


LINEAR POWER CONTROL SYSTEM FOR A NANOSATELLITE

DANNY MAKIMI ILUTO

 CAPE PENINSULA
UNIVERSITY OF TECHNOLOGY
LIBRARIES

Dewey No. THE 621.46 I L 4

CAPE PENINSULA
UNIVERSITY OF TECHNOLOGY



20132038

CAPE PENINSULA UNIVERSITY OF TECHNOLOGY
LIBRARY SERVICES
BELLVILLE CAMPUS

TEL: (021) 959-6210

FAX: (021) 959-6109

Renewals may be made telephonically.

This book must be returned on/before the last date shown.

Please note that fines are levied on overdue books

19 NOV 2013

21 NOV 2014

NOV 18 2014

19 DEC 2014
DEC 12 2014

BEL THE 621.46 ILM
(Green)

LINEAR POWER CONTROL SYSTEM FOR A NANOSATELLITE

by

DANNY MAKIMI ILUTU

**Thesis submitted in fulfillment of the requirements for the degree of Master of
Technology: Electrical Engineering in the Faculty of Engineering at the Cape
Peninsula University of Technology**

Supervisor: Prof. MTE KAHN

Bellville November 2011

CPUT Copyright Information

The thesis may not be published either in part (in scholarly, scientific or technical journals), or as a whole (as a monograph), unless permission has been obtained from the university

DECLARATION

I, Danny Makimi Ilutu, declare that the contents of this thesis represent my own unaided work, and that the thesis has not previously been submitted for academic examination towards any qualification. Furthermore, it represents my own opinions and not necessarily those of the Cape Peninsula University of Technology.

.....
Signed

.....
Date

ABSTRACT

Nanosatellite is an electronic device that requires a steady and reliable electrical power supplier (EPS) in order to drive all its electronic circuits. Its unpredictable failures can lead to extensive financial and time losses. The failures may be owing to the environment in which the satellite operates; the technique and the method used to generate power. In order to effectively minimise the risk of the EPS failures, a better technique is essential.

The direct energy transfer (DET) technique was chosen for this research because it provides high efficiency and high reliability, unlike the maximum power point tracking (MPPT) technique, which obtains maximum power from the solar cells by using a microcontroller. DET works on a fixed working point of current-voltage characteristic and responds to all satellite power system requirements.

The microcontroller is not a suitable device in satellite electrical power systems that requires high reliability, but is used because it is difficult to track the maximum power of solar cells without it. The analog MPPT system is another option, but the technique requires discrete components. Its deployment is limited because of the system's operating frequency and large electronic components such as the inductor and capacitor.

The main objective of this research was to design and develop a linear power control system for a nanosatellite. Sub-objectives were to examine and analyse existing techniques, which are used to design and develop the EPS of satellites, nanosatellites, the effectiveness and the potential types of energy reservoirs for space applications. Other sub-objectives were to investigate power densities' characteristics; charge times; physical size and complexity of charge cycles of the batteries; to develop a linear power control system (LPCS); to simulate the LPCS. Finally, to interpret the simulated results and then develop a prototype of a LPCS.

A low cost and feasibly sized linear power control system prototype, which is successfully developed, can enable continuous operation of a nanosatellite in space environment. The prototype is composed of power generation (solar cells), power storage (batteries), power distribution and power protection. LPCS captures solar energy and then distributes to the nanosatellite payload and subsystems.

Completion and testing of the prototype hence achieved the objectives of the research and design specifications of regulated power output (12V unregulated and 5V and 3.3V regulated). The design of LPCS has made a huge contribution to the satellite industry, and saves a lot of money in terms of reducing power supply size, weight and failure rates.

ACKNOWLEDGEMENTS

I wish to thank:

- My supervisor, Professor MTE Kahn, for his great support, guidance and encouragement throughout my research work, as well as for his diligence and generosity.
- The French South Africa Institute of Technology's (F'SATI) staff and students, especially Professor Robert Van Zil, for giving me the privilege to be a team member of the biggest project (CubeSat); Professor Elmarie Biermann, for her support by proof-reading and editing this thesis; and Francois Visserl, for his assistance in the completion of this project.
- My family, in particular my parents, for their faith, motivation and encouragement.
- Everyone who took an interest in my project.
- And, most importantly, my saviour, Lord Jesus Christ, for his love and giving me the strength to complete this thesis.

The financial assistance of the National Research Foundation through F'SATI towards this research is acknowledged. Opinions expressed in this thesis and the conclusions arrived at, are those of the author, and are not necessarily to be attributed to the National Research Foundation.

CONTENTS

DECLARATION.....	ii
ABSTRACT.....	iii
ACKNOWLEDGEMENTS.....	iv
LIST OF FIGURES.....	ix
LIST OF TABLES.....	x
LIST OF ABBREVIATIONS.....	xi
CHAPTER ONE.....	1
INTRODUCTION.....	1
1.1 Introduction.....	1
1.2 Background.....	1
1.3 Problem statement.....	1
1.4 Objectives of the research.....	2
1.5 Research methodology.....	3
1.6 Delineation of the research.....	3
1.7 Significance and contributions of the research.....	3
1.8 Structure of the thesis.....	4
1.9 Chapter summary.....	5
CHAPTER TWO.....	6
OVERVIEW OF NANOSATELLITE ELECTRICAL POWER SYSTEM.....	6
2.1 Introduction.....	6
2.2 Nanosatellite systems and applications.....	6
2.2.1 Nanosatellites.....	7
2.2.2 Nanosatellite system requirements.....	7
2.2.3 Nanosatellite power systems.....	8
2.3 Nanosatellite’s electrical source of power.....	8
2.3.1 Solar panels.....	9
2.3.1.1 Operating principle of a photovoltaic cell.....	10
2.3.1.2 Equivalent model of a photovoltaic cell.....	14
2.3.2 Batteries.....	16
2.3.3 Battery overview.....	16
2.3.4 Battery types.....	17
2.3.4.1 Primary batteries.....	17
2.3.4.2 Secondary batteries.....	17
2.3.5 Nuclear power.....	19
2.3.6 Heat generator.....	20

2.4	Working environmental	20
2.4.1	Orbits.....	20
2.4.1.1	Kepler's law.....	20
2.4.1.2	The earth in space.....	21
2.4.1.3	Types of orbits	22
2.4.2	Cosmological radiation.....	23
2.5	Chapter summary.....	24
CHAPTER THREE		25
LINEAR POWER CONTROL SYSTEM		25
3.1	Introduction.....	25
3.2	Theoretical consideration	25
3.2.1	Electrical power system	26
3.2.2	Types of electrical power systems	26
3.3	Switch mode power systems.....	26
3.4	Linear power systems.....	28
3.4.1	Types of linear power regulators	30
3.4.1.1	Standard power regulator	30
3.4.1.2	Low dropout power regulator	31
3.4.1.3	Quasi low dropout power regulator	32
3.4.2	Power regulator selections	33
3.4.2.1	Maximum load current	33
3.4.2.2	Input voltage.....	33
3.4.2.3	Output voltage precision (tolerance)	34
3.4.2.4	Quiescent current	34
3.4.3	Protection circuits	34
3.5	Selection of the design configuration	35
3.6	Design consideration.....	37
3.6.1	Solar panel.....	38
3.6.1.1	Solar panel's size.....	39
3.6.1.2	Cell alternatives	40
3.6.1.3	Radiation impacts	42
3.6.1.4	Thermal impacts	43
3.6.1.5	Final adjusted efficiencies.....	47
3.6.1.6	Series and parallel requirements.....	48
3.6.1.7	Solar cells power control system.....	50
3.6.2	Shunt regulation system	50

3.6.3 Battery management system	51
3.6.3.1 Charged characteristics of Lithium-Polymer batteries	52
3.6.3.2 Lithium-Polymer battery charger	56
3.6.4 Power distribution system	58
3.6.5 System power budget	58
3.6.6 System mass budget.....	60
3.7 Chapter summery.....	60
CHAPTER FOUR.....	61
DESIGN ANALYSIS AND TESTS	61
4.1 Introduction.....	61
4.2 Simulations.....	61
4.2.1 Solar cells.....	61
4.2.1.1 LTSpice simulation	61
4.2.1.2 Matlab/ Simulink simulation.....	63
4.2.2 Control systems.....	67
4.2.3 Power distribution systems.....	69
4.3 Hardware testing.....	71
4.3.1 Detailed hardware description.....	71
4.3.2 Solar panel.....	75
4.3.3 battery compatibility test.....	76
4.3.4 Power control and distribution efficiencies	77
4.4 Chapter summary.....	78
CHAPTER FIVE.....	79
CONCLUSIONS AND RECOMMENDATIONS	79
5.1 Introduction.....	79
5.2 Results and difficulties	79
5.2.1 Solar cells.....	79
5.2.2 Batteries	80
5.2.3 Battery and power management	80
5.2.4 Design of the electronics.....	80
5.3 Proposed future work and recommendations.....	80
REFERENCES	81
APPENDICES	84
APPENDIX A: Electrical power source equation.....	84
APPENDIX B: Adjustment of nominal cell efficiency and solar cells calculations	85
APPENDIX C: Solar cell specification sheets.....	88

APPENDIX D: Matlab codes.....	92
APPENDIX E: Power distribution and battery management systems pcb layout and schematic.....	97

LIST OF FIGURES

Figure 1.1: Thesis structure	5
Figure 2.1: Satellite power system concept from Wertz & Larson (1999:407).....	8
Figure 2.2: Spectrolab solar cell unit.....	9
Figure 2.3: Solar cell setup	10
Figure 2.4: Schematic diagram of a unit cell from Wenhan <i>et al.</i> (2007).....	11
Figure 2.5: PN junction photodiode and I-V characteristic curve.	12
Figure 2.6: I-Vcharacteristic curve of an illuminated PN junction.....	12
Figure 2.7: Characteristic curves of I-V and P-V from Castaner & Silvestre (2002).....	13
Figure 2.8: Electrical equivalent circuit model of a photovoltaic cell	14
Figure 2.9: Electrical model of an equivalent circuit photovoltaic generator.....	15
Figure 2.10: Voltaic cell connection from Linden & Reddy (2001).	16
Figure 2.11: MPP characteristic curve from Kaltschmitt <i>et al.</i> (2007:240).....	19
Figure 2.12: Illustration of Kepler's three laws from Maral <i>et al.</i> (2009:19).....	21
Figure 2.13: Representation of Van Allen belts in the magnetosphere	21
Figure 3.1: Basic layout structure of a typical DC-DC converter.....	27
Figure 3.2: Basic block diagram of SMPS with MPPT from Jordan (2006:17).....	28
Figure 3.3: Linear power regulator functional diagram Mohan <i>et al.</i> (2003:3).....	28
Figure 3.4: Diagram of a typical linear power regulator from Mohan <i>et al.</i> (2003:4).....	29
Figure 3.5: Standard power regulator circuit diagram from Chester (2011).	30
Figure 3.6: LDO power regulator circuit diagram from Chester (2011).	31
Figure 3.7: Quasi LDO power regulator circuit diagram from Chester (2011).....	32
Figure 3.8: System configuration of the LPCS from Jordan (2006:21).....	36
Figure 3.9: System configuration of the LPCS with redundancy from Jordan (2006:22).	36
Figure 3.10: Series-parallel arrangement of solar cells	38
Figure 3.11: Proposed structural design for LPCS system	40
Figure 3.12: High efficiency triple junction space solar cell developed on an ultra thin Ge substrate.....	41
Figure 3.13: Shunt regulated circuit diagram.....	51
Figure 3.14: Space Lithium-Polymer batteries from Clyde Space datasheet.....	52
Figure 3.15: Typical charge profile of 1C @ 20°C with defined voltage range for the application.	55
Figure 3.16: Discharge profile systems from Jordan (2006).	56
Figure 3.17: Battery management system circuit diagrams.....	58
Figure 3.18: LPCS power budget.....	59
Figure 4.1: 2.3V with 0.5mA Current-voltage characteristic curve	62
Figure 4.2: Power-voltage characteristic curve.....	62
Figure 4.3: Solar cell C-V characteristic vs irradiance	63
Figure 4.4: Solar cell C-V characteristic vs temperature.....	63
Figure 4.5: Solar cells average power simulation	65
Figure 4.6: Simulated control system circuit of LPCS.....	67
Figure 4.7: Simulation results of the linear control system	69
Figure 4.8: Simulated circuit of a regulated voltage.....	70
Figure 4.9: Simulation results of 3.3V regulated voltage	70
Figure 4.10: LPCS components	72
Figure 4.11: Base board power controller (BBPC), top view.....	72
Figure 4.12: Callout symbols drawing of BBPC.....	73
Figure 4.13: DC to DC regulator, Top view	74
Figure 4.14: Callout symbols drawing of power regulator.....	74
Figure 4.15: An ENE/CESI single junction GaAs solar cell from Clyde Space.....	75
Figure 4.16: 12.3 V 15 Whr Battery cell string for Nanosatellite from Clyde Space.	76

LIST OF TABLES

Table 2.1: Satellite classification	6
Table 3.1: Summary of the three types of linear power regulators.....	33
Table 3.2: Comparison of Spectrolab Incorporated and Emcore Corporation nominal efficiencies	41
Table 3.3: Mechanical design specification of UTJ solar cell	41
Table 3.4: Electrical design specification of UTJ solar cell	42
Table 3.5: Temperature gradients specification of UTJ solar cell	42
Table 3.6 (a & b): Summary of 1 MeV equivalent Electron Fluence (cm^{-2}) at solar maximum and minimum	43
Table 3.7: Predicted Solar Cell Temperature in summer	45
Table 3.8: Predicted Solar Cell Temperature in winter	46
Table 3.9: Preliminary adjustment of nominal cell efficiency.....	47
Table 3.10: Final average of nominal cell efficiency	48
Table 3.11: Series and Parallel Requirements	49
Table 3.12: Japanese CubeSat selected battery specifications.....	53
Table 3.13: PoLiFlex thermal specifications	53
Table 3.14: LPCS mass budget	60
Table 4.1: Solar panel test specifications	75
Table 4.2: LPCS test results	77
Table 4.3: Power distribution simulation and test results.....	77

LIST OF ABBREVIATIONS

AC	Alternating Current
BJT	Bipolar Junction Transistor
BOL	Beginning of life
CCCV	Constant Current Constant Voltage
DC	Direct Current
DET	Direct Energy Transfer
DoD	Depth of Discharge
EMF	Electromagnetic Fields
EOL	End of life
EPS	Electrical Power Supplier
ESA	European Space Agency
ESC	Electrostatic Charging
FO	Operating Factor
FOE	Operating Factors of the Eclipse
FOS	Operating Factors of the sun
GaAs	Gallium Arsenide
IC	Integrated Circuit
IR	Infrared
LDO	Low Dropout
LEO	Low Earth Orbit
Li-Ion	Lithium-Ion
LiPo	Lithium Polymer
LTSpice	Linear Technology Spice
MatLab	Matrix Laboratory
MPP	Maximum Power Point
MPPT	Maximum Power Point Tracking
NASA	National Aeronautics and Space Administration
NiCd	Nickel Cadmium
NiH ₂	Nickel Hydrogen
Opamp	Operational Amplifier
RF	Radio Frequency
RTG	Radioisotope Thermoelectric Generators
SOC	State of Charge
SPENVIS	Space Environment Information System
UTJ	Ultra Triple Junction
VARTA	Vertrieb Aufladung Reparatur Transportabler Akkumulatoren

CHAPTER ONE INTRODUCTION

1.1 Introduction

A nanosatellite is a standard term, which is applied to a satellite with a weight mass between 1 to 10 kg. Satellites of these sizes are called small satellites. Research and development within the field of nanosatellites have increased significantly within the last number of years owing to their small sizes, which make them affordable and open the horizon for universities to develop missions in these areas (Michael & Norma, 2002:276).

All nanosatellites require some sort of electrical power system to manage power flow within the satellite. The electrical power system for nanosatellites has three major operations, namely that of managing the power input from solar cells, charging the batteries and providing electrical power at the required voltages to all other satellite components (Maloney, Travis, Stogsdill & Waddle, 2007). The electrical power system also provides services such as over-current and under-voltage protection, and supplies the main nanosatellite microprocessor with telemetry data concerning its operations (Amils, Ellis-Evans & Hinghofer-Szalkay, 2007:170).

1.2 Background

For the last few decades the focus on the development of EPS and its progress has revolved around the needs and requirements of high power mission, mainly for communications applications (Lida, 2000:178). While the challenges to increase efficiency and reduce mass and volume of these applications are valid, the needs of nanosatellite missions have been more shaded.

The growing number and utility of nanosatellites highlights the need for careful and measured consideration for the specific power requirements on nanosatellite missions. The challenge for nanosatellite EPS designers is to produce an efficient and flexible design that avoids the need for system restructuring with each set of mission requirements (Sandau & Valenzuela, 2010:291).

1.3 Problem statement

EPS of a nanosatellite should be steady and reliable to drive all electronic circuits and components within the satellite. Unforeseen failures can lead to extensive financial and time losses. The failures may be owing to the environment in which the satellite operates; the technique and method used to generate power. In order to effectively minimise the risk of the EPS failures, a better technique is essential.

DET technique has been chosen for this research because it provides high efficiency and high reliability unlike the MPPT technique, which obtains maximum power from the solar cells by using a microcontroller. DET works on a fixed working point of current-voltage characteristic and responds to all satellite power system requirements.

Microcontroller is not a suitable device in satellite electrical power systems, which requires high reliability, but is used because it is difficult to track the maximum power of solar cells without it. The analog MPPT system is another option, but the technique requires discrete components. Its deployment is limited because of the system operating frequency and the large electronic components such as the inductor and capacitor.

This research focuses on the development of a LPCS that will manage the electrical power for nanosatellites. The LPCS will be competitive with other electrical power system designs, as implemented by Stanford University and Clyde Space. This LPCS design will be capable of receiving, storing, and distributing power, which is required by the satellite's subsystems and will be able to withstand space environment.

The LPCS will be designed to be environmentally friendly and its simple architecture will serve as a low cost power monitoring development platform for universities and organisations to engage in research for satellite power system projects.

1.4 Objectives of the research

The main objective of the research is to design and develop a linear power control system for a nanosatellite, while its sub objectives are:

- To examine and analyse the existing techniques used to design and develop the EPS for nanosatellites;
- To examine the effectiveness and the potential types of energy reservoirs for the space applications;
- To investigate the power densities' characteristics; charge times, physical size and complexity of charge cycles of the batteries;
- To develop and simulate the LPCS;
- To analyse and interpret the simulated results; and
- To develop and propose ideas for LPCS development.

With the objectives of this project introduced, the following research questions are significant:

- Can an LPCS be developed to endure and accurately operate nanosatellites in the harsh environmental conditions encountered in high altitude and low earth orbit?
- What are the existing techniques and methods used to power nanosatellites?
- Can the same techniques and methods be used to develop LPCS to power the nanosatellites of the sizes between 5 to 10 kg that will be launched in a low earth orbit environment?
- Will the LPCS be able to deliver the power requirement for nanosatellite subsystems?
- Is the size of LPCS according to the nanosatellite's standard?
- What kind of solar cells, batteries and regulations should be used?

1.5 Research methodology

A literature search concerning implementing LPCS for a nanosatellite was chosen to lead to further investigation into different EPS techniques, including the DET, solar cells technology, battery chemistries and power regulations. A comparison between feasible EPS techniques for satellites was made from where future recommendations and improvements were suggested. Subsequently, feasible EPS techniques relating to LPCS for a nanosatellite and their surroundings were identified from where the design prototype was constructed. Laboratory simulations and test scenarios on these solutions were executed and the feasibility of this design was evaluated.

1.6 Delineation of the research

The research was based on the EPS for a nanosatellite and did not provide a generic EPS solution for all categories of nanosatellites. The proposed solution is limited to nanosatellites of mass between 5 to 10 kg. Although the research offers a brief comparison study of the different types of linear power regulators and their feasible techniques as reference, the LPCS technique implemented is limited to the use of solar cells, storage batteries, charging and discharging regulators, as well as the shunt regulation technique.

1.7 Significance and contributions of the research

Several EPS techniques and topologies already exist to supply nanosatellites with the required electrical energy. Amongst these techniques is the popular MPPT, which uses a microcontroller (although less reliable) to easily track and obtain maximum power from solar cells (Michael & Norma, 2002:45). However, for more reliability, the microcontroller is not a suitable device to use, but it is difficult to track the maximum power of the solar cells without it (McEvoy, Markvart & Castaner, 2011: 713).

Building an analog MPPT system is another option, but the analog technique requires discrete components. To limit the system operating frequency, involves the use of a bulky inductor and capacitor. As a result of the shortcomings of the above EPS technique, the LPCS adopts the DET technique. The DET technique is simple to implement and works on a fixed working point on a current-voltage characteristic and responds to all satellite power requirements and provides better efficiency and high reliability. Completion of LCPS research should add value to nanosatellite power systems.

1.8 Structure of the thesis

The structure of this research paper is outlined in Figure 1.1 below. Excluding Chapter 1, the thesis covers satellite electrical power system techniques and analytical methods that were employed to design and develop the electrical power system in order to achieve the objectives of the research. Chapter 2 provides an overview of nanosatellite's electrical power system, and highlights the applications of nanosatellites and its working environments. In Chapter 3 the design studies of the electrical power system are given, as well as the selected topology for the LPCS, including both system power and mass budgets that play an important role in the design study. Chapter 4 presents the system simulations; practical test results; and the comparison of simulation and practical results, while Chapter 5 concludes and recommends future improvements that can be done on LPCS.

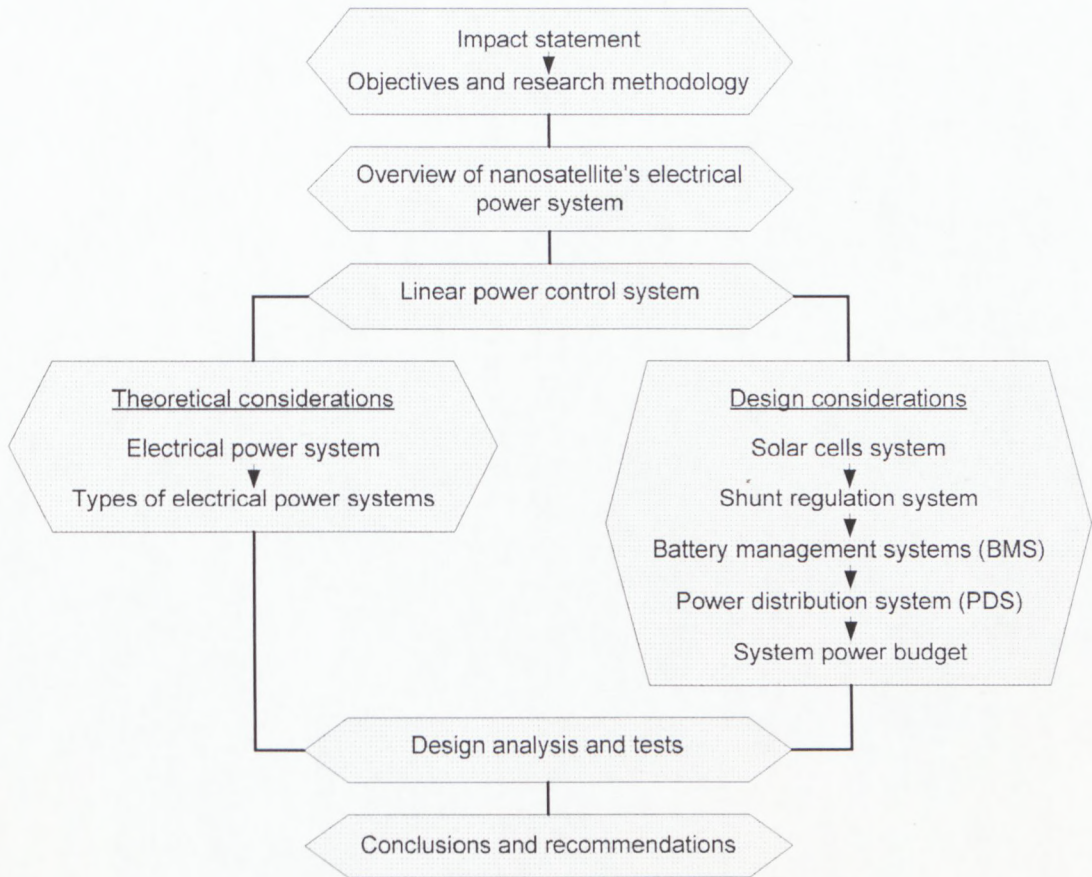


Figure 1.1: Thesis structure

1.9 Chapter summary

An LPCS for a nanosatellite is an electrical power system, which produces electrical power to operate satellite payload and other electronic subsystems at optimal levels. Included in the system are the solar cells, recharged batteries and various regulations and distribution components that were chosen according to their reliability and ability to fit within the constraints imposed by the nanosatellite's mission.

CHAPTER TWO OVERVIEW OF NANOSATELLITE ELECTRICAL POWER SYSTEM

2.1 Introduction

Discussion of the following aspects highlights understanding of the use of nanosatellites, and the methods and techniques employed to supply nanosatellites with electrical power.

- Nanosatellite systems and applications;
- Types of electrical power systems available for powering nanosatellite subsystems; and
- Environmental effects of low earth orbit (LEO).

2.2 Nanosatellite systems and applications

Nanosatellites are objects that orbit the earth and sometimes the sun. They are highly specialised instruments that do different tasks every day. There are many different types of nanosatellites that can do different things. Weather satellites, for example, take pictures of how the weather is, whereas communication satellites transmit TV or telephone signals to earth. Each satellite has many different parts, but the two common parts that all satellites have are the payload and the bus (Inglis & Luther, 1997:1-5).

A payload is any equipment that satellite uses to carry out its work. This equipment can be the camera, antenna, radar, as well as certain electronic devices. For example, the weather satellite uses the camera as the payload to take pictures of cloud formations, while the communication satellite uses large antennas to transmit television signals or telephone signals to the ground. The bus is the part of a satellite that carries the payload and all its equipment in space. In other words, the bus holds all the satellite's parts and provides electrical power for its operations (Wertz & Larson, 1999: 245).

The satellites are classified by their relative sizes, weights and work that they do. There are seven groups of satellites, which orbit the earth. Each group has its own location in space (Michael & Norma, 2002:1-3). Table 2.1 below lists satellite groups, as well as their location in space.

Table 2.1: Satellite classification (SRREY)

Type of satellite	Group	Weights	Space location
Big	Large satellite	> 1000 kg	Geostationary orbit
	Medium sized satellite	500 – 1000 kg	Medium orbit
Small	Mini satellite	100 – 500 kg	Low earth orbit
	Micro satellite	10 – 100 kg	Low earth orbit
	Nano satellite	1 – 10 kg	Low earth orbit
	Pico satellite	0.1 – 1 kg	Low earth orbit
	Femto satellite	< 100 g	Low earth orbit

Within this classification, the term small satellite is used to cover all spacecrafts within an orbit mass of less than 500 kg. The small satellite, which is used in the case study in this project, is a nanosatellite.

2.2.1 Nanosatellites

Nanosatellites have literally been around since the dawn of the space age, but have been dominated by the large satellites' programmes in the industry. However, as a reaction to shrinking budgets, emphasis in the 1990s in industry on smaller, faster, and better has focused increased attention on the capabilities and advantages that nanosatellites can bring to satellites' industries (Sandau, Roser & Valenzuela, 2010:19). Although nanosatellites projects might not perform complex missions that require huge instruments or high power communication payloads, there remain many missions whereby nanosatellites can be efficiently used, including:

- Meteorological satellites, which are used for weather reports;
- Scientific satellites, which are used in scientific applications such as studying the universe, remote sensing, exploring the earth mineral resources, and so on;
- Navigational satellites, which are used in global positioning systems; and
- Military satellites, which are used for imaging enemy territory, and eavesdropping of enemy components.

All nanosatellites must have limited power budgets and must operate within a space radiation environment, which is harmful to the reliability of semiconductor electronics components (Lang, 2011:155).

2.2.2 Nanosatellite system requirements

The technologies used in terrestrial and airborne applications are applicable in the same way in satellites, but there are some additional requirements and specifications.

Because of degrading space environment, nanosatellites must be designed specifically for shock and vibration during launch, extreme temperatures, temperature cycling, temperature gradients, radiation exposure and vacuum conditions, while maintaining high reliability over extended lifetimes. Nanosatellites also limit on-board resources for on-board processing and communications to the ground. The small mass and size of these satellites limit the amount of energy provided by solar panels as well, therefore, power availability is a constrain on both processor and communications systems of the satellite. Their RF systems radiate only about 0.5 watts of power and generally use omni antennas without gain to avoid any unnecessary tracking (Mahalik, 2006:201).

2.2.3 Nanosatellite power system

The function of the power system is to generate electrical power by using solar cells, backup batteries, as well as regulate and distribute circuitries (Kramer, 2002:74). In order to improve the reliability and stability of the system, the system configuration power budget and on-board components of electrical power must be well designed and selected. A nanosatellite, like all other satellite power system concepts, is illustrated in Figure 2.1 below.

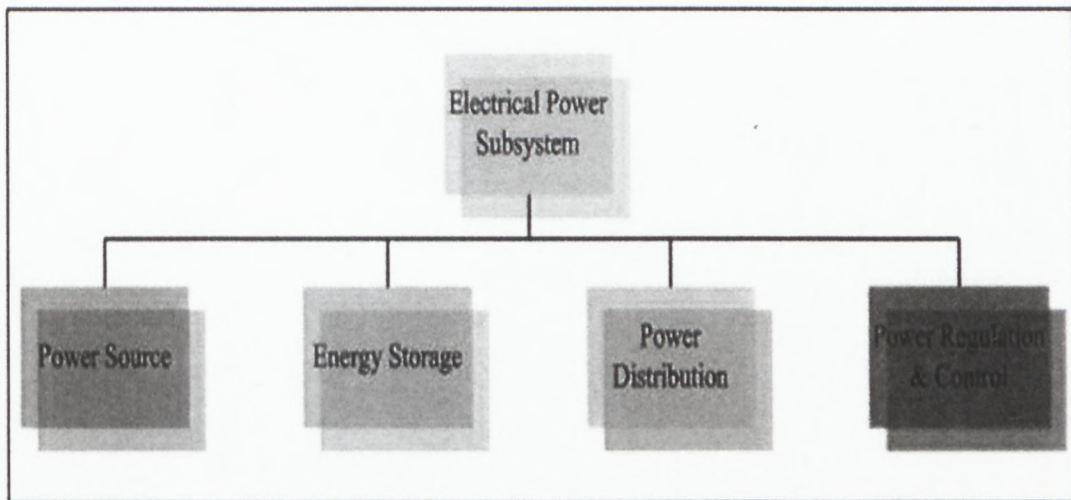


Figure 2.1: Satellite power system concept
(Adapted from Wertz & Larson, 1999: 407)

Nanosatellite electrical energy needs depend on the intended mission of the satellite and the payload that the satellite needs to carry. These variables influence the amount of electricity that the satellite will use. Depending on the size, mass and mission, the nanosatellite electrical power varies from a few watts to hundreds of watts. This power may be derived from solar array, rated at 2.3 V and approximately 1 W.

2.3 Nanosatellite's electrical source of power

Reliable, abundant and portable energy is developing and sustaining human presence in space. These needs are normally met with chemical and solar energy sources. However, chemical sources have a limited operating life, while solar energy sources have limited maximum available output in addition to being unfeasible for missions far from the sun (Fortescue, Stark & Swinwr, 2003:325-349).

Factors that should be considered for choosing a satellite's power source include cost, durability, and effectiveness (amount of power generated).

The following are some possible power sources for satellites:

- Solar panels;
- Batteries;
- Nuclear power; and
- Heat generators.

2.3.1 Solar panels

Solar energy has become the most popular satellite source of power because of its cost and weight and the fact that it provides the energy continuously. There exist two types of solar panels, namely flat-plate collectors and the photovoltaic cell. The flat-plate collector is a type of solar panel that is useful on earth, while the photovoltaic cell is used in space activities (Maini & Agrawal, 2011:143).

The photovoltaic cell converts light directly into electric power. The voltage output and the current delivering capability of an individual solar cell are small and should be linked to one another to form electrical power input, which is sufficient to supply any satellite subsystem and payload. The solar panel consists of a set of a large number of solar cells, which are connected in series and parallel to each other. The series-parallel arrangement is to obtain the desired output voltage with the required power delivery capability.

The typical voltage produced by Spectrolab solar cell is 2.3V with a load current capacity of about 500mA. Figure 2.2 below illustrates solar cells from Spectrolab datasheet (see Appendix C).

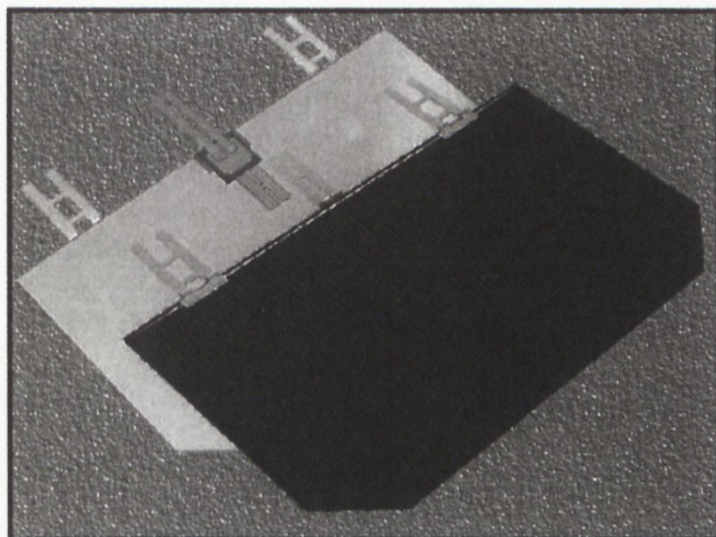


Figure 2.2: Spectrolab solar cell unit

Solar efficiency is the ratio of the maximum electrical power of a solar cell to the radiant power on the solar cell area. The efficiency figure for ultra triple junction solar cells is 28.3%. The most commonly used semiconductor material to make solar cells is silicon, and another is Gallium Arsenide. Gallium Arsenide solar cells are lightweight and more efficient. The solar panel provides electrical power when the satellite is in direct sunlight, but when the solar panel cannot provide power, the batteries take over (Castaner & Silvestre, 2002:1-18).

Satellites' solar panels comprise of a number of photovoltaic cells, which are connected together. This arrangement produces enough electricity to power a satellite's computers, radios, cameras, and other equipment, as well as recharges the satellite's back-up batteries. Figure 2.3 below shows how a solar cell can be setup to generate power to a load.

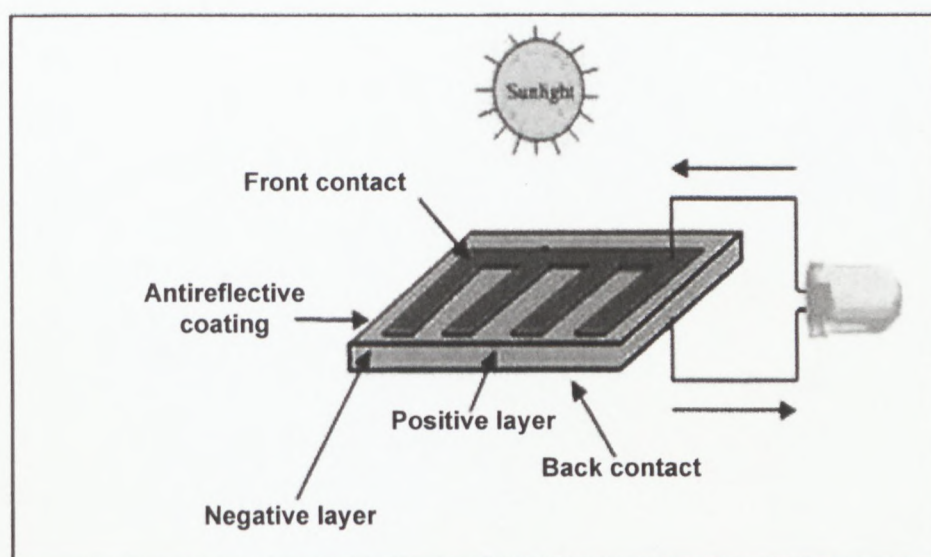


Figure 2.3: Solar cell setup

2.3.1.1 Operating principle of a photovoltaic cell

A photovoltaic cell is similar to a photo diode. Its operation is based on the properties of semiconductor materials. The photovoltaic cell allows the direct conversion of light energy into electrical energy. Its operating principle is based on the photovoltaic effect (Boeker & Grondelle, 2011: 152).

A cell consists of two thin layers of a semiconductor. These two layers are doped differently; for layer N, a contribution of electron devices and the P layer is a deficit of electrons. These two layers are potentially different (Luque & Hegedus, 2003:50-147). The energy of light protons captured by the outer electrons of the N layer allows them to cross the potential barrier and to generate a continuous electrical current.

To make a collection of this current, electrodes are deposited by screen printing on both layers of the semiconductor, as shown in Figure 2.4. The upper electrode is a gate, which allows passage of light rays. An anti-reflective layer is then deposited onto this electrode to increase the amount of light, which is absorbed (Wenhan, Green & Watt, 2007:1-75).

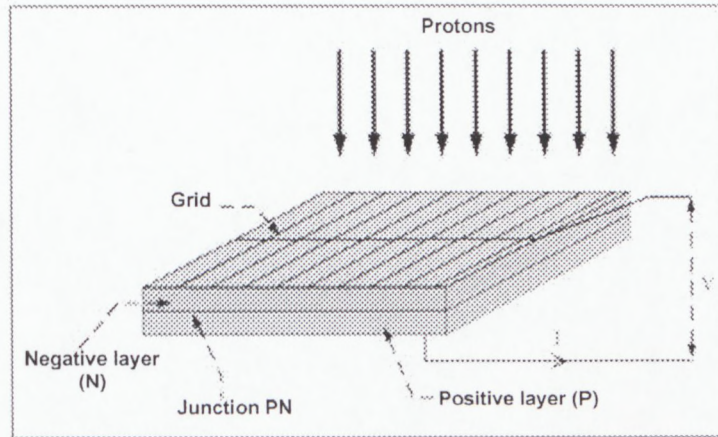
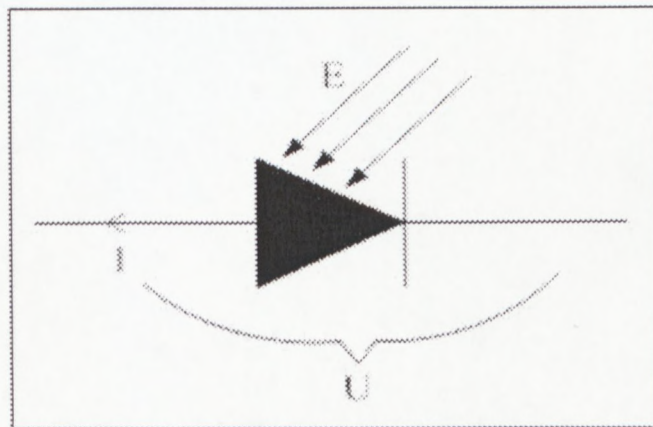
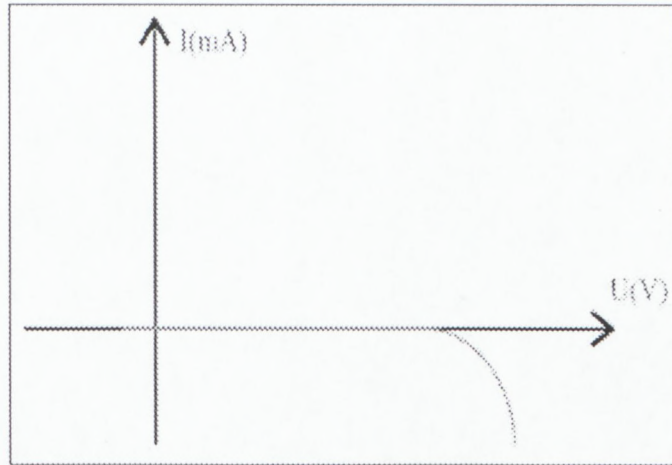


Figure 2.4: Schematic diagram of a unit cell
(Adapted from Wenhan *et al.*, 2007:1-75)

In darkness the cell behaves like a diode and presents the current-voltage characteristic curve similar to that of a PN junction diode, as shown in Figures 2.5a and b.



(a)



(b)

Figure 2.5: PN junction photodiode and Current-voltage characteristic curve
(Adapted from Wenhan *et al.*, 2007:1-75).

Figure 2.6 below shows the current-voltage characteristic curve of the photodiode (PN junction). When the photovoltaic cell diode is illuminated, electric current is produced even higher than the intensity of the illumination itself. This current is often proportional to the sun is illumination.

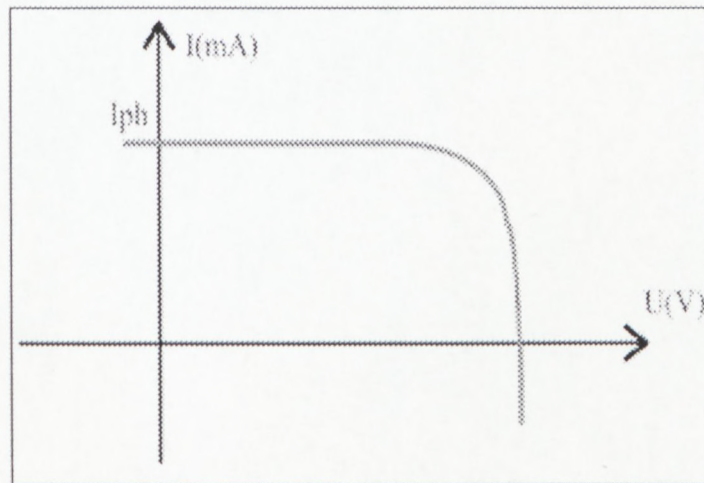
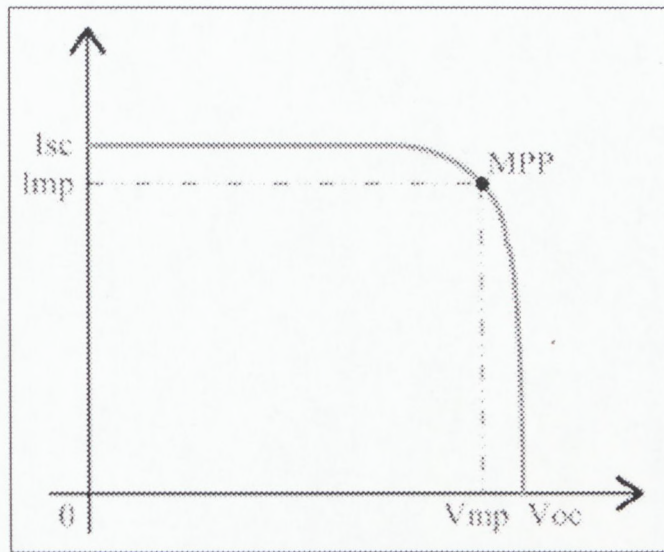


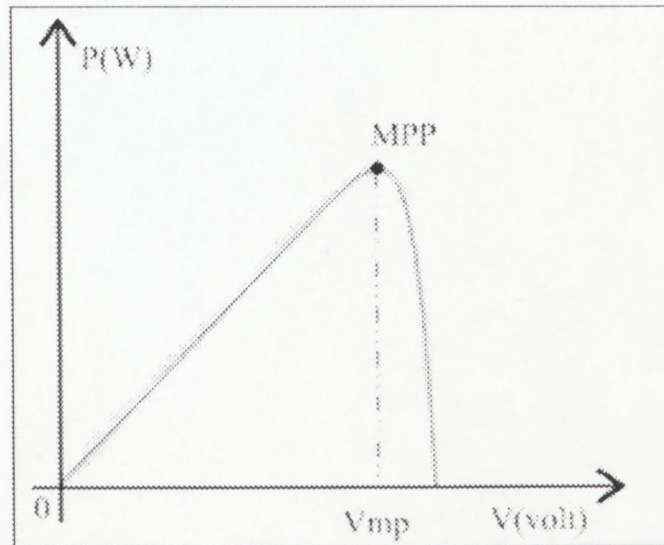
Figure 2.6: Current-voltage characteristic curve of an illuminated PN junction (photodiode)
(Adapted from Luque & Hegedus, 2003:50-147)

In this same sequence of ideas, the photovoltaic cell can also produce the characteristic curve, which is similar to the photodiode. The difference is the level of material resources that is used.

Figures 2.7a and b below show the characteristic curves of current-voltage and power-voltage of the photovoltaic cell, respectively.



(a)



(b)

Figure 2.7: Characteristic curves of current-voltage and power-voltage
(Adapted from Castaner & Silvestre, 2002:1-18)

V_{mp} is the optimal voltage of PV panel for maximum power and I_{mp} is the optimal current.

2.3.1.2 Equivalent model of a photovoltaic cell

The mathematical model, which is associated with a photovoltaic cell, is derived from the PN junction photodiode by adding the current source I_{ph} , which is proportional to the sun illumination and some internal elements. The expression of the current (I) of the solar cell is given by:

$$I = I_{ph} \times \left(I_d - \frac{U + (R_s \times I)}{R_{sh}} \right) \quad \text{Equation 2.1}$$

$$I_d = I_{od} \times \left(e^{\frac{q(U + (R_s \times I))}{k \times T}} - 1 \right) \quad \text{Equation 2.2}$$

Where

- I_{ph} : photo current or the current generated by the illumination (A),
- I_{od} : saturation current of the diode (A),
- R_s : series resistance (Ω),
- R_{sh} : shunt resistance (Ω),
- K : Boltzmann constant ($k = 1.38 \times 10^{-23}$),
- q : electron charge ($q = 1.602 \times 10^{-19} \text{C}$),
- T : cell temperature (°K).

From these expressions, the basic equivalent circuit of the photovoltaic cell can be represented as follows:

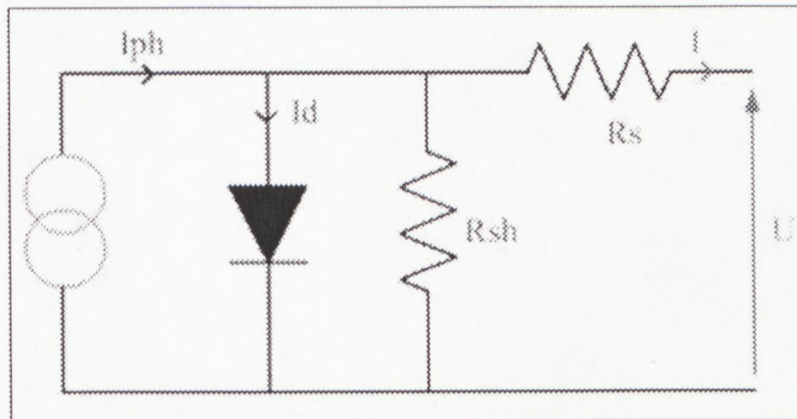


Figure 2.8: Electrical equivalent circuit model of a photovoltaic cell
(Adapted from Camarinha-Matos, 2011: 512)

In this equivalent circuit, the diode models the behaviour of the cell in the dark period. The current generator models the current I_{ph} generated by the illumination of the solar radius. Finally, the two resistors model the internal losses; series resistance (R_s) models the ohmic losses of the material, while the shunt resistance (R_{sh}) models the eddy current that passes through the cell.

The photovoltaic cell is a basic generator of low power *vis-à-vis* the needs of most domestic, industrial or space applications. To produce more power, more cells must be assembled to create a module or a photovoltaic panel. The series connection of cells easily increases the voltage of the assembly, while the parallel increases the current. Figure 2.9 shows the electrical equivalent circuit model, which is closest to the practical photovoltaic generator. This presentation is a model with two diodes of different form factors and different constitutive laws with respect to temperatures.

The term of current (I) for the model with two diodes photovoltaic generator is:

$$I = I_{CCstd} \times \frac{G}{1000} (\Delta I_T (T - T_{ref}) + 1) - K_1 T^3 e^{\frac{-E_g}{KT}} \left(e^{\frac{q(V+R_s I_{SC})}{n_1 KT}} - 1 \right) - K_2 T^{\frac{5}{2}} e^{\frac{-E_g}{KT}} \left(e^{\frac{q(V+R_s I_{SC})}{n_2 KT}} - 1 \right) - \frac{V}{R_{sh}}$$

Equation 2.3

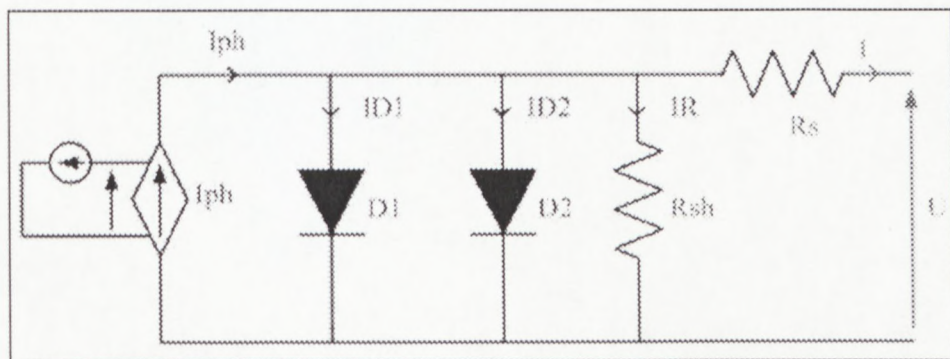


Figure 2.9: Electrical model of an equivalent circuit photovoltaic generator
(Adapter from Solanki, 2009:103)

The shunt resistance (R_{sh}) is a leakage resistance. The value of this resistance must be high ($\approx 1 \text{ M}\Omega$), and the series resistance value must be low ($\leq 0.01 \Omega$) to approximate the simulation of reality.

2.3.2 Batteries

Battery is a backup device, which is used to supply the satellite subsystems in the absence of the sun or at huge demand of the energy (Maini & Agrawal, 2011: 148). In order to have a robust and efficient system, the battery should work to its full potential.

The connection of the battery depends on the technique that is used, but one common point is to maximise battery capacity usage, which relates to how energy is properly restored to a rechargeable battery. No single technique is ideal for all battery chemistries; each technique corresponds to a particular application and to a particular chemistry. The technique, which is employed in this design, is based on the lithium family.

2.3.3 Battery overview

As mentioned above, a battery is a device that converts stored chemical energy that is contained in its active materials directly into electric energy by means of an electrochemical oxidation reduction reaction called redox. This reaction employs the transfer of electrons from one material to another through an electric circuit (Scott, 2004:1).

As shown in Figure 2.10, the battery is composed of a number of voltaic cells; each voltaic cell constitutes two half cells, which are connected in series by a conductive electrolyte that contains anions and cations. One half of the cells consist of anodes (positive electrode) and other half consist of cathodes (negative electrode). An electrolyte and an electrode migrate to the anions for a negative charged to cations for a positive charge (Linden & Reddy, 2001:8).

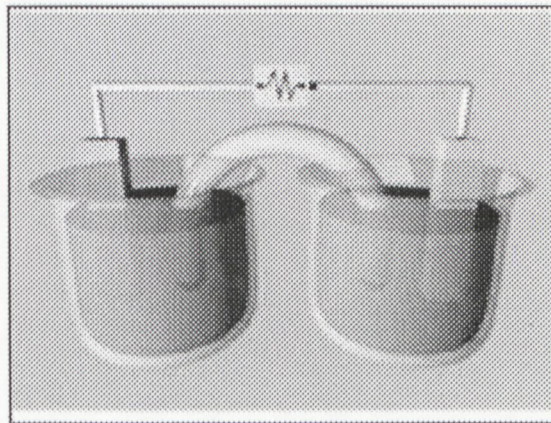


Figure 2.10: Voltaic cell connection
(Adapted from Linden & Reddy, 2001:1-8)

2.3.4 Battery types

Batteries are classified into two main categories, namely primary and secondary.

2.3.4.1 Primary batteries

Primary batteries have an irreversible reaction and limit of used period. They transform chemical energy into electrical energy. When an initial supply of reactants is exhausted, energy cannot be restored to the battery by electrical means. These batteries cannot work under high-drain applications with 75Ω loads (Linden & Reddy, 2001:1-5). The most common primary batteries are:

- Zinc-carbon batteries;
- Alkaline batteries; and
- Lithium metal batteries

2.3.4.2 Secondary batteries

Secondary batteries can be recharged; the chemical reactions are reversed by supplying electrical energy to cells, hence restoring their original composition. Certain secondary batteries work well under high-drain applications. The most common of secondary batteries include:

- Lead-acid battery;
- Gel battery;
- Absorbed glass mat;
- Dry cell;
- Nickel-cadmium;
- Nickel metal hybrid; and
- Lithium family (Li-Ion and LiPo).

The three kinds of batteries that are mostly used in satellite applications are Nickel Cadmium (NiCd), Nickel Hydrogen (NiH₂) and Lithium-Ion (Li- ion) batteries.

❖ NiCd batteries

Nickel Cadmium batteries are well known for space applications and are characterized by:

- Low output voltage (1,2V);
- Low energy density (~ 10 WH/ kg); and
- Suffer from memory effects that mean the discharge capacity of the battery is reduced when it is repetitively discharged incompletely and then recharged.

❖ NiMH batteries

These batteries are also known for space applications and are characterized by:

- No memory effect;
- Low output voltage (1,2V); and
- High energy density (~ 60 WH / kg) compared to NiCd batteries.

❖ Lithium family batteries

Li-ion batteries are characterised by:

- Higher energy density than NiCd and NiMH batteries (well over 100wh /kg);
- Produce approximately three times the voltage of rechargeable NiCd and/ or NiMH batteries (3,7V and/or more);
- No memory effect;
- Have an extremely flat discharge profile;
- Wider operating temperature interval than NiCds and NiMHs batteries; and
- Suffers from overcharging, which may cause the battery to explode.

Amongst these batteries, Lithium family batteries are mostly used because of their high energy density, which reduces the power system volume and weight, and is characterised by the wide range of temperature fluctuations compared to NiCd and NiMH.

The difference between Li-Ion and LiPo cells is that in Li-Ion cells, the rigid case presses the electrodes and the separator onto each other, whereas in polymer cells this external pressure is not required because the electrode sheets and the separator sheets are laminated onto each other (Kiehne, 2003:149). The following are criteria, which are used for the selection of batteries:

- Dimension of individual cells (flat or circular);
- Longevity (maximum life cycle);
- Voltage output;
- Capacity and mass; and
- Test for space applications.

One problem in connecting a solar panel to a rechargeable battery is that the solar panels and battery do not work at the same maximum efficiency at the same voltage. This means that there is a mismatch between them. To avoid this situation, either maximum power point tracker (MPPT) or direct energy transfer (DET) techniques should be used. Figure 2.11 shows the current-voltage characteristic curve. In the curve the maximum power point (MPP) is calculated as the largest possible area of the dotted square. The voltage and current are the values, which are supplied by the solar panels.

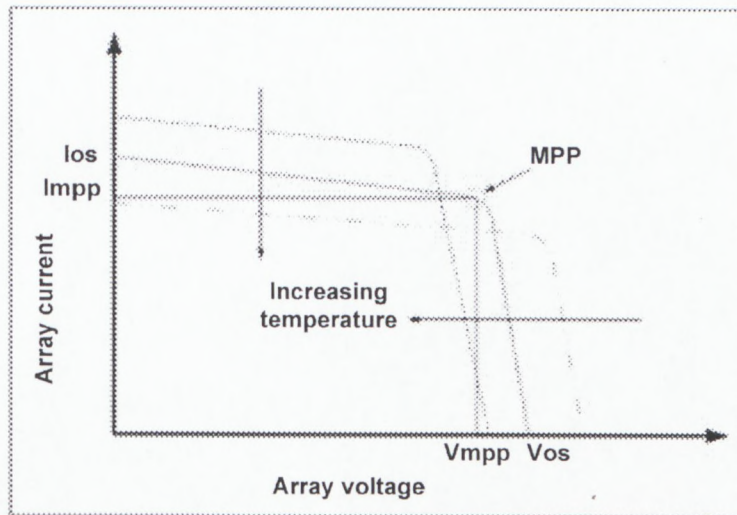


Figure 2.11: MPP characteristic curve
 (Adapted from Kaltschmitt, Streicher & Wiese, 2007:240)

2.3.5 Nuclear power

Nuclear energy systems have provided another source of electrical power for satellites since the 1960s.

Two technologies, which are currently available for space uses of thermal energy liberated by nuclear processes, are radioisotope thermoelectric generators (RTGs) and nuclear reactors.

RTGs utilise the heat released in the spontaneous decay of radioisotopes, specifically Plutonium-238. Nuclear reactors exploit the controlled fission of heavy nuclei (such as Uranium-235) in a sustained neutron chain reaction of the two technologies, and RTGs are generally used when power requirements are below 1 kWe (Eisenbud & Gesell, 1997:325).

The advantages of using nuclear energy sources are:

- Compact size;
- Low-to-moderate mass;
- Viability in hostile environments; and
- Independence of distance and orientation to the sun and high reliability.

When power requirements exceed the hundreds of kilowatts (kW) for an extended period, nuclear energy is the only realistic power option.

2.3.6 Heat generator

The heat generator is also a source of satellite power, which uses heat energy in solar radiation to generate electricity. A parabolic dish of mirrors reflects heat energy of solar radiation through a boiler, which in turn feeds a generator and converts solar energy into electrical power. This mode of power generation is new and efficient only if the satellite is exposed to solar radiation. The heat generator can also be used in conjunction with rechargeable batteries (Maini & Agrawal, 2011:143).

2.4 Working environmental

The space within the satellites consists of degrading environmental conditions such as high temperatures, high ultraviolet ranges, high electric charges, and so on. Despite these conditions, satellites are supposed to perform its operations, whilst respecting its orbital trajectory.

2.4.1 Orbits

The orbits of satellites have numerous forms and orientations; some are circular and others have elongated ellipse forms. These orbits can be located at low altitude just above the earth's atmosphere, approximately 250 km of the altitude or exceed 30000 km. The orbit of a satellite is chosen to respond to the best of the mission's needs (Montenbruck & Eberhard, 2005:2).

2.4.1.1 Kepler's law

The celestial mechanics took its modern face based on the work of Kepler in 1609. His work was based on measurements that were made by Tycho Brahe on Planet Mars. The following are three Kepler's laws:

- The orbits of a satellite around the earth are ellipses, which the earth occupies;
- The areas swept by the vector of the earth and the satellite are identical for the same duration; and
- The squares of the times revolution are proportional to the cube of the semi-major axis of the orbit.

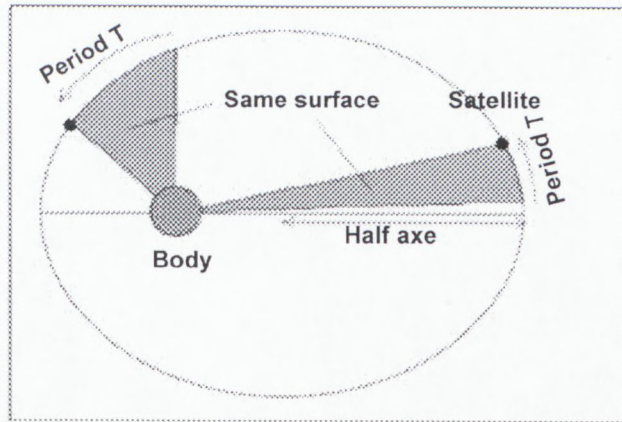


Figure 2.12: Illustration of Kepler's three laws
(Maral, Bousquet & Sun, 2009:19)

2.4.1.2 The earth in space

The earth is a sphere, which is slightly flattened at the poles with an equatorial diameter of 6370 km. The earth makes a complete rotation on itself in 23 hours 56 minutes, hence called sidereal day. The moon, its natural satellite is situated at 380,000 km above the earth, and rotates on itself and around the earth in 28 earth days (Green, 1985).

The earth is surrounded by two belts called Van Allen in the magnetosphere at 5,000 km and 20,000 km of altitudes, which push satellites into their orbits. The Van Allen belts were discovered by a man of the same name following the launch of the satellite Explorer 1 in January 1958, and consist of charged particles and radioactive energy that are trapped in the magnetic structure created by the earth magnetic field (Maral *et al.*, 2009:28).

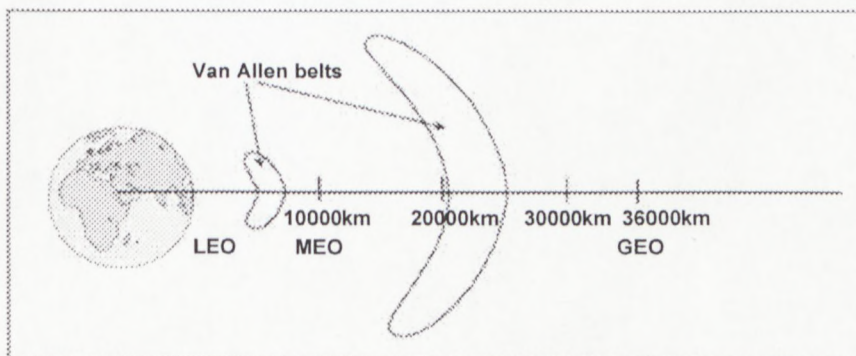


Figure 2.13: Representation of Van Allen belts in the magnetosphere
(Adapted from Edward, 1887:37)

2.4.1.3 Types of orbits

The orbits of satellite systems are classified into four categories, which are:

- Low earth orbit;
- Polar orbit;
- Geosynchronous orbit; and
- Geostationary orbit.

❖ Low earth orbit (LEO)

The low earth orbit is located just above the earth's atmosphere at an altitude where the atmosphere force does not hinder the speed of satellite too much (by convention, the low orbit is located at an altitude of less than 2 000 km) (Montenbruck & Eberhard, 2005: 2). One rocket requires less power to place a satellite on LEO orbit. The LEO orbit is used by scientific satellites to explore deep space.

The Hubble Space Telescope, for example, is located at 610 km of LEO's orbit, as well as other missions such as amateur radio satellites, the constellations of mobile telephony and remote sensing terrestrial (the A-train) (Ali, 2002).

❖ Polar orbit

Polar orbit is a circular low orbit, which is situated by convention between 300 and 1 000 km altitude with the inclination angle close to 90°, whereby satellites pass above or near the poles. Because of the rotation of the earth, every satellite located on a polar orbit passes regularly above all the points of the surface. The polar orbits are generally sun-synchronous orbits. This type of orbit retains a constant angle in a direction of sun-earth, which means that the orbit turns 360° per year. Sun-synchronous orbits allow satellites to move at the same solar time above a given place. This characteristic makes it an orbit that is ideal for satellite observation of the earth (for example, meteorological satellites).

The rotation of the orbit is done naturally by using orbit disruption that is generated by the flattening of the terrestrial globe. The orbit midi/midnight is a particular case of sun-synchronous orbit where the solar time that sets the passage is around noon or midnight for the longitudes of the equator. The orbit twilight in a similar way, is a sun-synchronous orbit whose time fixed solar crossing coincides with the lift or the sunset (Barrett & Curtis, 1999:91).

❖ **Geosynchronous orbit**

Earth-synchronous or geosynchronous satellites are placed into orbit so that their rotation period matches exactly with the earth's rotation (the period is 24 hours a day to make one rotation). However, the plane of geosynchronous orbit is generally not the equatorial plane. Apart from geostationary satellites, as explained below, the satellites at this orbit are used for communications at high latitudes, particularly in Russia and Canada. The satellites are placed in highly elliptical orbits, which enable them to appear to hover above one point on the earth for most of the day. In twenty four hours, the satellites move over the earth in a figure of eight pattern, which is centred on a fixed longitude. When activities are intense, the satellites move slowly and quick movement occurs in less activity (Bagad & Chitode, 2007:273).

❖ **Geostationary orbit**

The geostationary orbit (also called Clarke) is a circular orbit, which is located in the plane of the equator to an altitude of 35 786 km above the earth with a radius of 42 164 km. At this altitude, the period of revolution of the satellite corresponds exactly to the period of rotation of the earth, or 23 hours, 56 minutes and 4 seconds (24 hours). With regard to the earth, a geostationary satellite seems still in the sky, which makes it a perfect orbit for the telecommunications satellites and for some satellites of observation (for example, weather), which must cover a fixed area. Three geostationary satellites are sufficient for the whole of the earth's surface. The launch of a geostationary satellite requires altitude, which is a powerful launcher.

For telecommunications, the distance crossed by a signal transitted through this type of satellite creates a perceptible delay by a user. Telecommunications satellites, which do not follow this type of orbit, are called scrolling satellites (Montenbruck & Eberhard, 2005:4).

2.4.2 Cosmological radiation

Radiation energy affects electronic and other technological equipment, which are exposed to it, as well as the cells of human beings. The term radiation, which is cited here, refers to the space of electromagnetic waves that consist of electrons, photons and neutrons.

Interaction with these waves may amend the chemical composition of the devices and also that of the atmosphere. The continuous flux of cosmic radiation from the outside of the solar system, the transitional flux produced by the sun and the variation of space weather conditions, therefore, affect the technology and life of the systems that are not protected by the atmosphere and the magnetic field of the earth (Jones, Lambourne and Adams, 2004:417).

The design of a linear power control system must be made resistant against various types of shocks (damages) that it could be subjected to. A degree of perfection of EPS requirements depend on the evolution and period of the intensity of particles and the number of solar events, as well as the phase of the solar cycle. The operation of the satellite on the atmosphere is also affected by energetic particles. These particles modify the state of the atmosphere, particularly in the polar atmosphere, where the space is less protected by the magnetic field of the earth. A majority of protons moderate with energy, and penetrate the object at altitudes that are low enough of about 50 to 70 km above sea level (Kusky, 2010:174).

2.5 Chapter summary

This chapter has detailed the basic definitions of space and satellite. Satellite links and orbits were classified. The road map of satellites was also discussed with emphasis applications. The advantages of satellite electrical power systems were also brought out with comments on different types of electrical power generations.

CHAPTER THREE LINEAR POWER CONTROL SYSTEM

3.1 Introduction

LPCS is a nanosatellite's EPS, which is designed to provide electrical power that is required by a nanosatellite. Its major function is to capture solar energy from the sun and albedo with solar panels during daylight, store a portion of the energy into rechargeable batteries, and then supply it to the satellite subsystems and payload. The LPCS employs the required techniques to provide permanent electrical energy to a nanosatellite.

This chapter covers two important points of the research, namely the theoretical and design considerations. The theoretical consideration describes the methods and techniques that are used when designing electrical power systems of satellites, while design consideration explains the physical developments of the entire project, as well as the calculations.

3.2 Theoretical consideration

The theoretical consideration describes the techniques used and lists the important aspects considered in developing electrical power systems for nanosatellites. Two major techniques, which are commonly used in satellite electrical power systems are the maximum power point tracking (MPPT) and the direct energy transfer (DET) (Wertz & Larson, 1999: 425). Selection of one of the above techniques depends on the mission of what the satellite is designed for and its size. A majority of satellites use the MPPT technique to obtain maximum power from the solar cells by using a microcontroller as a tracking device.

However, for more reliability, the microcontroller is not a suitable device to use in satellite applications but it is also difficult to track maximum energy called maximum power point (MPP) of the solar cells without a microcontroller. Building the analogue MPPT system is another option, but this technique requires the presence of discrete components. To limit the system operating frequency requires the use of bulky electronic components such as inductors and capacitors. This is not acceptable because of the size and weight of the nanosatellite. Unlike the MPPT, the DET directly connects solar cells to the load. This technique works on a fixed working point on current-voltage characteristic and responds to all small satellites electrical power generation requirements with high efficiency and reliability.

Based on the constraints of the MPPT technique, the LPCS adopts the second technique, which is DET for its simplicity and reliability. Redundancy is also employed to maintain the fidelity of the system.

3.2.1 Electrical power system

The LPCS provides permanent electrical power to operate nanosatellites' payload and subsystems by using solar cells, rechargeable batteries and controllers. In space, solar panels generate the electrical power from the sun's rays and albedo. This power is usually produced during the day. At night, there is no way to produce power because of the absence of solar radiations in spite of the presence of infrared rays, which are emitted by the earth and, which are often exploited, but with a lower performance (Graham & Turk, 2006:456)

During the supply process, some energy is stored into batteries in order to continuously provide electrical power to the satellite in the dark or peak period. In summary, the most important functions of the LPCS are:

- To generate electrical power;
- To store this electrical power; and
- To protect and distribute this stored power.

3.2.2 Types of electrical power systems

The aim of the electrical power system for satellites is to change from one form of energy into another form. This process of changing the state of the energy is called power conversion (Mohan, Undeland & Robbins, 2003:1). The power conversion system consists of the input, output and controller. The two power system topologies are:

- Switch mode power systems; and
- Linear power systems.

3.3 Switch mode power systems

Switch mode power systems are electronic power converters that incorporate switched regulators in order to be highly efficient in the conversion of electrical power. These power converters are used in many appliances such as computers, television sets, stereo systems, aerospace systems and so on, where weight is an important consideration. In fact, a majority of modern consumer electronic devices use switch mode power systems (Pressman, 1992:10).

There are literally many different circuit configurations for switch mode power systems. However, all these configurations are classified into two basic categories, namely:

- Step-down or buck converters; and
- Step-up or boost converters.

Figure 3.1 below shows the basic layout of a switch mode power system. The input power to the converter can be an AC or DC source. For the AC source, the line power is first rectified and filtered and then fed to the converter input. For a DC source as a battery or solar cell, the unregulated power is directly fed to the converter input and then its output is directly connected to the load.

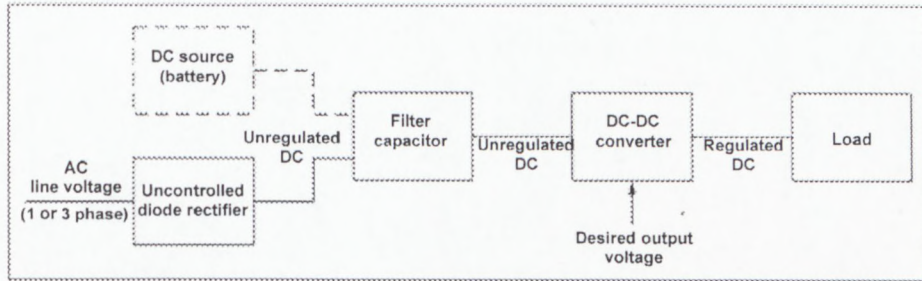


Figure 3.1: Basic layout structure of a typical DC-DC converter

In satellite's applications, switch mode power system topology is often recommended when the need of the current is greater than 5A (Pressman, 1992:9-10) and maximum energy from solar cells are required. The DC to DC power converter, known as maximum power point tracker (MPPT), is inserted into the system to stabilise electrical power from solar cells and then fed into the load.

This technique often poses problems of instability and interference to the loads. Employing this technique requires great attention not only in terms of frequency, but also in the use of microcontrollers. As mentioned earlier, it is possible to track the MPP with an analogue system, but it is not conceivable for the small satellite projects whereby size and weight are limiting factors. Moreover, the MPPT also requires redundancy circuits, which are avoided in the reliability system. The concept of this technique is illustrated in Figure 3.2 below, which shows all functional blocks.

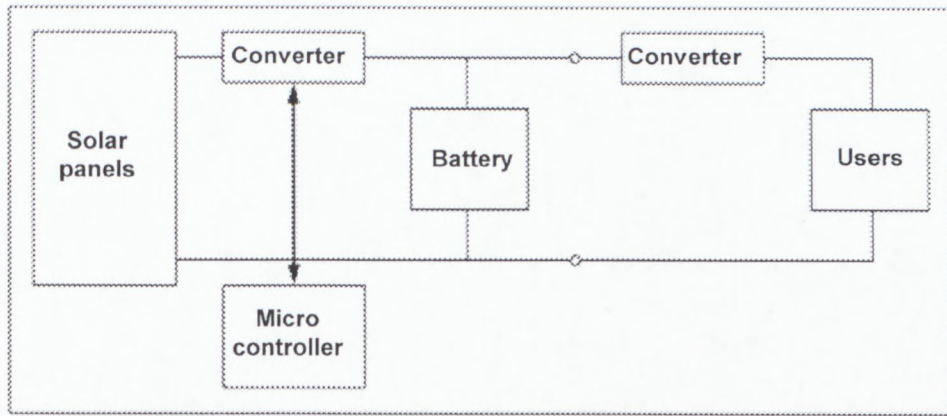


Figure 3.2: Basic block diagram of SMPS with MPPT
(Adapted from Jordan, 2006:17)

3.4 Linear power systems

Linear power systems, which are also called linear power regulators or voltage regulators, provide constant DC output voltages and contain circuitries that continuously hold the output voltages at desired values, regardless of changes in load current or input voltage (Pressman, 1992:4-9). Chester (2011) notes that linear power regulators operate by using voltage controlled current sources to force fixed voltages to appear at the regulators output terminals. Figure 3.3 below shows the basic functional block diagram of linear power regulators.

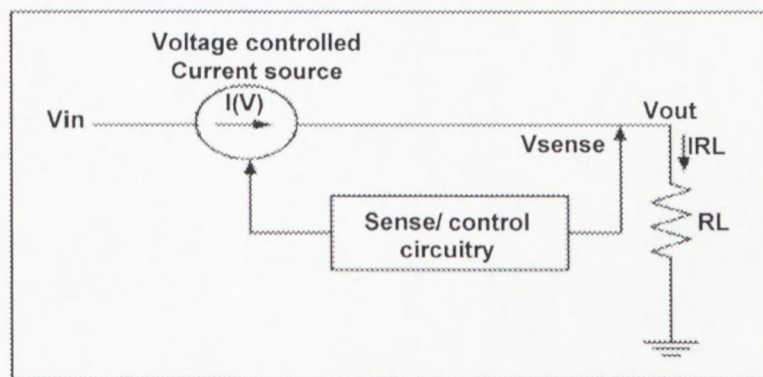


Figure 3.3: Linear power regulator functional diagram
(Adapted from Mohan *et al.*, 2003:3)

In the diagram, the control circuitry is incorporated to monitor the output voltage and to adjust the required load current source to hold the output voltage at the desired value.

The design of the current limiting source defines the maximum load current that the regulator can source, and still maintain regulation. The output voltage is controlled by using a feedback loop circuitry.

The linear power regulators require lagging times to correct the output voltages after changes in the load current demand. This lagging time defines the characteristic that is called a transient response, which is a measure of how fast the regulator returns to steady-state conditions after a load change (Chester, 2011). The schematic diagram in Figure 3.4 below details the operational function of the control loop of all linear power regulator types.

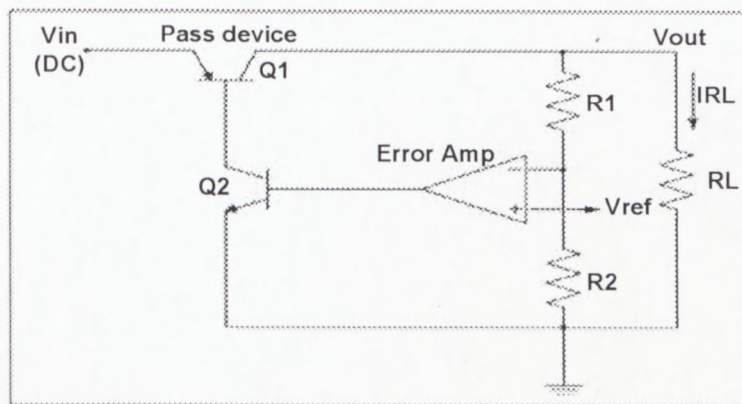


Figure 3.4: Diagram of a typical linear power regulator
(Adapted from Mohan *et al.*, 2003:4)

The regulator's pass device Q1 is a PNP transistor. In the regulator the current flowing out of the collector of the pass transistor, which is also the load current, is controlled by Q2 and the voltage error amplifier. The feedback loop that controls the output voltage is obtained by using R1 and R2 to monitor the output voltage, whilst applying this voltage to the inverting input of the voltage error amplifier. The current through the resistive divider R1 and R2 is assumed to be negligible compared to the load current. The non-inverting input of the voltage error amplifier is connected to a reference voltage to adjust its output voltage and the current through Q1 and to force the voltages at its inputs to be equal. The major role of a feedback loop in this schematic representation is to continuously hold the regulated output voltage at a fixed value, regardless of changes in load current.

3.4.1 Types of linear power regulators

The following are three basic types of linear power regulators:

- Standard power regulator;
- Low Dropout or LDO power regulator; and
- Quasi LDO power regulator.

The operation of the three regulators is almost the same, but the two important differences between them are that the dropout voltage is defined as the minimum voltage drop, which is required across the regulator to maintain output voltage regulation, and the ground pin current, which is required by the regulator when driving rated load current. Increased ground pin current is unwanted in the circuit because of a waste of energy. It is important to note that the linear regulator operation with the smallest voltage across dissipates the least internal power and has the highest efficiency (Rashid, 2010:249).

3.4.1.1 Standard power regulator

The standard power regulator is the first voltage regulator that was made and which used NPN Darlington configuration as a pass device (see Figure 3.5 below).

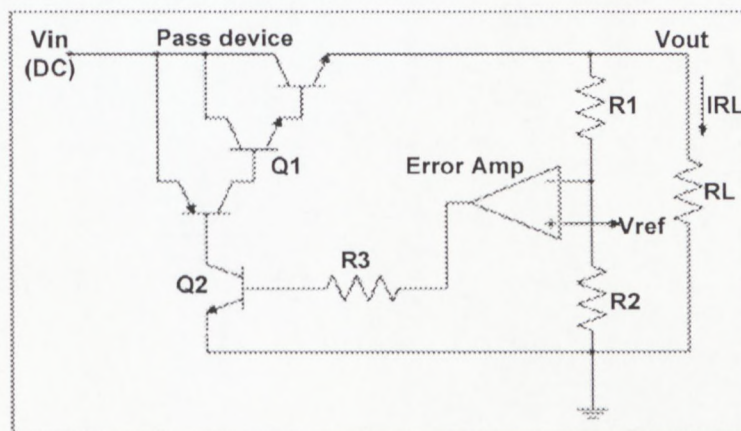


Figure 3.5: Standard power regulator circuit diagram
(Adapted from Chester, 2011)

In order to maintain a constant output voltage in the standard power regulator's topology, the minimum dropout voltage (ranged between 1.5 and 3V) across the pass transistor, should be determined by using the following equation:

$$V_{D(MIN)} = 2V_{BE} + V_{CE}$$

Equation 3.1

The ground pin current of this power regulator is low (around 10mA). The reason for this is that the current through the base of the pass transistor is equal to the load current divided by the gain of the pass device. The network of the pass device is composed of one PNP and two NPN transistors, which means that the total current gain is extremely high (≥ 300), resulting in little current, which is necessary to drive the base of the pass transistor and less power dissipation. This makes the standard power regulator the lowest power dissipated regulator in terms of current (Chester, 2011).

3.4.1.2 Low dropout power regulator

The low-dropout power regulator (LDO) comprises only one PNP transistor, as illustrated in Figure 3.6 below. The minimum voltage dropout across the regulator to maintain regulation value is merely the voltage across the PNP transistor, which is given in the following equation:

$$V_{D(MIN)} = V_{CE} \quad \text{Equation 3.2}$$

The maximum specified dropout voltage across the pass transistor in LDO power regulator is usually about 0.7V to 0.8V at full current with typical values around 0.6V.

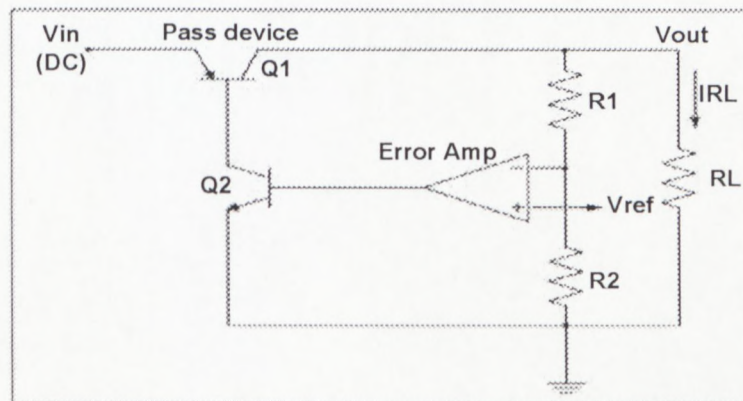


Figure 3.6: LDO power regulator circuit diagram
(Adapted from Chester, 2011)

The dropout voltage is directly related to load current, which means that at low values of load current the dropout voltage may be as little as 50 mV. Therefore, the LDO power regulator is the best power regulator in terms of the output voltage. Its ground pin current is approximately equal to the load current divided by the gain of the pass transistor. This is higher (approximately 45mA), compared to the standard power regulator (Chester, 2011).

3.4.1.3 Quasi low dropout power regulator

Illustrated in Figure 3.7, the quasi low dropout power regulator is a variation of the standard power regulator, which uses an NPN and PNP transistor as pass devices. The minimum voltage dropout across pass devices to maintain regulation is given in equation 3.3 and its maximum dropout voltage is rated at about 1.5V.

$$V_{D(MIN)} = V_{BE} + V_{CE}$$

Equation 3.3

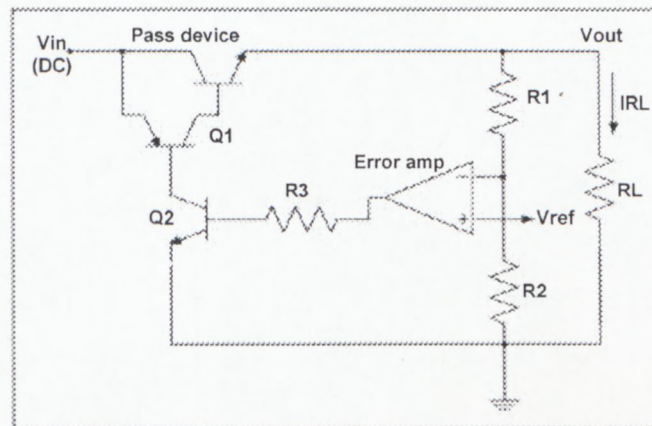
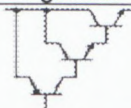
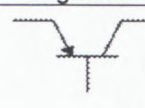
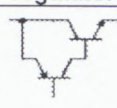


Figure 3.7: Quasi LDO power regulator circuit diagram
(Adapted from Chester, 2011)

The dropout voltage of quasi LDO power regulator depends on the temperature and the load current, since the expected voltage value cannot go lower than about 0.9V at 25°C even if the light load is connected. The dropout voltage of quasi-LDO is higher compared to the LDO power regulator and lowers than the standard power regulator. The ground pin current of the quasi-LDO is fairly low ($\leq 10\text{mA}$), which is as good as the standard power regulator (Chester, 2011). The summary of the three linear power regulators is given in Table 3.1 below.

Table 3.1: Summary of the three types of linear power regulators

Type	Standard power regulator	LDO power regulator	Quasi-LDO power regulator
Circuit configuration			
Voltage dropout limit	$V_{D(MIN)} = 2V_{BE} + V_{CE}$ ~ 1.7V to 2.5V	$V_{D(MIN)} = V_{CE}$ ~ 0.1V to 0.7V	$V_{D(MIN)} = V_{BE} + V_{CE}$ ~ 0.9V to 1.5V
Ground pin current limit	$I_G = \frac{I_L}{\beta}$; ($\beta \geq 300$) $I_G \leq 10 \text{ mA}$	$I_G = \frac{I_L}{\beta}$; ($\beta \leq 30$) $I_G \leq 20 \text{ to } 40 \text{ mA}$	$I_G = \frac{I_L}{\beta}$; ($\beta \geq 250$) $I_G \leq 10 \text{ mA}$
Maximum load current	$I_{L(MAX)} = 10A$	$I_{L(MAX)} = 1A$	$I_{L(MAX)} = 7.5A$
Advantages	Low cost and high load current.	Less dropout voltage across the regulator ($\geq 0.7V$) and cost savings.	High load current and better than LDO regulator.
Disadvantages	High dropout voltage across the regulator ($\leq 2.5V$).	Low load current.	High dropout voltage across the regulator ($\geq 1.5V$). better than standard regulator

3.4.2 Power regulator selections

The following requirements should be evaluated in order to choose the best regulator for a specific application:

- Maximum load current;
- Input voltage;
- Output voltage precision (Tolerance); and
- Quiescent current.

3.4.2.1 Maximum load current

In the process of selecting a type of power regulator for a specific application, a careful consideration of maximum load current is required. The selected power regulator should be able to provide sufficient current to the load under worst-case operating conditions, if the system performance should be reliable.

3.4.2.2 Input voltage

The source of electrical energy influences, which type of power regulator is best suited for a specific application; for example, in solar and battery-powered applications, the LDO and/or the quasi-LDO power regulators are the best choice because of their low dropout voltages that reduce the number of cells, which result in cost saving.

3.4.2.3 Output voltage precision (tolerance)

According to Chester (2011), "The nominal regulated output tolerances have to be approximately 5%". This level of accuracy is adequate for most applications. Apart from this specification, many new regulators have tighter output tolerances (better than 2%), and separate output specifications that cover room temperature with full operating temperature ranges and full-load and or light-load conditions (Chester, 2011).

3.4.2.4 Quiescent current

The quiescent current is current, which is drawn by the circuit at open-circuit conditions. This current determines the working life of the system by showing either that the source can be shut down or does not deliver significant amounts of current to the load. This is important in solar and battery powered applications.

The quiescent currents that most LDO power regulators have optimised are limited between 75 to 150mA, and provide significant improvement over other power regulators, which draw several milliamps (Chester, 2011).

3.4.3 Protection circuits

Apart from the requirements listed above, protection is the most important part that should be added to the list. Linear power regulators require protection circuits to make them virtually immune to damage from both excessive load currents and high operating temperatures (Rashid, 2010:249). The following are three major protection circuits, which are incorporated into regulators:

- Thermal shutdown;
- Current limiting; and
- Voltage error amplifier.

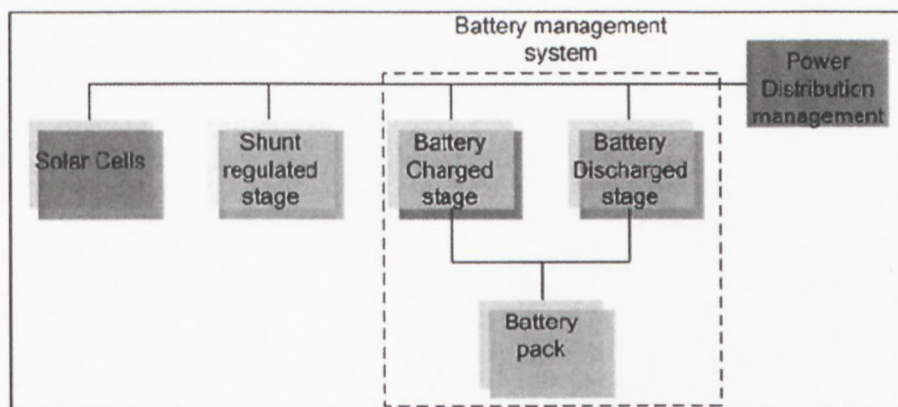
These circuits comprise the three distinct and separate control loops with a definite hierarchy that allows one to override the other. In other words, the power regulator will operate in constant voltage mode, where the voltage error amplifier regulates the output voltage to a fixed value. This is true only when both the load current and junction temperature are at accurate or below their limit threshold values. If the load current increases, the current limiting circuitry will override the voltage error amplifier, and force the load current to set the limiting value. The voltage error amplifier will take over only if the current limiting circuits to release control, which means that the load current is sufficiently reduced. The same concept is also applied for temperature. If the temperature approaches the limit threshold (approximately at 160°C), the thermal shutdown will cut driving the power transistor, thereby reducing load current and internal power dissipation (Rashid, 2010:249).

Power regulators hold their output voltages at fixed only when they are in constant voltage mode. In current limiting, the output voltage will be reduced as required to hold the load current at the set limiting value. In thermal limiting, the output voltage drops and the load current can be reduced to any value (including zero) (Chester, 2011). Based on this information, the LDO power regulator is the selected linear power regulator for this research because of its low dropout voltage and its best performance.

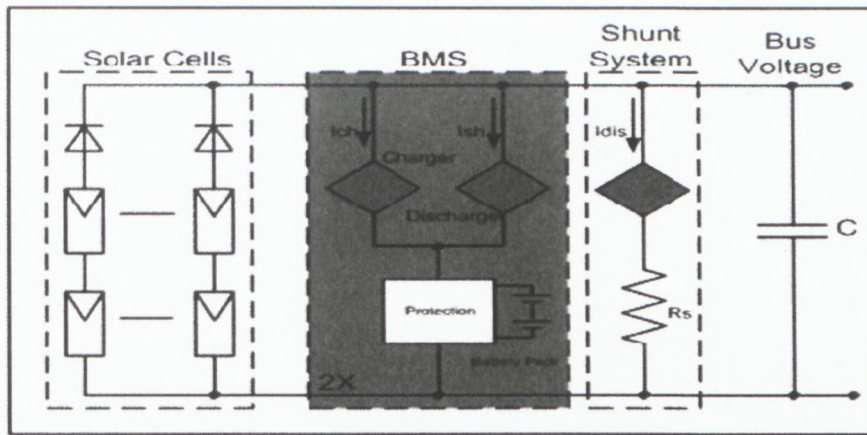
3.5 Selection of the design configuration

The selection of the topology depends on the mission that the satellite is expected to perform. During the mission, the satellite will be exposed to violating phenomena that can cause failure. Hence, the design of the LPCS should be simple and robust to withstand all attacks encountered in the space environment such as temperature, radiations, and especially hostile vacuum. The suggested architecture is illustrated in Figure 3.8 (a & b) below and consists of the following main parts:

- Solar cells;
- Shunt regulated stage;
- Battery management system; and
- Power distribution management.



(a) LPCS block diagram



(b) Fixed working point architecture

Figure 3.8: System configuration of the LPCS

(Adapted from Jordan, 2006:21)

The basic operation of the LPCS is in fact based on the parts named above. The system uses the technique in which the battery pack is directly connected with solar panels via a battery management system. This technique is called direct energy transfer (DET). Solar cells are arranged in a series-parallel configuration to produce the required power for the entire satellite.

The shunt regulated system is employed as a control to bypass the excess power from batteries, and/or when the bus voltage exceeds the threshold value. The battery charged and discharged stages are also used to control voltage levels of batteries to prevent the occurrence of overcharging or undercharging conditions. In order to increase the reliability in the system, it was decided to place a redundancy in the design. Below is another representation of the architecture.

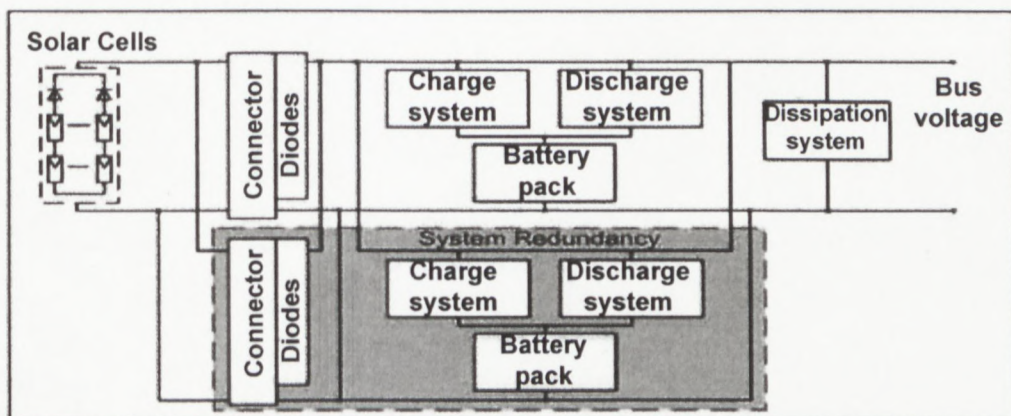


Figure 3.9: System configuration of the LPCS with redundancy

(Adapted from Jordan, 2006:22)

3.6 Design consideration

Designing the electrical power system for a nanosatellite is challenging, since the only energy source that is available is the sun. The area of solar panels is the most important factor, which determines the available power for the satellite. With its small surface, the available power that is provided by the solar panels is limited. Another problem with nanosatellite is the unavailable surface for payloads such as sensors, probes, antennas and so on. These payloads also need space for them to function, thus the available area for solar cells is a problem.

Conversely, the design technology of semiconductors goes faster compared to solar cells, which present another problem. In practice, if many payloads are integrated into the system, the huge demand for electrical power will be observed during the mission. The growth of solar cell technology is not faster to provide higher efficiency cells required to power all payloads. Presently, the greater solar efficiency in the market is 28.3%, Ultra Triple Junction (UTJ) GaAs cells manufacturing by Spectrolab (USA).

With these constraints in mind, the LPCS attempts to maximise the overall efficiency of the power system. The design of the LPCS is dedicated for nanosatellites of the masses, which range from 5 kg to 10 kg, and whereby the solar panels will be body-mounted on all six sides. This configuration guarantees the presence of electrical power, while the satellite is in the sun's view. In addition to the body-mounted panel configuration, the deployable panels can also be added, but should be budgeted.

The system uses the direct energy transfer technique with a robust battery pack. Both solar cells and batteries are well sized in order to provide necessary power to the payloads and other components during daylight and eclipse periods.

Once orbiting the earth, battery cycles vary, therefore, a vigilant charge and discharge management is carefully implemented for proper battery maintenance. In order to simplify the design and to save hardware, charge will be regulated by using shunt systems to prevent an overcharged state from occurring.

The LPCS provides three different output voltages to the nanosatellite modules. The first output voltage is a 12V unregulated bus voltage. This voltage is the battery voltage and is used by the modules to generate voltages that are required only by them. The remaining two voltages are regulated at 5V and 3.3V, respectively. These two voltages are implemented by using high-efficiency DC/DC converters.

The main motivation of the research is to design a high-efficiency independent system that will provide the required power to sustain a meaningful operation of a nanosatellite by providing the accurate control for operation consideration, as stipulated in sections 1.3 and 1.6.

3.6.1 Solar panels

One of the main sources of satellite electrical power systems is solar panel. Solar panel is composed of a number of photovoltaic cells that are connected in a series-parallel shape. These photovoltaic cells convert the solar energy directly to the electrical energy for use while the satellite is illuminated. This energy is stored in a storage element, which supplements the solar panel during shadow or eclipse periods.

Figure 3.10 below shows the series-parallel arrangement of solar cells. This arrangement is lay down in order to augment power level (voltage and current) after the setup of the power budget, which was discussed in section 3.4.5.

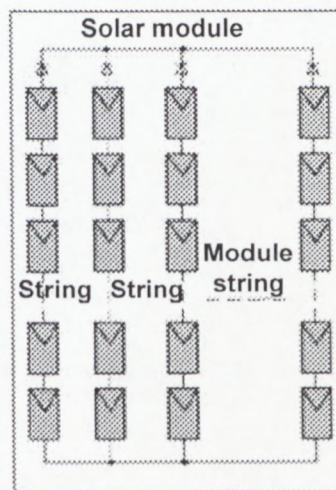


Figure 3.10: Series-parallel arrangement of solar cells

The important considerations for how much power the LPCS will collect during its orbit include the size of solar cells, nominal photovoltaic cell efficiency, and the length of eclipse periods. These considerations are dependent on the following factors, which are solar intensity variations, solar incidence angle, thermal considerations and radiation effects during the satellite's lifetime.

3.6.1.1 Solar panel's size

Sizing solar panels take two basic approaches. The first approach is given by equation 3.4, and is followed by the equation 3.5.

$$P_{scell} = \frac{\frac{P_e T_e}{X_e} + \frac{P_d T_d}{X_d}}{T_e} \quad \text{Equation 3.4}$$

$$P_o = S \times \eta_{Cell} \left[\frac{\text{Watts}}{\text{Area}} \right] \quad \text{Equation 3.5}$$

The amount of power per unit area, P_o , is the product of solar intensity (S) and the nominal solar cell efficiency (η_{Cell}). Due to the alteration of solar intensity and the degradation of solar cell efficiency over time by the thermal cycling in and out of eclipses, micrometeoroid strikes, plume impingement from thrusters, and material out gassing, the change in the nominal efficiency can be observed (Melone, 2009:44-170). This change results in an end of life (EOL) value for P_o denoted P_{EOL} . The required area is then given in equation 3.6 (Wertz & Larson, 1999).

$$A_{scell} = \frac{P_{scell}}{P_{EOL}} \text{ [Area]} \quad \text{Equation 3.6}$$

This approach is valuable mostly for the design of satellites that are independent of the size and orientation of solar panels. The second approach is used when size, mass, and deployment vehicle (for example the PPOD) and volume are required for the design. In this case, the design of solar panels should be properly investigated in order to optimise the maximum area available for solar power collection. The LPCS project uses a combination of both approaches with an emphasis on the latter.

Although several different solar panel configurations were investigated, the body-mounted structure was selected because of its advantage in power area ratio. Figure 3.11 below shows the proposed structural design for the LPCS system.

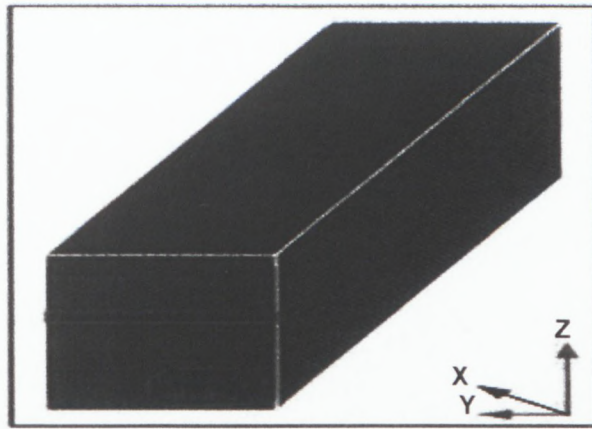


Figure 3.11: Proposed structural design for LPCS system

The idea of the above structure was taken from the paper of Chad W. Melone (Melone, 2009:4). The structure is a shape of a 6 unit nanosatellite and 3 coordinate axes. The absolute outer dimensions of X faces are 21.35 cm in width and 34.6 cm in height, resulting in a total surface for each face of approximately 740 cm^2 . Doubling this comprises $1,480 \text{ cm}^2$. The surface should be adjusted down to leave some space for payloads. Assuming that the surface that payloads can occupy is about 28 cm^2 , subtracting this area from the outer dimensions, results in approximately $1,450 \text{ cm}^2$. When one adds Z face dimensions ($\approx 197 \text{ cm}^2$), the total surface available to place solar cells is about $1,650 \text{ cm}^2$. This surface is big enough to supply nanosatellite missions by using the direct energy transfer technique.

3.6.1.2 Cell alternatives

The two popular satellite photovoltaic cell manufacturers are Emcore Corporation (Albuquerque, New Mexico, US) and Spectrolab Incorporated (Sylmar, California, US). The PV product lines of these manufacturers are comparable in every way, including nominal efficiency, size, price, radiation degradation, thermal properties, and so on, as in Table 3.2. Their full specification sheets can be found in Appendix C.

Table 3.2: Comparison of Spectrolab Incorporated and Emcore Corporation nominal efficiencies

Company	Solar cell name	Nominal efficiency
Spectrolab Incorporated	Triple Junction solar cell	25.1%
	Improved Triple Junction (ITJ)	26.8%
	Ultra Triple Junction (UTJ)	28.3%
	NeXt Triple Junction (XTJ)	29.9%
Emcore Corporation	Advanced space solar cell (ATJM)	27%
	Advanced space solar cell (ATJ)	27.5%
	Space solar cell (BTJM)	28%
	Space solar cell (BTJ)	28.5%
	Space solar cell (ZTJM)	29%
	Space solar cell (ZTJ)	29.5%

Regarding power, mass, cost and area requirements for nanosatellites, traditional silicon solar cells are increasingly being replaced by high efficiency multi-junction solar cells on space solar generators, as tabulated above. The selected solar cells for this research are high efficiency triple junction' cells (UTJ), with an average efficiency of 28.3 % at the beginning of life (BOL), as illustrated in Figure 3.12 below.

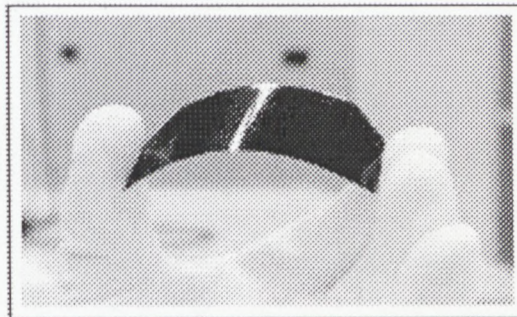


Figure 3.12: High efficiency triple junction space solar cell developed on an ultra thin Ge substrate

(Adapted from Jordan, 2006)

The design specifications of UTJ solar cell, including the mechanical data, the electrical data and temperature gradients, are given in Tables 3.3 and 3.5 below.

Table 3.3: Mechanical design specification of UTJ solar cell (Spectrolab datasheet)

Designation	Quantity
Dimension	6,89 × 39,5 cm
Cell area	27,216 cm ²
Average weight	2,3 g

Table 3.4: Electrical design specification of UTJ solar cell (Spectrolab datasheet)

Designation	Symbol	Unit	BOL @ 28,3 °C
Average open circuit	V_{OC}	[V]	2,665
Average short circuit	I_{SC}	[A]	0,464
Voltage at max power	$V_{P_{max}}$	[V]	2,350
Current at max power	$I_{P_{max}}$	[A]	0,444
Load voltage	V_{Load}	[V]	2,310
Maximum power	P_{max}	[W]	1,043
Average efficiency	η	[%]	28,3
Average load efficiency	η	[%]	28

Table 3.5: Temperature gradients specification of UTJ solar cell (Spectrolab datasheet)

Designation	Unit	BOL	5×10^{14} (1 MeV e/cm ²)
dV_{OC}/dT	[mV/°C]	- 5,9	- 6,3
dI_{SC}/dT	[mA/°C]	0,136	0,163
$dV_{P_{max}}/dT$	[mV/°C]	- 6,5	- 6,7
dP_{max}/dT	[mW/°C]	2,72	=//=

3.6.1.3 Radiation impacts

The European Space Agency (ESA), under its Space Environment Information System (SPENVIS), provided a modelling tool to predict the electron value (1 MeV electron) that experiences solar cells once in the orbits. This value is compared with a solar cell manufacturer's stated radiation degradation coefficients to determine effective solar cell efficiency. The comparison of the electron value with that of the cell manufactured can be done only when the operational orbit is designated; for this research, a 500 km circular orbit was considered with an approximate inclination angle of 98°. The output fluence values that SPENVIS gave goes up to a maximum thirty-day period. These values multiply by twelve results to the fluence values of the power system for a one-year mission.

Since the research is based on global information of the electrical power system, both solar minimums and maximums were considered. Table 3.6a and b, taken from Melone (2009:28), claimed that the 1 MeV equivalent electron values for both cases and all their information references to a thickness of a cover-glass, as shown in the leftmost column.

These fluence values are referred to in terms of the following parameters:

- Maximum power (P_{max}) of the solar cell;
- Open circuit voltage (V_{OC}) of the solar cell; and
- Short circuit current (I_{SC}) of the solar cell.

Table 3.6a and b: Summary of 1 MeV equivalent Electron Fluence (cm⁻²) at solar maximum and minimum (Melone, 2009:28)

Coverglass thickness			Total			Trapped Electrons			Trapped Protons		
g (cm ⁻²)	mils	micron	P _{max}	V _{OC}	I _{sc}	P _{max}	V _{OC}	I _{sc}	P _{max}	V _{OC}	I _{sc}
0	0	0	1.13E+15	1.32E+15	1.57E+15			1.57E+12	1.13E+15	1.32E+15	1.57E+15
0.0056	1	25.41	1.08E+13	1.24E+13	1.04E+13			1.36E+12	9.43E+12	1.11E+13	8.98E+12
0.0168	3	76.36	4.66E+12	5.27E+12	3.49E+12			1.15E+12	3.51E+12	4.12E+12	2.34E+12
0.0335	6	152.27	3.43E+12	3.43E+12	2.32E+12			9.54E+11	2.48E+12	2.90E+12	1.37E+12
0.0671	12	305	2.68E+12	3.02E+12	1.66E+12			7.15E+11	1.97E+12	2.30E+12	9.50E+11
0.112	20	509.09	2.22E+12	2.52E+12	1.28E+12			5.31E+11	1.69E+15	1.98E+12	7.50E+11
0.1675	30	761.36	1.90E+12	2.16E+12	1.00E+12			3.91E+11	1.51E+12	1.77E+12	6.09E+11
0.335	60	1522.73	1.48E+12	1.71E+12	6.78E+11			1.86E+11	1.30E+12	1.52E+12	4.93E+11

Coverglass thickness			Total			Trapped Electrons			Trapped Protons		
g (cm ⁻²)	mils	micron	P _{max}	V _{OC}	I _{sc}	P _{max}	V _{OC}	I _{sc}	P _{max}	V _{OC}	I _{sc}
0	0	0	1.14E+15	1.34E+15	1.57E+15			8.01E+11	1.14E+15	1.34E+15	1.57E+15
0.0056	1	25.41	3.50E+13	4.09E+13	3.45E+13			7.07E+11	3.43E+13	4.02E+13	3.38E+12
0.0168	3	76.36	1.24E+13	1.45E+12	1.01E+13			6.06E+11	1.18E+13	1.39E+12	9.52E+12
0.0335	6	152.27	6.83E+12	7.92E+12	4.83E+12			5.07E+11	6.32E+12	7.42E+12	4.32E+12
0.0671	12	305	4.24E+12	4.90E+12	2.54E+12			3.85E+11	3.85E+12	4.52E+12	2.16E+11
0.112	20	509.09	3.24E+12	3.75E+12	1.75E+12			2.88E+11	2.95E+15	3.46E+12	1.46E+11
0.1675	30	761.36	2.69E+12	3.11E+12	1.28E+12			2.17E+11	2.48E+12	2.90E+12	1.07E+11
0.335	60	1522.73	2.13E+12	2.48E+12	9.06E+11			9.91E+10	2.03E+12	2.38E+12	8.07E+11

The comparison of Tables 3.6a and b shows that the proton fluence values are highest at solar minimum, while electron fluence values are highest at solar maximum. In Spectrolab's specification sheet of 28.3% efficiency cells, the radiation degradation coefficient begins at 1E+14 of 1MeV equivalent fluence. This is two orders of magnitude higher than the values for solar maximum and one order of magnitude greater than the values for solar minimum. Therefore, no radiation degradation adjustment should be made for the Spectrolab cells.

3.6.1.4 Thermal impacts

The efficiency of solar cells depends on the position or the time of the satellite in orbit (in dark or in light). In darkness, the efficiency is higher than in light. As the satellite leaves the dark, the efficiency decreases. When it is positioned under full sun, the efficiency becomes low.

According to Melone (2009: 29), "the non- body mounted flat solar cells in LEO have a typically temperature of 67 °C, while the body mounted solar cells heat up 5 °C more". Pearsall and Hill (2001: 28) state: "The efficiency of solar cells degrades by approximately 0.5% per degree when the temperature exceeds 28 °C". The analytical model can further refine these estimations.

The analytical model of the research is taken from pages 29 to 36 of Melone (2009:30-36). The model allows the determination of the design components, as well as their values, and all begin with these formulas:

$$T_{SCell} = \left[\frac{\alpha_F S \cos(\phi) + \alpha_b S a I F_a + \varepsilon_b E F_e - \eta f_p S \cos(\phi)}{(\varepsilon_f + \varepsilon_b) \sigma} \right]^{\frac{1}{4}} \quad \text{Equation 3.7}$$

$$F_a = F_e \cos(\beta) \cos(v) \quad \text{Equation 3.8}$$

$$F_e = \sin^2 \cos(\rho) \cos(\lambda) \quad \text{Equation 3.9}$$

Where:

- T_{SCell} : is solar cells temperature;
- α_F and α_E : are front and back sides' absorption of the cell, respectively;
- S : is the solar flux (power per unit area);
- ϕ : is the incidence angle of the sunlight;
- a : is a factor applied to the earth's thermal flux to approximate the albedo flux;
- F_a : is the product of multiple radian measured angles describing how much of the solar cell's area is pointing at the albedo of the earth;
- F_e : is the product of multiple radian measured angles describing how much of the solar cell's area is pointing at the earth;
- ε_F and ε_E : are front and back sides' emissions of the solar cell, respectively;
- E : is the earth flux (power per unit area);
- η : is the nominal solar cell efficiency;
- f_p : is the solar cell packing factor;
- β : is the angle the orbit plane makes with the sun direction unit vector;
- v : is an angle that defines where the satellite is in its orbit relative to the solar sub point;
- ρ : is the angular radius of the earth at the satellite's altitude;
- λ : is the incidence angle of the earth's thermal flux on the solar cell; and
- σ : is the Stefan-Boltzman constant.

As mentioned previously, the body-mounted is the selected configuration for the project, but the configuration causes the heat between the body and the solar cells, which is known as heat transfer. Hence, the appropriate margin is inserted in the design to prevent this phenomenon. This margin or packing factor cannot be higher than 93%. In this research 85% was applied. The value for the solar power per unit area varies with the position of earth in its orbit around the sun.

Donabedian and Gilmore (2003) assert that the highest value at winter time is 1,414 W/m², while the lowest value at summer is 1,322 W/m². These values are taken from the solar cell manufacture's specification sheet, as well as other additional values that are shown in Tables 3.7 to 3.9, including the nominal solar cell efficiency, the front side solar cell absorption value and the front side solar cell emitting value. The back sides values of the absorption and emission are chosen from this range (0.17 and 0.92) (Wertz & Larson, 1999: 28-40). The Stefan-Boltzman constant value is 5.67×10⁻⁸, while the sun incidence angle can be chosen from zero according to the orientation of the satellite.

The values of the albedo adjustment factor and the earth's thermal flux are 0.3 and 326 W/m² respectively. The beta angle is chosen to be zero, while the earth thermal flux angle begins at reasonable average value (≈45°). The satellite altitude sets the angular radius of the earth. In practice, the value of zero is chosen as the starting point of the satellite in its orbit, relative to the sub-solar point (ν) (Melone, 2009:31).

Table 3.7: Predicted Solar Cell Temperature in summer (Spectrolab) (Adapted from Melone, 2009:29)

Predicted Solar Cell Temperature in Summer				
Item	Equation	Symbol	SMAD	Source
Altitude		h	500	Given
Inclination of a satellite's orbit		i	1.6999507	Given
Solar/orbit angle		β	0	Given
Orbit angle from sub-solar point (SSP)		ν	0	Given
Radiator normal WRT Nadir		λ	0.7853982	Given
Earth angular radius	$\sin^{-1}(R_e/R_o)$	ρ	1.187	calcul
Earth view factor		F_e	0.608	calcul
Albedo view factor	$F_a = F_e \cos(\beta) \cos(\nu)$	F_a	0.6080385	calcul
Solar cell temperature (⁰ K)	$T_{Scell} = \left[\frac{\alpha_f S \cos(\phi) + \alpha_b S a l F_a + \epsilon_b E F_e - \eta f_p S \cos(\phi)}{(\epsilon_f + \epsilon_b) \sigma} \right]^{\frac{1}{4}}$	T_{Scell}		
Albedo		al	0.3	Given
Emissivity solar cell side		ϵ_f	0.85	Given
Emissivity back side		ϵ_b	0.92	Given
Front side absorption		α_f	0.92	Given
Back side absorption		α_b	0.17	Given
Cell packing factor		f_p	0.8	Given
Cell efficiency		η	0.251	Given
Max direct solar flux ~ W/m ²		S	1322	Given
Solar incidence angle (rad)		ϕ	0	Given
Max earth IP emission @ surface		E	326	Given
Solar cell temperature (⁰ K)	$T_{Scell} = \left[\frac{\alpha_f S \cos(\phi) + \alpha_b S a l F_a + \epsilon_b E F_e - \eta f_p S \cos(\phi)}{(\epsilon_f + \epsilon_b) \sigma} \right]^{\frac{1}{4}}$	T_{Scell}	328.88	calculation

Table 3.8: Predicted Solar Cell Temperature in winter (Spectrolab) (Adapted from Melone, 2009:30)

Predicted Solar Cell Temperature in Winter				
Item	Equation	Symbol	SMAD	Source
Altitude		h	500	Given
Inclination of a satellite's orbit		i	1.699951	Given
Solar/orbit angle		β	0	Given
Orbit angle from sub-solar point (SSP)		v	0	Given
Radiator normal WRT Nadir		λ	0.785398	Given
Earth angular radius	$\sin^{-1} (R_e/R_o)$	ρ	1.187	calcul
Earth view factor		F_e	0.608	calcul
Albedo view factor	$F_a = F_e \cos(\beta) \cos(v)$	F_a	0.608039	calcul
Solar cell temperature ($^{\circ}\text{K}$)	$T_{Scell} = \left[\frac{\alpha_f S \cos(\phi) + \alpha_b S a l F_a + \epsilon_b E F_e - \eta f_p S \cos(\phi)}{(\epsilon_f + \epsilon_b) \sigma} \right]^{\frac{1}{4}}$	T_{Scell}		
Albedo		al	0.3	Given
Emissivity solar cell side		ϵ_f	0.85	Given
Emissivity back side		ϵ_b	0.92	Given
Front side absorption		α_f	0.92	Given
Back side absorption		α_b	0.17	Given
Cell packing factor		f_p	0.8	Given
Cell efficiency		η	0.28	Given
Max direct solar flux ~ W/m ²		S	1322	Given
Solar incidence angle (rad)		ϕ	0	Given
Max earth IP emission @ surface		E	326	Given
Solar cell temperature ($^{\circ}\text{K}$)	$T_{Scell} = \left[\frac{\alpha_f S \cos(\phi) + \alpha_b S a l F_a + \epsilon_b E F_e - \eta f_p S \cos(\phi)}{(\epsilon_f + \epsilon_b) \sigma} \right]^{\frac{1}{4}}$	T_{Scell}	327.47	calculation

In this same series of thoughts, the new values of efficiencies are adjusted by first beginning with the currents and voltages (at BOL for 28 °C), which conform to the following formula:

$$NV = SV + (\Delta T \times TC) \quad \text{Equation 3.10}$$

Where:

- NV: is a new value;
- SV: is a specification value;
- ΔT : is a temperature change; and
- TC: is a temperature coefficient

The following tables summarise the calculations of the efficiencies and the Appendix B shows the full calculations on solar cells.

Table 3.9: Preliminary adjustment of nominal cell efficiency (Spectrolab) (Adapted from Melone, 2009:32)

Adjustment of nominal efficiencies of Spectrolab Solar Cell			
	Summer	Winter	Note
Predicted Temperature [degree C]	55.7	60.5	From paper
Base Temperature [degree C]	28	28	Manufacturer Specification sheet
Temperature delta [degree C]	27.7	32.5	Line3 - Line4
Voltage Coefficient [V/degree C]	-0.0067	-0.0067	From paper
Nominal Max Power Voltage [V]	2.35	2.35	Manufacturer Specification sheet
Average Max Power Voltage [V]	2.16441	2.13225	Line8 + (Line7*Line5)
Current Coefficient [$\mu\text{A}/\text{cm}^2/\text{degree C}$]	9.00E-06	9.00E-06	From paper
Nominal Max Power Current [A]	0.0164	0.0164	Manufacturer Specification sheet
Average Max Power Current [A]	1.66E-02	1.67E-02	Line12 + (Line11*Line5)
Nominal Efficiency	0.283	0.283	Manufacturer Specification sheet
AMO [W/cm^2]	0.1353	0.141	Solar constant at Air Mass Zero (AMO)
Power [W]	3.60E-02	3.56E-02	Line9 * Line13
Average Efficiency	2.66E-01	2.52E-01	Line17 * Line16

3.6.1.5 Final adjusted efficiencies

The parameters used to determine the final average efficiency were: nominal efficiency, the radiation adjustment, the temperature adjustment, design and assembly adjustment. Design and assembly parameters present circuit losses, which are created by line connections and other imperfections. These parameters values range between 77% and 90% (Wertz & Larson, 1999: 28-40). A value of 85% was chosen for the research. In order to maintain an overall of 85% adjustment for the power that solar cells will deliver for the design and the assembly, the square root of 0.85 was applied to both voltage and current.

Table 3.10: Final average of nominal cell efficiency (Spectrolab) (Adapted from Melone, 2009:34)

Final Average of a nominal Efficiencies of Spectrolab Solar Cell			
	Summer	Winter	Note
Nominal Efficiency	0.283	0.283	Manufacturer Specification sheet
Average Radiation	1	1	Decided
Temperature Adjustment	0.954	0.881	From paper
Design and Assembly Adjustment	0.84	0.84	Manufacturer Specification sheet
Final Average Efficiency	0.226785	0.209431	Line24 * Line25 * Line26 * Line27
Temperature Adjustment			
Temperature Adjustment Voltage [V]	2.35	2.35	Manufacturer Specification sheet
Square Root of Design & Ass.	0.92	0.92	From paper
Final Average Voltage [V]	2.162	2.162	Line30 * Line31
Current Adjustment			
Temperature Average Current [A]	0.0163	0.0163	Manufacturer Specification sheet
Square Root of Design & Ass.	0.92	0.92	From paper
Final Average Current [A]	0.014996	0.014996	Line34 * Line35
Final Average			
Final Average Voltage * Final Average Current	0.032421	0.032421	Line32 * Line36
Solar Constant at Air Mass Zero [W/cm ²]	0.1353	0.141	From paper
Final Average Efficiency	0.239626	0.229939	Line38 / Line39

Tables 3.7, 3.8, 3.9 and 3.10 above show the behaviour of solar cells in all seasons. During the summer period, the electrical power of solar cells per unit of the surface is low, which makes the cells' voltage higher; consequently, the cells power is lower. In winter, the temperature of the cells is low compared to summer.

This low temperature ensures the highest solar cell's efficiency, which results in the production of high power. The final result showed that the winter solstice scenario is worst for both types of cells.

3.6.1.6 Series and parallel requirements

The number of solar cells required in series is determined by the level of voltage that is required by the satellite's system (bus voltage). The connection in parallel strings of series cells also depends on the overall current requirement of the entire satellite. Adjusted values of the voltage and the current are used in order to know exactly how many solar cells should be placed in series and in parallel to generate the required power. All these calculations are done in Excel, as shown in Table 3.11 below. These calculations also allow a comparison of the area required by calculations and the available space of the satellite.

Table 3.11: Series and parallel requirements

Solar cell series and parallel requirements (Spectrolab)			
	Summer	Winter	Note
Battery nominal voltage [V]	12.3	12.3	Battery specification sheet
Voltage required to charge battery [V]	14.35	14.35	Battery specification sheet
Margin [%]	3.00%	3.00%	Decided
Net voltage required [V]	14.7805	14.7805	Line47 + (Line47 * Line48)
Average power [W]	12	12	From Matlab
Current required [A]	0.811881	0.811881	Line50 / Line49
Net current required [A]	0.836237	0.836237	Line51 + (Line51 * Line48)
Dimension of a cell [6.89cm * 3.95cm]	#	#	From Specification Sheet
Area of solar cell [cm ²]	27.2155	27.2155	From specification sheet
EOL voltage [V]	2.162	2.162	The final average voltage [Line32]
EOL current density [A/cm ²]	0.014996	0.014996	The final average current [Line36]
Number of cells connected in series	6.836494	6.836494	Line49 / Line56
Number of cells connected in parallel	2.048979	2.048979	Line52 / (Line54*Line57)
Number of cells required	14.00784	14.00784	Line59 * Line60
Total cells area required [cm ²]	381.2302	381.2302	Line61 * Line54
Solar cells body mounted configuration			
Total area available on the unit [cm ²]	1981.156	1981.156	Dimension calculation
Packing factor	0.58	0.58	Decided
Effective area available [cm ²]	1149.071	1149.071	Line66 * Line67
Unsed area available [cm ²]	767.8404	767.8404	Line68 - Line62

Referring to Appendix B, section 5, lines 3 and 4 are the values given in design. Line 3 is the value of the voltage of the battery pack and line 4 is the voltage level to recharge the batteries. Line 5 is the value, which is taken arbitrarily to adjust the level of margin in order to increase the voltage level to enable the system to function normally. The overall system power is given in line 7. This power is taken from the simulation done with Matlab (see codes in Appendix D).

The value of 12 W is an adjusted power value taken from Matlab simulation. In practice, this value can be higher when the satellite points directly to the sun. Because the margin level is included in the series and parallel calculations for both voltage and current, some portion of power is also used for it. The power portion value is selected arbitrarily. In this research, 2.5% power margin was used for both voltage and current. The system required current was calculated from the simulation power divided by the Net Voltage Required. Similarly to the voltage, a margin was included. The solar cell area value was taken directly from the solar cell manufacturer's specification sheet (27.2155 cm²).

Lines 13 and 14 were taken from the final average of the nominal cell efficiency table (see Appendix B, section 5). The required string voltage was then divided by Line 13 and rounded up to calculate the number of cells required in series.

Similarly, the required overall current was divided by the product of Line 14 and Line 11, and then rounded up to calculate the number of parallel strings required. Line 17 was the product of Lines 15 and 16, while Line 15 was the product of Line 17 and Line 11. Calculations show that the cell area required was smaller than the available area of the satellite. Lines 23 to 24 show the method that was used to arrive at an available area of 1149.071 cm².

3.6.1.7 Solar cells power control system

The theme of power control system applies to the technique that is used to control the transfer of power from a power source to an energy storage device and load resistance. In this research, the power source was a panel of photovoltaic cells and the energy storage device was a bank of battery cells.

As mentioned previously, batteries are highly sensitive to overcharge and undercharge conditions, thus photovoltaic cells cannot be directly connected to them otherwise this would cause the battery permanent damage, resulting in a catastrophic failure of the satellite mission. The control of power source and energy storage interface can be done in several different ways. However, Helvajian (1997: 207) describes two basic techniques used on modern satellites, namely MPPT and DET. The DET technique is much simpler to implement and is cheaper in terms of cost, while the MPPT technique is designed to extract the maximum amount of power from the photovoltaic cells.

The last technique uses microcontroller as a main control device. One of the aims of this research is to ensure the reliability and robustness of the system, while the microcontroller is not a suitable device in terms of reliability. Building the analogue system could help, but this technique requires the presence of discrete components that could reduce the fidelity of the satellite's operation (Jordan, 2006). The basic technique used to allocate power to the load in a DET system is shunt regulation. In this technique, current is diverted from loads by shunt resistors, which along with the load appear in parallel to the power source, as shown in Figure 3.12 below (LPCS block diagram).

The shunt resistors dissipate power not used by the loads. For thermal reasons, this resistor is typically placed outside the main satellite bus, often on the solar panel yoke.

3.6.2 Shunt regulation system

The bus voltage should be stable for the best operation of the satellite in either a sunlight or eclipse period. The voltage regulation in sunlight is based on a shunt regulator. The Zener diode is incorporated into the circuit to give the voltage reference signal, while the voltage divider gives a signal proportional to the actual bus voltage, as illustrated in Figure 3.13.

The operational amplifier (Opamp) generates an error signal that commands the switching transistor and latter regulates the shunt current. The Opamp in the system acts as a sensor and control logic.

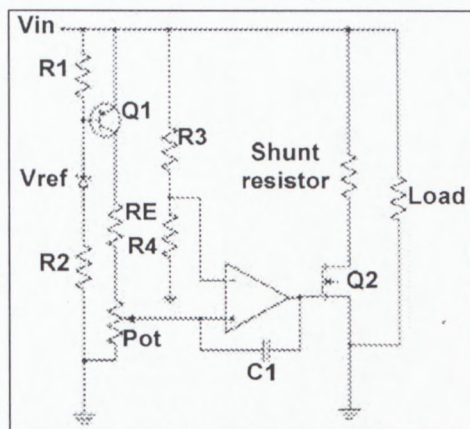


Figure 3.12: Shunt regulated circuit diagram

The Zener diode current increases at the same rate as the bus voltage. This increase forces the current in the voltage divider node to also increase. Because of the properties of the zener, the error signal becomes larger and increases the current in the shunt row. Therefore, the current through the batteries will reduce. Consequently, the bus voltage maintains constant all the time. The Opamp is directly connected to the bus voltage and the ground. Regarding the system configuration and considering the constraints of Opamp's output power, there is a small current, which flows through the shunt row, the zener and the voltage divider, therefore, a power dissipation of some watt is accepted in the system.

3.6.3 Battery management system

The design of a robust electrical and thermal management system of the battery's pack within the satellite is imperative. During the satellite's operation, the voltage, current and temperature differences vary. This variation leads to electrical imbalances from cell to cell and decreases the battery's pack performance to nearly 25% (Pistoia, 2008: 125-154). Active battery management is required in the system to avoid the instability phenomena from occurring during the satellite's operation.

The control of the level of charge and discharge of batteries is essential to protect batteries from an over and/or undercharged state. This can be done if the electrical characteristics of the selected batteries are known.

Hence, to determine a suitable battery for the project, feasibility studies based on battery weight, temperature, duration of life, and so on (as discussed in Chapter 2) were conducted, and Lithium-polymer (LiPos) cells from the Lithium's family were selected, amongst others. See Figure 3.14 below.

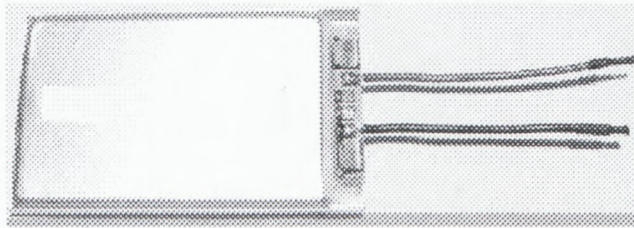


Figure 3.13: Space Lithium-Polymer battery
(Adapted from Clyde space datasheet)

The main advantage of the Lithium Polymer battery over NiCad and NiMH, is the weight. Added to this advantage, the Lithium-Polymer cell has no memory effect and is light. The LiPos cell is the best available Lithium chemistry, which is used in satellite activities. Conversely, this battery is a bit fragile. Straying outside strict voltage limits usually damages it, as defined in section 2.3.4.2. The Lithium-Polymer cell can also be easily damaged physically if it overheats, as it releases oxygen, which causes it to swell and if the temperature reaches 150 °C, its thermal runaway will cause a fire (Munshi, 1995:284).

3.6.3.1 Charged characteristics of Lithium-Polymer batteries

❖ Charged voltages

Lithium-Polymer batteries are designed to be charged up to 4.2 V per cell at a charge current of about 1 coulomb and should not be discharged below 3V with a nominal rating of 3.6V or 3. These batteries have a limited number of charged and discharged cycles, normally around 300 to 500. Once the threshold level of charged voltage is reached the current declines, until the cell is fully charged. This characteristic of the charger is called constant current constant voltage (CCCV). The cell voltage is not expected to drop below about 3V per cell. Operating these batteries outside the defined ranges causes a loss of capacity and inability to deliver the full current or the complete death of the cells, which means that the cell is no longer able to perform its function (Munshi, 1995:284). Thus, the charging and discharging of cells should be maintained within the specified limits, as described above.

❖ Temperature

Lithium-Polymer batteries are sensitive to the temperature, as mentioned above. At high temperature ($\approx 150\text{ }^{\circ}\text{C}$), the cells puff up and do not work as well.

Also, in low temperature ($\approx 0\text{ }^{\circ}\text{C}$) their voltage tends to drop. To keep the voltage at its nominal level, the temperature control should be inserted within the battery pack. This controller also prevents the premature electrostatic charge (ESC) cut-off phenomenon from occurring.

❖ Alternative batteries and thermal control design

Suitable Lithium-Polymer batteries were also selected based on existing EPS missions. The first mission was that of the Japanese CubeSat CUTE-I followed by the Swiss Cube mission (Jordan, 2006). The specifications of the Japanese CubeSat (CUTE-I) battery are shown in Table 3.12 below.

Table 3.14: Japanese CubeSat selected battery specifications

CubeSat	Battery type	Life expectancy [Cycles]	Charge operating temperature [$^{\circ}\text{C}$]	Discharge operating temperature [$^{\circ}\text{C}$]
CUTE-I	Li-Ion	500	0 to 40	-20 to 60

Jordan (2006) asserts that it is possible to use batteries with standard temperature ranges only if the thermal design works well, since the temperature inside the satellite depends mostly on design. Conversely, SwissCube used VARTA Lithium Polymer batteries, which are also called PoLiFlex. The thermal requirements of PoLiFlex are similar to the standard thermal requirements of Li-Ion batteries, as shown in Table 3.13 below.

Table 3.15: PoLiFlex thermal specifications (Jordan, 2006)

Parameters	Unit	Significant values	Suitable value	Notes
Gravimetric density	energy [Wh/l]		370	High
Volumetric density	energy [Wh/kg]		200	Very high
Charge operating temperature	[$^{\circ}\text{C}$]	0 to 45		The appreciation depends on the thermal design
Discharge operating temperature	[$^{\circ}\text{C}$]	-20 to 60		The appreciation depends on the thermal design
Life expectancy >70% of capacity	[Cycles]		500	Standard
Charge retention 1 year at -20 to 20 $^{\circ}\text{C}$ 3 month at -20 to 45 $^{\circ}\text{C}$ 1 month at -20 to 60 $^{\circ}\text{C}$	[%] of capacity	>70		The appreciation depends on the thermal design

The VARTA PoLiFlex battery could work for LPCS, but had certain important limiting factors, which were required by the LPCS project's objectives. Therefore, the space lithium polymer battery SLPB from Clyde space was opted for this design. There are several reasons for opting for Clyde Space battery technology:

- It has a solid reputation for quality, safety and reliability;
- It does not exhibit the memory effect seen in NiCds and NiMHs batteries. This allows the battery to be charged from any state of charge without degradation of performance; and
- It is strongly recommended by Clyde Space (manufacturer of electrical power systems and other accessories for small satellites).

The procedures set by ESA to test Lithium-Polymer batteries for space applications found SLPB without any bulging problems, whereas all other cells did.

These tests were conducted as follows:

- Capacity at C/10 under vacuum;
- Radiation up to 500krad;
- DPA;
- Capacity at -10C, 0C, 20C and 40C;
- Resistance;
- Self discharge;
- Missions scenario tests:
 - Charge C/2 and Discharge C/4 (5 cycles),
 - Charge C/10 and Discharge C/2 (5 cycles), and
 - Charge C/10 and Discharge C/15 (5 cycles);
- EMF vs SOC;
- Cycling tests at reduced pressure (15-20 mbar) -30% DoD, C/2; and
- Charge/Discharge >5000 cycles.

The SLPB cell has a nominal capacity of 1210 mAh and energy density ranges between 120Wh/kg to 150Wh/kg. This allowed the DoD to be at 30% for this application. The available capacity to supply the satellite during the eclipse was 360mAh. This energy was sufficient for the mission. Figures below shows the typical charge profile of a SLPB battery and the voltage range for a DoD of 30%:

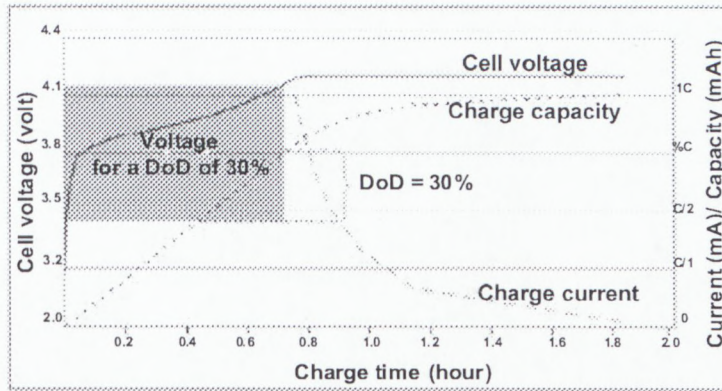
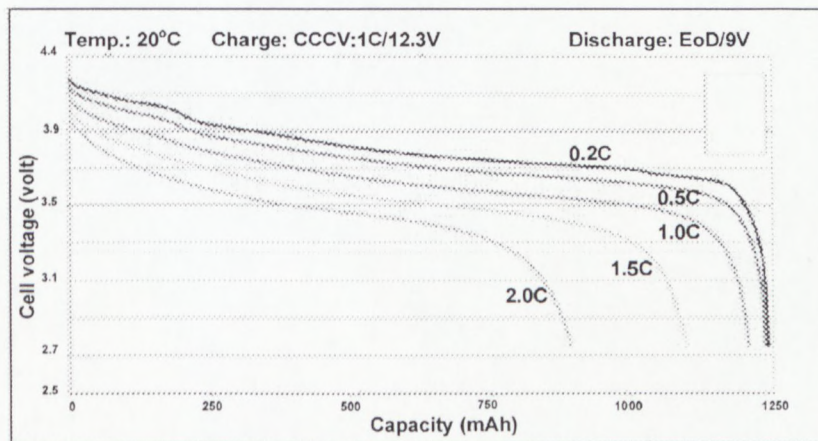
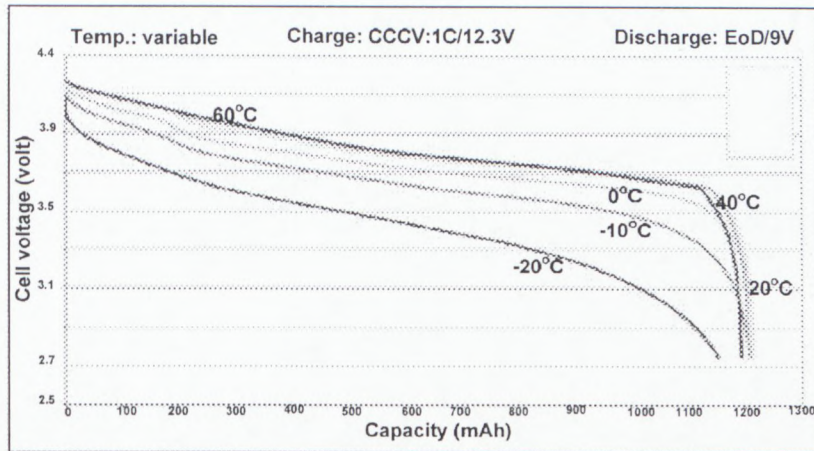


Figure 3.16: Typical charge profile of 1C @ 20°C with defined voltage range for the application (Adapted from Jordan, 2006)

The DoD is 30% of the capacity if only one battery pack is used. But this system uses two battery packs at the same time. This is to reduce the DoD to about 15%. The low DoD capacity increases the reliability and the working life expectancy of the system. There will not be a problem if one battery pack breaks down, since the system will survive with the other battery and then the DoD will be 30% again. The other aspect that had been taken into consideration was the discharge profile. This profile varies accordingly with the charging current and temperature, as shown in Figure 3.16 a and b, respectively.



(a) Discharge profile vs charge current @ 20°C



(b) Discharge profile vs temperature @0.2C

Figure 3.17: Discharge profile systems

(Adapted from Jordan, 2006).

In the case of using one battery pack at a temperature of approximately -20°C , the discharging current increased to about 0.7C , and the battery capacity critically reduced. This led to a design of a robust thermal controller system. The system was designed to monitor the battery temperature. At a temperature of about 75°C , the charging current is isolated from the battery pack and when the temperature decreases below 0°C , the discharging current stops flowing to the loads (Jordan, 2006). The heating system is also incorporated in the design to keep the battery temperature above 0°C . It has been assumed that the satellite will perform approximately 15 orbits (cycles) per day and because the design is dedicated for the mission that lasts for at least one year. Consequently, the number of cycles can be determined by using the following equation:

$$\text{Cycles per year} = \text{Number of Orbits} \times \text{Number of the days of the year} \quad \text{Equation 3.11}$$

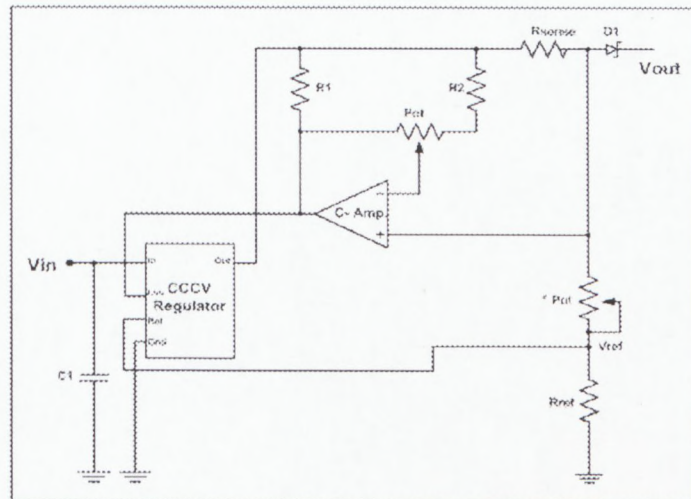
$$15 \text{ orbits/day} \times 365 \text{ days/year} = 5475 \text{ cycles/year.}$$

However, the DoD is 30% for one battery pack and because 1/3 of the eclipses will not consume a lot of energy, the number of cycles will be higher than 2000. Based on this reasoning, it is not obvious to confirm 5475 cycles with only one battery pack. This can be done if both battery packs work correctly. Hence, the batteries will last for one year or more.

3.6.3.2 Lithium-Polymer battery charger

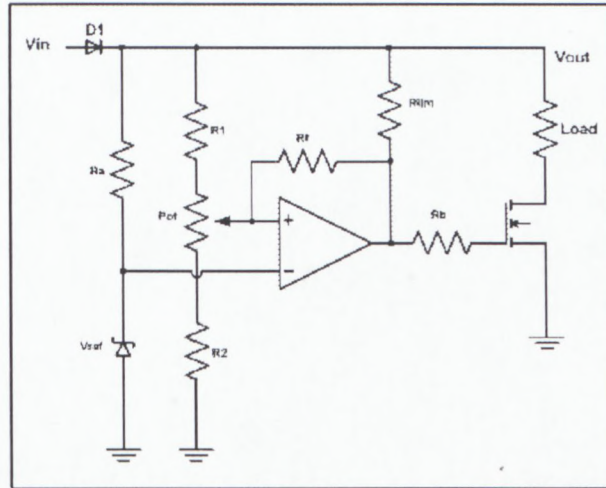
Charging Lithium-Polymer batteries can be an extremely simple exercise by using the voltage and current limits system. Many adjustable power systems can do this. The management system of this research is composed of two main functional circuits, namely the charge regulator and discharge regulator.

The charge regulator is basically a current regulator that senses the battery voltage to allow the end of the charge cycle. Figure 3.17 a and b below show the battery charge and discharge regulators, respectively.



(a) LPCS' Battery charge regulated circuit diagram using CCCV regulator

The circuit is slightly more complex, but works quite fine with a current range from about 100mA to 2A. R_{Sense} is a current sensing resistor, which feeds the opamp with a voltage that varies according to the flow of current. The nominal value of this resistance ranges between 0.01Ω and 0.1Ω . The larger R_{Sense} , being the smaller starting current. Therefore, this resistance (R_{Sense}) should be carefully selected. The gain of the opamp is set by the ratio, which is created by R_2 and $Pot1$ and also on the value of R_{Sense} above. The regulator device selected is L200, which has an internal limit current of 2A. The output voltage is set by the combination of R_{Ref} and $Pot2$. There is some sort of leakage current from cells that are connected backward to the charger, while the circuit is not powered. This leakage is less than 20mA, hence is not significant. Nevertheless, $D1$ (Schottky diode) is placed to prevent this loss, but more importantly, protects the circuit from reverse polarity and any disasters that may arise.



(b) LPCS' Battery discharge regulator using current controlled Opamp

Figure 3.18: Battery management system circuit diagrams

For the discharge regulator stage, since the number of series-parallel connection of cells is dimensioned on values of bus voltage and battery cell charge voltage, the bus voltage drops below the normal voltage at darkness. To avoid battery voltage from dropping below the threshold limit, the discharge regulator is incorporated into the system. This discharge regulator controls the output voltage and assures that the voltage is always at the nominal bus voltage.

3.6.4 Power distribution system

The power distribution system provides power, which is required by different loads. In this research, there were three different voltages that were provided for the nanosatellite operation.

The unregulated bus voltage (12V) was the voltage that was measured across the loads and battery management system. This voltage was used to supply payloads and other devices on board the satellite. The remaining two voltages were regulated at 5 V and 3.3 V. Full details of the LPCS power distribution is given in Chapter Four.

3.6.5 System power budget

The objective of the power budget is to verify that the power consumption on board the nanosatellite does not exceed the power produced by solar panels. The power budget is defined on a time interval i.e. what power the load will require for the day or night, or at the peak demand. The model presented in this project was a simplified power budget model, which was taken from Jordan (2006:64). In the model only the average power consumption during the day and during eclipse was considered.

The following are power consumptions:

- Average energy produced with the solar cells during daylight: 12Wh;
- Average energy produced with the solar cells during eclipse: 0Wh;
- Average energy consumed with users during daylight with 30% of margin: 8.4Wh;
- Average energy consumed with the users during eclipse with 30% of margin: 525mWh;
- Efficiency of charge: >90%; and
- Efficiency of discharge: >90%.

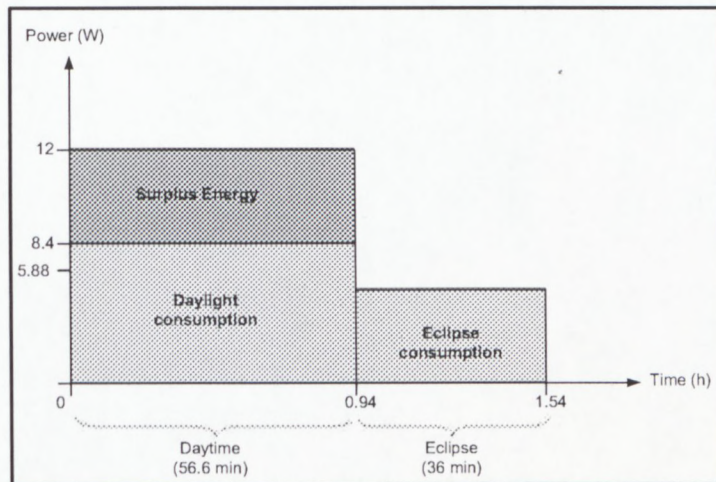


Figure 3.19: LPCS power budget

Therefore, the energy stored in the battery is given in equation 3.12.

$$E_{Bat} = 700 \text{ mWh} \times 0.90 = 630 \text{ mWh}$$

Equation 3.12

This amount of energy represents a capacity of:

$$C = \frac{630 \text{ mWh}}{12.3} = 51.22 \text{ mWh}$$

Equation 3.13

The capacity available on the battery is 360mAh, hence there is no problem.

3.6.6 System mass budget

The estimated mass of the entire LPCS comprises the following devices:

- Solar cells;
- Protective cover of the solar cells;
- Aluminium structure that the solar cells are mounted to;
- PDS components;
- BMS components;
- Control circuits; and
- The harnessing to interconnect the above components.

The solar cell mass per unit area is given by the manufacturer datasheet. This value is multiplied by the product of the packing factor and the overall solar panel area to give the total mass for the solar cells. The protective cover is assumed to have the same weight as the solar cells. The structure that holds solar cells is a bit heavy compared to other devices. The mass for the PDS components and control circuits are estimated to be the same as those that are provided by Clyde space. The mass for BMS system is also given from the manufacturer datasheet and is then multiplied by 2 because of the system's redundancy. Finally, a 4% overhead estimate for harnessing is also included. Table 3.14 below summarises the mass budget of LPCS.

Table 3.14: LPCS mass budget

	Quantity	Units	Area (m ²)	Number	Total (kg)
Aluminium structure	499	mg/cm ²	0.14499		0.78
Solar cells	84	mg/cm ²	0.115992		0.1
Solar cell cover	84	mg/cm ²	0.115992		0.1
BMS	0.22	kg		2	0.44
Regulation and control	0.2	kg		1	0.2
Cabling (4% of total)					0.06
Total mass					1.68

3.7 Chapter summery

Every electronic circuit is designed to work with certain voltage, which is generally considered constant. The LPCS was provided constant voltages and contained circuitry, which were continuously, hold the output voltages to the design values regardless of changes in load current or input voltage. This chapter has shown the techniques and methods, which were used to design electrical power supply for a nanosatellite, outlining all details used in the design.

CHAPTER FOUR DESIGN ANALYSIS AND TESTS

4.1 Introduction

A satellite power system consists of a primary power source, a secondary rechargeable power source, power distribution and power control. Both power sources should be well sized in order to provide the necessary power to the satellite's subsystems and payload during the daylight and eclipse period (Maral *et al.*, 2009:562).

In order to choose and size the system's components, two simulation packages were used. These simulations helped to identify the behaviour of each stage in the system by monitoring its main parameters, including the solar array output voltage and current, the bus voltage and current, the battery output voltage, current and state of charge; and to verify the power supplied by the solar generators, as well as the batteries with respect to the required power. Following the simulation sections, the hardware tests were performed to confirm the results, which were obtained during the simulation processes.

4.2 Simulations

4.2.1 Solar cells

The system control is an imperative factor on the design of the EPS for nanosatellites. It controls the transfer of power from source to an energy storage device or a dissipative load. The LPCS employs the DET technique where its advantages were disputed previously. In the case of this study, the source was solar cells and the storage devices were battery cells. Because battery cells are highly sensitive to over and/or undercharging conditions, solar cells are not recommended to be connected directly to battery cells to avoid battery damage and failure of the mission. The power delivered by solar cells is not stable and varies with space environment conditions. The most crucial conditions that influence solar cells' power are solar intensity (irradiance) and operating temperature.

In order to predict the robustness and efficiency of the system, several simulations were performed, including individual solar cell simulation with LTSpice and Matlab software and the average power that solar cells can provide once orbiting earth.

4.2.1.1 LTSpice simulation

The solar cell simulation allows the determination of the individual cell voltage, current and power. In this case, the Spectrolab 2.3V with 0.5mA cell model was simulated with LTSpice. Figures 4.1 and 4.2 below are simulation results, which show current-voltage and power-voltage characteristic curves, respectively.

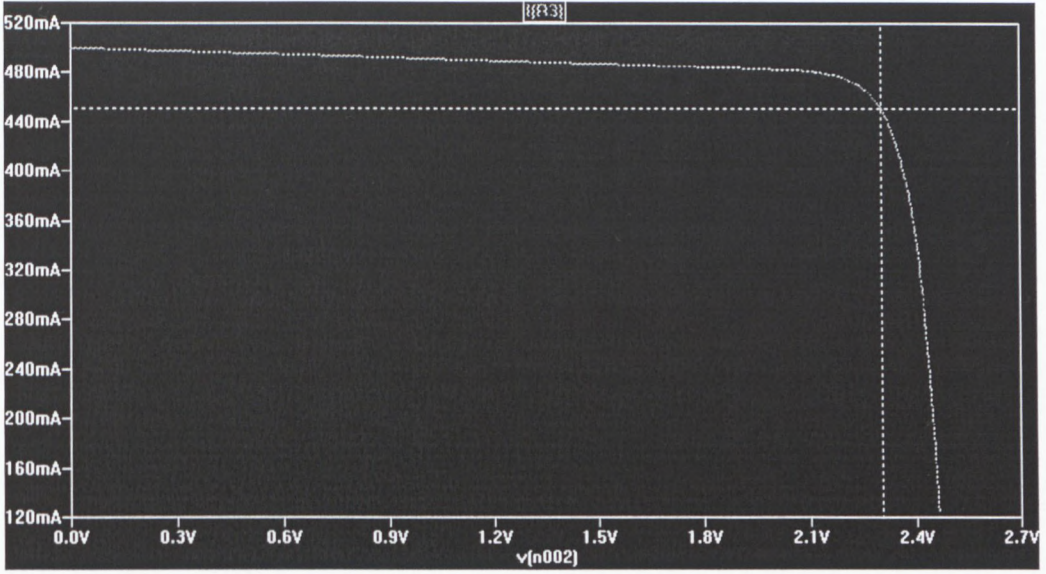


Figure 4.1: 2.3V with 0.5mA current-voltage characteristic curve

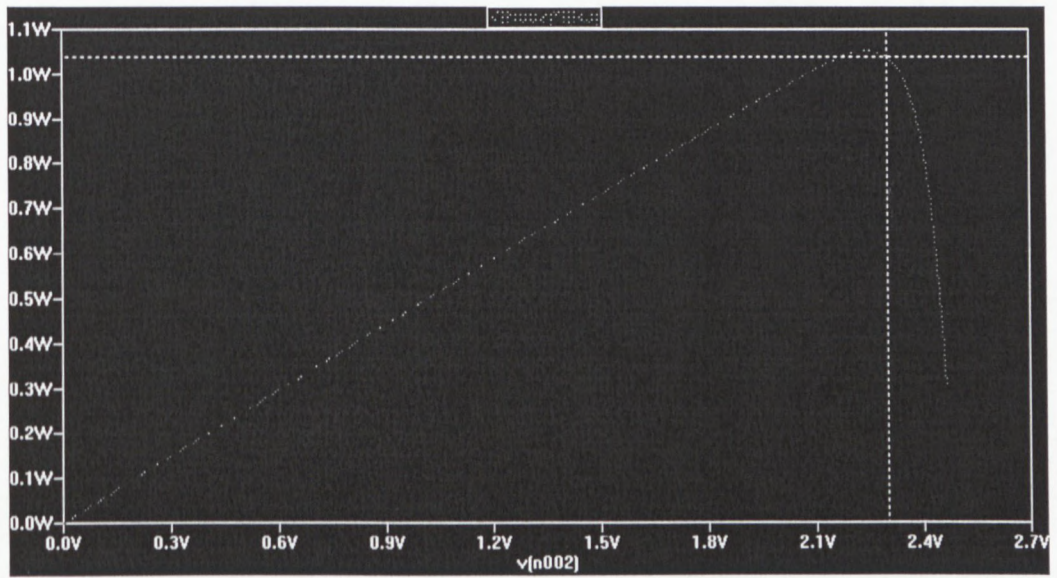


Figure 4.2: Power-voltage characteristic curve

4.2.1.2 Matlab/ Simulink simulation

The Matlab simulations predict the system average power and show the behaviour of the solar cell with respect to changes in space environment conditions. As mentioned above, the temperature and irradiance affect the operation conditions of the solar cells. Decreasing irradiance shifts the current down with little effect on the voltage, as shown in Figure 4.3, whilst increasing temperature shifts the voltage down with little effect on the current (Figure 4.4). Conforming to the value of the individual solar cell open-circuit voltage and short-circuit current characteristics, which were obtained from solar cell simulation with LTSpice and the calculations done in Chapter three, the series-parallel combination of solar cells are performed, as shown in Figures 4.3 and 4.4 below (Matlab codes are given in the Appendix D).

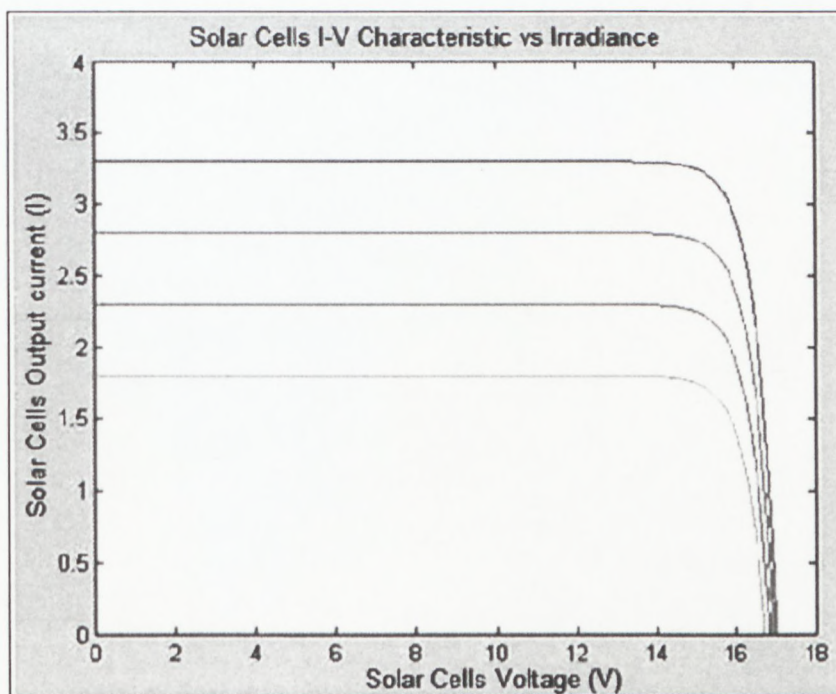


Figure 4.3: Solar cell C-V characteristic vs irradiance

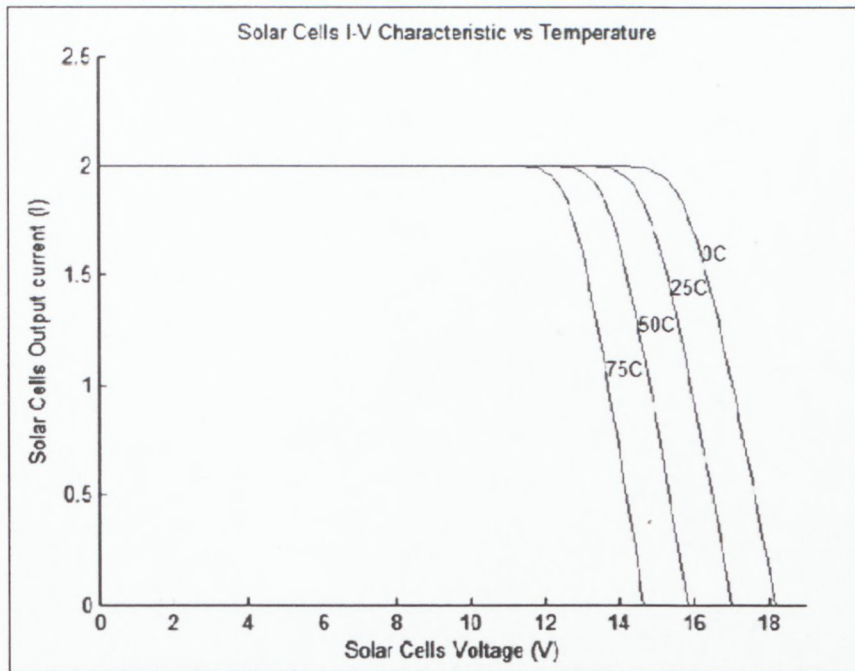


Figure 4.4: Solar cell C-V characteristic vs temperature

Besides environmental conditions, another Matlab code simulation was done to show the worst-case scenario and the average power available from solar cells by rotating the satellite at different angles. This led to the calculation of the power of the individual load, including the power required by the EPS circuitry, magnetometer, transmitting and receiving circuits, OBC and any other equipment onboard the satellite.

Appendix D shows the Matlab programming code. The program begins with the sun pointing directly at one side at an angle of 0° , then the nanosatellite was rotated along the vertical axis so that the best and worst case power values could be seen. The result of the simulation is shown in Figure 4.5 below.

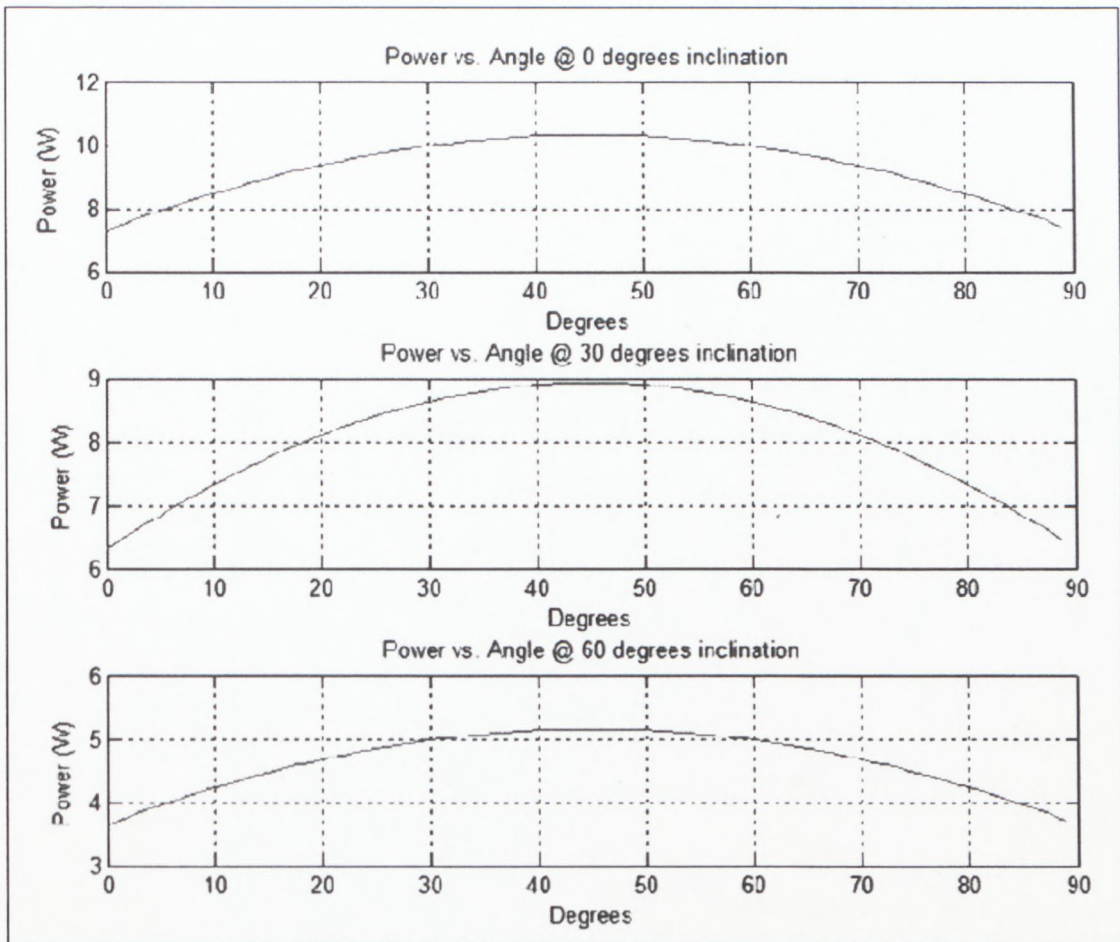


Figure 4.5: Solar cells' average power simulation

From Figure 4.5 above, it may be concluded that the best case scenario power is approximately 11W when the sun directly pointed to one side of the satellite.

The worst case scenario was when the satellite was inclined at 60 degree relative to the sun's position, and when the sun shone directly between two panels, which gave a power of approximately 5.3W.

In order to determine the minimum average power, the following analysis was performed. As stated previously, the LPCS is designed to perform a mission at an altitude of 500km (circular orbit) with a solar power of 12W. The satellite subsystems and payload will consume this power evenly throughout the mission. Of course, since the satellite will be going into eclipse, the solar cells cannot provide this power continuously, thus a backup system is required.

Calculation of the average power was done once the maximum eclipse time was determined. A total of 92.76 minutes was the total orbital period (P) of the satellite and was given by equation 4.1:

$$T = 2\pi\sqrt{x^3/\mu} \quad \text{Equation 4.1}$$

Where T is the period (in second), x is the semi-major axis of the orbit and mu is the standard gravitational constant for earth, which is $398,600 \text{ km}^3\text{s}^{-2}$. By taking 6378 km as the radius of the earth (R_{Earth}), the maximum eclipse time could be found. First the nanosatellite positioning angle alpha was calculated by using equation 4.2 and the result is 22° .

$$\alpha = \cos^{-1}(R_{\text{Earth}}/(R_{\text{Earth}} + H)) \quad \text{Equation 4.2}$$

The total orbital period was also expressed in terms of an operating factor (FO = 1). The operating factors of the eclipse (FOE) and sun (FOS) periods were given as:

$$FOE = \frac{(180^\circ - 40^\circ)}{360^\circ} = 0.389 \quad \text{Equation 4.2}$$

$$FOS = FO - FOE = 0.611. \quad \text{Equation 4.3}$$

Therefore, the maximum eclipse and sun times were 36.08 minutes and 56.68 minutes, respectively, and form equations 4.4 and 4.5.

$$\text{Max eclipse time} = FOE \times P \quad \text{Equation 4.4}$$

$$\text{Max sun time} = P - \text{Max eclipse time}. \quad \text{Equation 4.5}$$

Now the minimum average power was calculated by using equation 4.6, which produced a value of 8.433 W.

$$P_{av} = \frac{P_{sc}}{(P/(P - \text{Max eclipse time}))} \quad \text{Equation 4.6}$$

Where P_{sc} , was the total power delivered by the solar cells.

4.2.2 Control systems

When connecting solar cells to rechargeable batteries and loads, it is usually necessary to control the operation mode of the batteries, as stated above, to assure their expected life time. The control of the electrical power system can be performed with a number of different circuit types. The simplest type is the simple on-off linear control system that consists of a linear shunt regulation, as well as charging and discharging systems. This type has advantages of simplicity, small power dissipation, low cost and high reliability.

Figure 4.6 shows a simulated system control circuit of the LPCS. This control system performs at least two crucial operations, namely protecting the batteries from overcharge in times of high sun intensity and little consumption, and the other is protecting it from excessive discharge during eclipse periods.

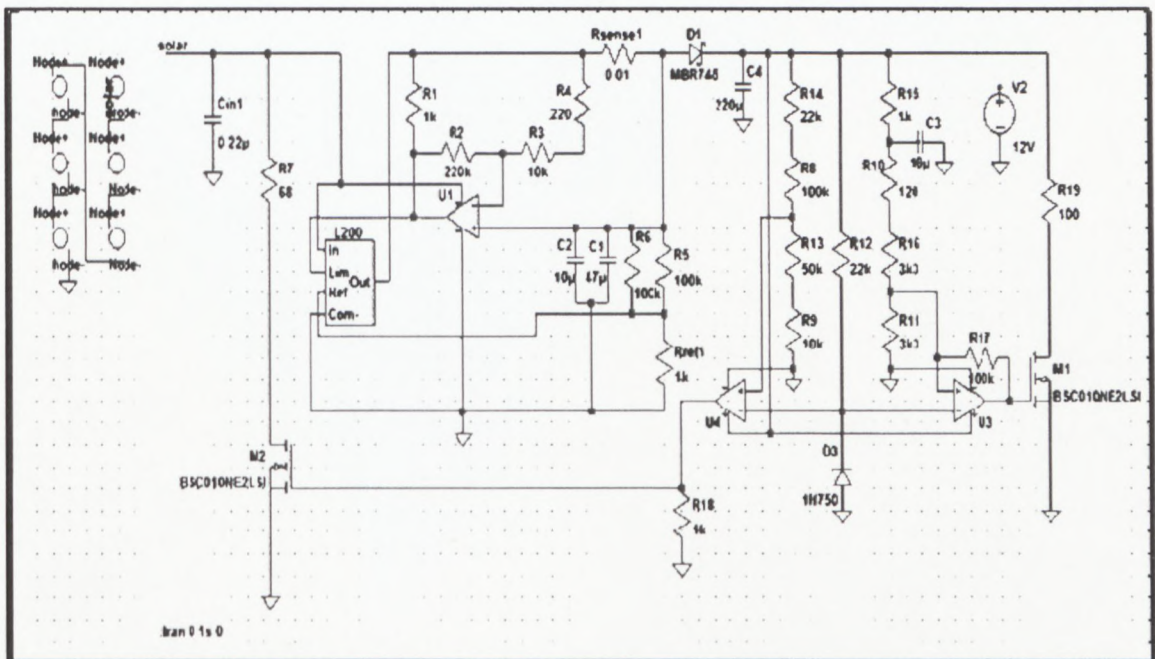


Figure 4.6: Simulated control system circuit of LPCS

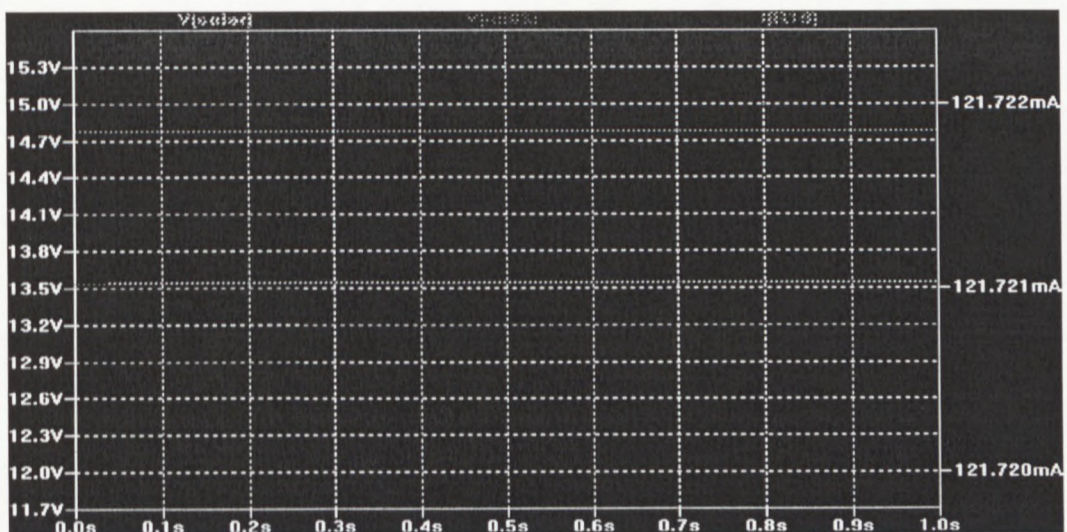
The shunt resistance dissipates excess energy from solar cells, which keeps output voltage constant all times. During high sun intensity, when solar cells' output is equal or greater than the load and batteries are fully charged, the load obtains its power from solar cells, while batteries remain at a fully charged state. During eclipse periods, the discharging regulation watches over the batteries' voltage and drops off the load when the batteries become discharged too much. The simulation's results of both linear shunt and the battery's controlled systems are shown in Figure 4.7b below. The bus voltage is set at about 13V of the sunlight's position, as shown in green waveform (Figure 4.7b).

The system regulation is based on a shunt regulator, which composes of the Opamp, the power transistor, the power resistor, zener diode and the voltage divider network.

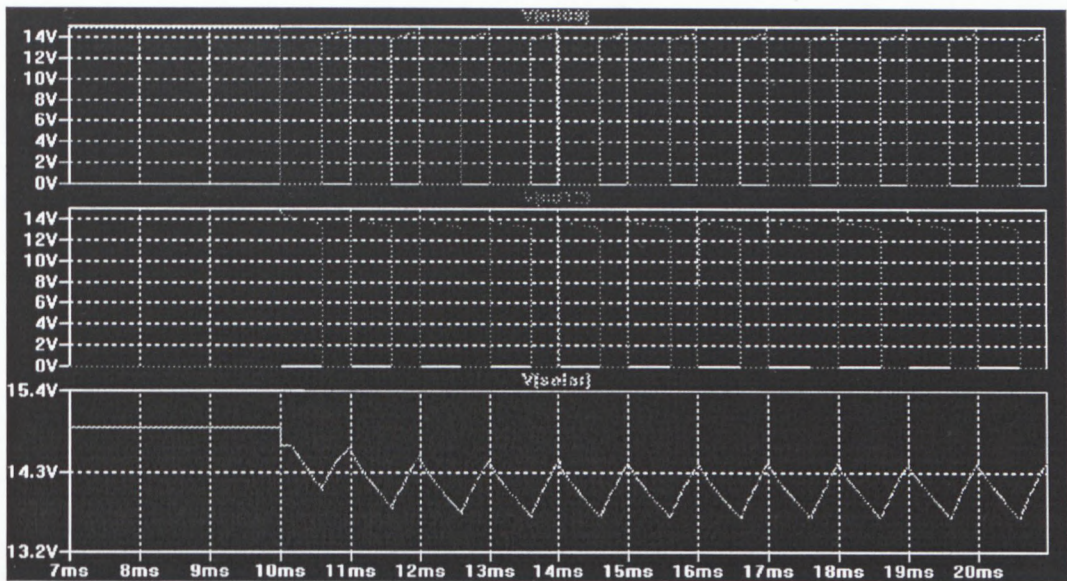
The Zener diode is incorporated into the circuit to give the voltage a reference signal, while a voltage divider network gives a voltage, which is proportional to the actual bus voltage. The operational amplifier (Opamp) generates the error voltage (shown in blue waveform), which commands the switching device (BJT) (Red waveform) and the latter regulates the shunt current. The Opamp in the circuit acts as a sensor and logic controller.

When the bus voltage increases, the voltage at the non-inverting pin of the Opamp increases and the Zener diode is set to be constant at about 4.12V and connected to the inverting pin of the Opamp. The comparison of these voltages gives the error voltage (Blue waveform, Figure 4.7b), which increases or decreases with respect to the change of the voltage divider that is connected at the non-inverting pin. The battery's discharged controller works the same way as the shunt regulator system, but the difference is that the power resistance is replaced with a load resistance.

Figure 4.7 (a) illustrates the simulation's results of the entire LPCS controller. The output system voltage, which is also the charging voltage, is shown in blue line with a value of 12.2 V. The green line (14.8V) is an input voltage from the solar panel and current of 122 mA for the charged cycle. When the batteries are charged, the current splits into three parts, the huge amount of current goes to the load, while some go to the batteries for charging purpose. A little current flows through the shunt resistance. When the batteries are fully charged, the current stops flowing through the batteries, and all current flows through both shunt resistance and load.



(a) Control system's output voltage and current



(b) Shunt and battery discharged controllers

Figure 4.7: Simulation results of the linear control system

4.2.3 Power distribution system

The LPCS provides three voltages to the nanosatellite subsystems and payloads. The first is an unregulated bus voltage (12 V). This voltage is essentially batteries voltage and is used by the subsystem to generate voltages that are needed only by that subsystem. The remaining 5 V and 3.3 V voltages are regulated supplies.

This is implemented by using high-efficiency DC/DC linear converters, which provide typical voltages of 5V and 3.3V. Figure 4.8 below shows the simulated circuit by using the adjustable linear voltage regulator with 110mA loads of current.

4.3 Hardware testing

Whereas Chapters Three and Four, section 4.2, focused on the design and simulation of the linear power control system, section 4.3 examines the operating characteristics and possible limitations of the system in the space environment. These tasks are required for any EPS design effort. Several questions arise regarding the ability of the LPCS to operate in space. Some of them were discussed in Chapter One, section 1.4. Before considering each of these questions in turn, it is important to recall the motivation by considering the LPCS. In particular, this stems from the guiding principles that were introduced in Chapter One, sections 1.6 and 1.7. It was shown throughout Chapter Three that the LPCS meets all of these criteria. With that notion as a starting point, the hardware was tested and characterised, as outlined in subsequent sections.

4.3.1 Detailed hardware description

Before delving into the tests that were conducted, it was important to have a basic understanding of the system design and intended operations of the LPCS, in general, as well as of other parts that are associated with it like solar panels and batteries, in particular. The information given for solar panels and batteries were derived from Clyde Space documentation, namely (Clyde Space Ltd: small satellite solar panels).

An LPCS consists of two printed circuit boards, batteries and solar panels, as depicted in Figure 4.10 below. This model of satellite's electrical power system can provide various voltages, currents, and power levels. The base board shown may be used alone, but provides unregulated voltage.

Because the regulated voltages are required to supply certain communication circuits, a DC to DC regulator board was used in conjunction with a base board, while 3.3 and 5 regulated voltages were provided, but at an efficiency cost.

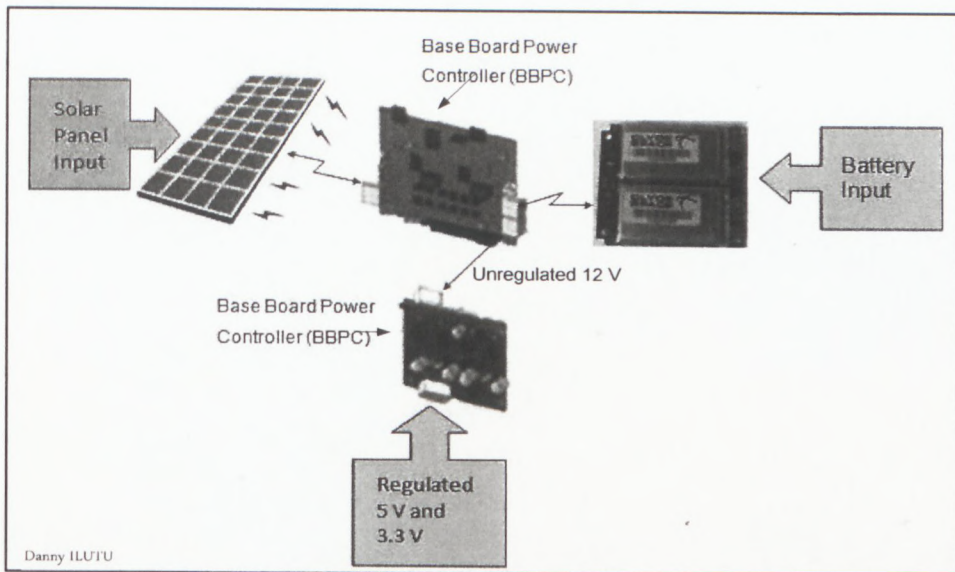


Figure 4.10: LPCS components

The following figures show close-ups of the base board (Figure 4.10) and the DC to DC regulator board (Figure 4.12), as delivered, namely without any modifications.

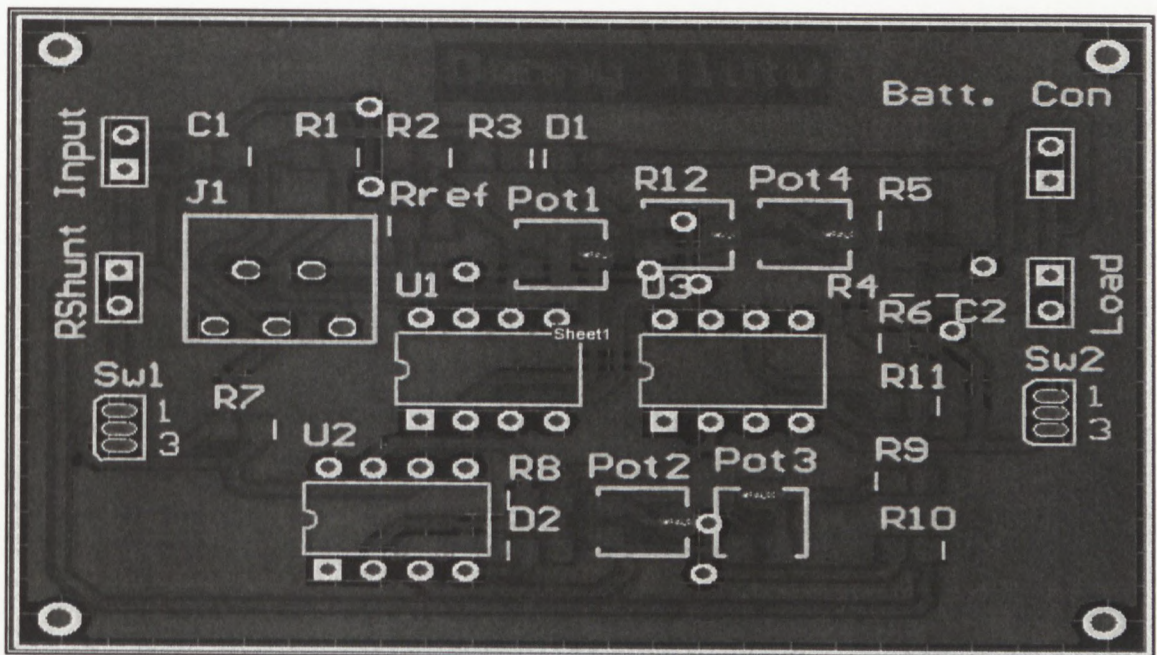


Figure 4.11: Base board power controller (BBPC), top view

Knowledge of the nomenclature of connections is crucial and makes the configuration of the system easier for all users. Beginning from the top left and moving in a counter-clockwise direction, connector nomenclature is listed below and is shown schematically in Figure 4.12:

- J1: Two pin connector (positive voltage and ground) linked solar panels and base board power controller (BBPC);
- J2: Two pin connector, connected shunt resistance;
- J3: Two pin connector, battery connector input; and
- J4: Two pin connector, communications interconnect between BBPC and power distributed board.

Figure 4.12 shows a line drawing version of the picture in Figure 4.11. The connectors listed above are labeled with circular callout symbols in Figure 4.12. Comparing Figures 4.11 and 4.12 clearly identifies and shows the positions of the connectors.

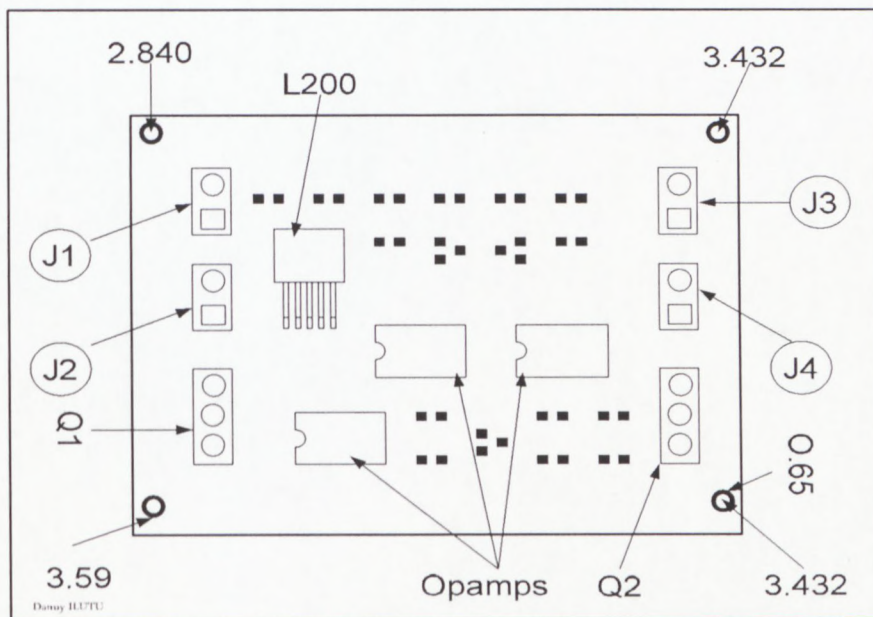


Figure 4.12: Callout symbols drawing of BBPC

Again starting at the top left of Figures 4.13 and 4.14, and moving in a counter-clockwise direction, the connector nomenclature is:

- J5: Two pin connector (unregulated 12 V from BBPC);
- J6: Two pin connector (regulated 5 V), load output; and
- J7: Two pin connector (regulated 3.3 V), load output.

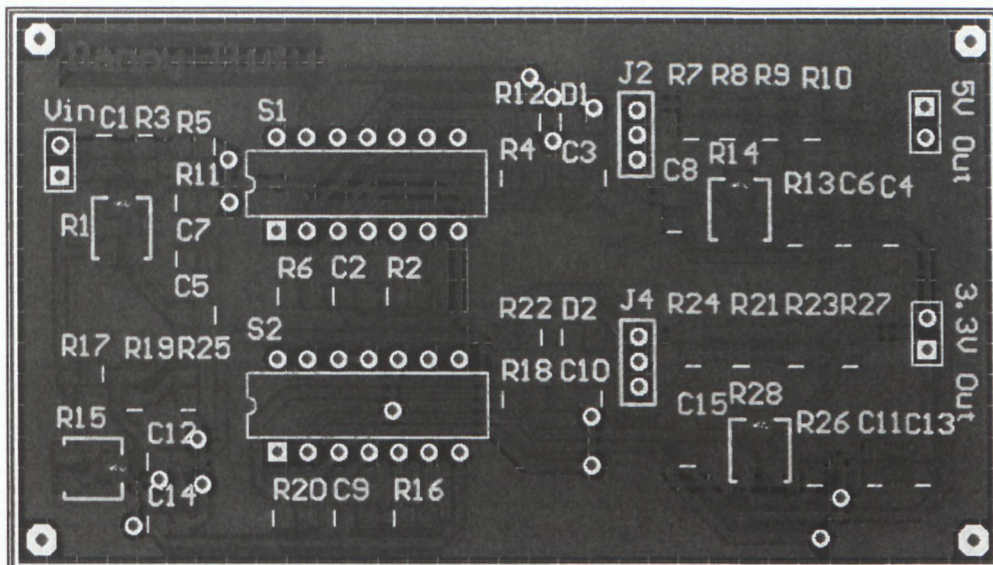


Figure 4.13: DC to DC regulator, Top view

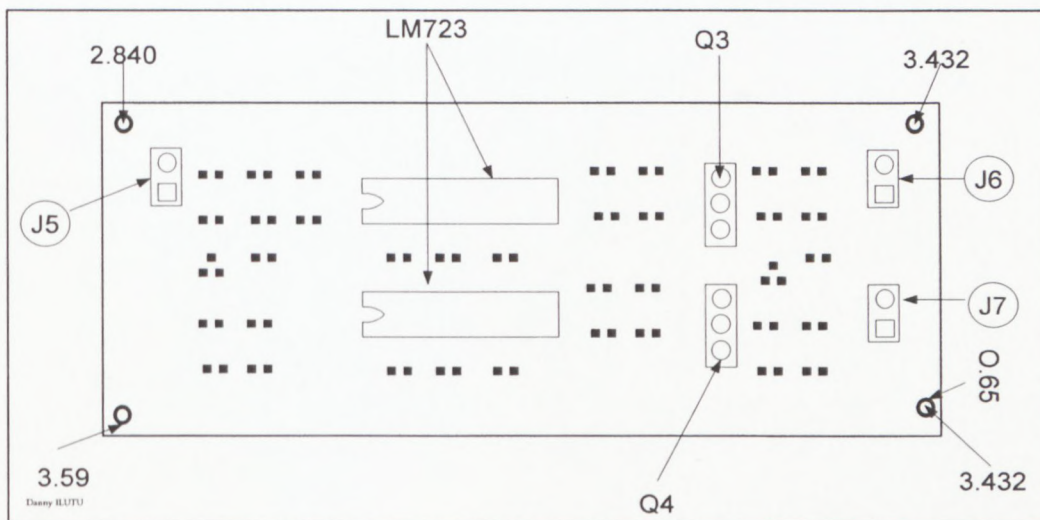


Figure 4.14: Callout symbols drawing of power regulator

Passive components (resistors and capacitors) maintain their electrical characteristics over relatively wide operating temperature ranges. The connection's material that is selected (nylon) has a wide operating temperature range, as well and a high outgassing rate in a vacuum, which is relative to many other materials.

Active components (integrated circuits) are designed with various operating temperature ranges depending on manufacturer designs and processes. The one that was used has wide operating temperature ranges to accommodate space environment temperatures.

4.3.2 Solar panel

LPCS is easily configured for use with solar panels. A Clyde Space technical note supplies guidance to implement solar panels for small satellites (Clyde Space Ltd: small satellite solar panels). The application note was followed and battery charge/discharge information was collected. An ENE/CESI single junction GaAs solar cell interconnected with the following specifications, and was selected and used (Figure 4.15) (Clyde Space Ltd: small satellite solar panels).

Table 4.1: Solar panel test specifications

Specification	value
Operating voltage (Vmp)	16.45 V
Operating current (Imp)	0.443 A
Rated power (Pmax)	7.29 W
Dimensions	21.35 cm × 34.6 cm
Weight	0.6 LBS

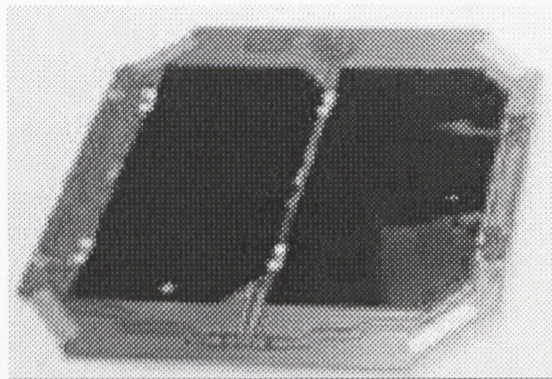


**Figure 4.15: An ENE/CESI single junction GaAs solar cell
(Clyde Space Ltd: small satellite solar panels)**

4.3.3 Battery compatibility test

As mentioned previously, Lithium Polymer (Li-Pols) batteries were selected. These batteries have undergone a number of tests to verify its performance in a space environment. These tests included the following:

- Capacity at C/10 under vacuum;
- Radiation up to 500 krad;
- DPA;
- Capacity at -10°C , 0°C , 20°C and 40°C ;
- Resistance;
- Self Discharge;
- Mission Scenario tests;
- EMF vs SOC;
- Cycling tests at reduced pressure (15 – 20 mbars); and
- -30 % DoD, C/2 charge/Discharge > 5000 cycles.

Other tests were also performed on flight cells to verify their integrity for space use. The batch of batteries passed these tests and matched the capacity and voltage characteristics over temperature.

The 6U battery that was selected has the same main battery board with two series cells, which are mounted flat, side-by-side on a PC104 sized, CubeSat kit compatible PCB as 3U battery, as shown in Figure 4.16 (Clyde Space Ltd: Evaluation of Lithium Polymer technology for small satellite applications).

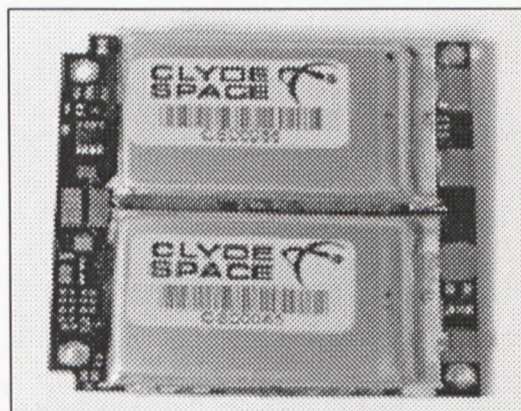


Figure 4.16: 12.3 V 15 Whr Battery cell string for Nanosatellite

(Adapted from Clyde Space Ltd: Evaluation of Lithium Polymer technology for small satellite applications)

Two additional, two cell battery daughter boards can then be integrated with this main PCB to increase the batteries' capacity and to provide further voltage (12.3 V at 300 mA). This configuration results in a 2s3p battery (2 series cells per string and 6 strings in parallel). The capacity of each 2s3p is 3.75 Ah at a maximum voltage of 12.3 V. The main battery PCB (PC104) weighs approximately 80 g, while each daughter battery unit weighs 62 g.

4.3.4 Power control and distribution efficiencies

To accurately predict the amount of power that must be collected by the solar panels to support the loads and battery charging, system efficiencies must be identified, measured and accounted. The LPCS equivalent circuit was thoroughly developed in Chapter Three, Section 3.5 and is shown in Appendix A. The faster the batteries are charged or discharged, the higher the C and less efficient. Again the ambient temperatures beyond the battery's optimum operating range can also cause efficiency to drop. The batteries are rated for discharge from -10 °C to 40 °C, and charge from 0 °C to 35 °C.

The basic setup of the system consisted of batteries and external power supply, which was connected to the base board. Batteries were not connected during the discharge stage. The DC to DC regulators were connected to the base board and the load was connected to the DC to DC regulator. The load measurements were made with only one load attached at a time to isolate the DC to DC regulator's efficiency for each voltage that it supplied. The power controller efficiency was measured during discharge for all loads that were connected, and then each load was connected individually. This power was also measured during charge when no loads were connected, followed by all loads and batteries that were connected. A summary of the findings is given in Table 4.2 below.

Table 4.2: LPCS test results

Designation	Efficiency (%)	Measured As	Voltage (V)	Current (A) (28Ω)
Shunt regulator	75	Very good working condition	=/=	=/=
Battery charged regulator	55	Good working condition	13.4	0.300
12 V Unregulated voltage	=/=	Bus voltage	12.3	Load current
5 V regulator voltage	45	Excellent working condition	5 V	0.9
3.3 v regulator voltage	45	Excellent working condition	3.3 V	0.12

The comparison of the hardware and simulation results is given in table 4.3 below.

Table 4.3: Power distribution simulation and test results

Designation	Simulation	Practical	comment
Shunt regulator	=/=	=/=	Excellent
Battery charged regulator	=/=	=/=	Excellent
12 V Unregulated voltage	12.7 V	13.4 V	Almost equal
5 V regulator voltage	5 V	5.2 V	Approximately equal
3.3 v regulator voltage	3.3 V	3.42 V	Approximately equal

From Table 4.3 above, the practical results approximate the simulated results and slight discrepancies in both results were a result of tolerance in the components and the inaccuracy in the voltmeter that was used.

4.4 Chapter summary

The LPCS for a nanoatellite was comprised of four major parts, included primary power source (solar cells), secondary power source (rechargeable batteries), power distribution and power control. Both power sources were well sized and were provided power required for nanosatellite's subsystems and payload. The system was simulated and the hardware tests were performed, and the comparison of both simulation and hardware test results was done, which was showed their approximate. The power distribution and power control were made of two different PCBs.

CHAPTER FIVE CONCLUSIONS AND RECOMMENDATIONS

5.1 Introduction

A linear power control system (LPCS) is a nanosatellite's EPS, which is designed to continuously provide electrical energy that is required to operate nanosatellites' payload and other electronic subsystems at optimal levels. Included in the system are solar cells, rechargeable batteries and various regulation and distribution components that are chosen for their reliability and ability to fit within the constraints imposed by the mission itself.

This final chapter presents a summary of the results and difficulties that were encountered during the realisation of this project. It shows the different stages or components that were placed together for a perfect functional system, which fits within the requirements of the project as mentioned in chapter 1. Future improvements will make this system sturdier, more powerful, and more modular to accommodate upcoming missions.

5.2 Results and difficulties

A low cost and feasibly sized linear power control system prototype was successfully developed. This EPS will enable continuous operation of a nanosatellite in space environment. The prototype was composed of power generation (solar cells), power storage (batteries), power distribution and power protection. LPCS was captured solar energy and then distributes to the nanosatellite payload and subsystems. Completion and testing of the prototype hence achieved the objectives of the research and design specifications of regulated power output (12V unregulated and 5V and 3.3V regulated). The design of LPCS has made a huge contribution to the satellite industry, and saves a lot of money in terms of reducing power supply size, weight and failure rates.

5.2.1 Solar cells

- The GaAs triple junction solar cells from Clyde Space were selected and bought. These solar cells were tested and qualified for space activities;
- The solar cell's simulation or the electrical model is functional and efficient;
- The preliminary measurements of solar cells were done by F'SATI researchers and significant working points became known, but it was necessary to redo some measurements with a solar generator and a temperature sensor in order to obtain good identification of each cell; and
- The preliminary comparison between simulations of the electrical model and physical measurements was satisfactory.

5.2.2 Batteries

Clyde Space's Lithium Polymer batteries were selected and bought. The choice of this type was justifiable for, among others, reliability, performance and had undergone extensive evaluation in collaboration with ESA to assess their suitability for space environment, including leak and bulge tests.

5.2.3 Battery and power management

- Simulations that were concluded proved that the management strategy of the battery and power system was theoretically functional and efficient;
- The hot redundancy guarantees good reliability;
- Preliminary tests validate the model of DC/DC linear converters; and
- The measurement of the current was not precise enough, which means that the measured values were not satisfactory, and should be improved by inserting accurate current control loops.

5.2.4 Design of the electronics

The electronics were designed with reliable and efficient components that were able to support thermal constraints, and hence spare as much energy as possible. In Addition, the PCBs were designed, approved and manufactured. All the necessary tests were performed and the results were excellent.

5.3 Proposed future work and recommendations

The following parameters are recommended for further improvement of the system's performance:

- Validate the current control loops;
- Validate the bus voltage control loop;
- Design current limitations for each user;
- Define a priority order to enable the management of current limitations;
- Define exactly what kinds of loads to use and appropriate sensors in order to protect the entire system;
- Temperature of the batteries (two sensors) => use the TMP35, 36 or 37 of the analogue device;
- Voltage of the batteries (two measurements);
- Conduct an analysis of the heat distribution on the PCB and validate the engineering test model (functioning, vacuum, temperature); and
- Test the thermal efficiency of the battery with the thermal designer.

REFERENCES

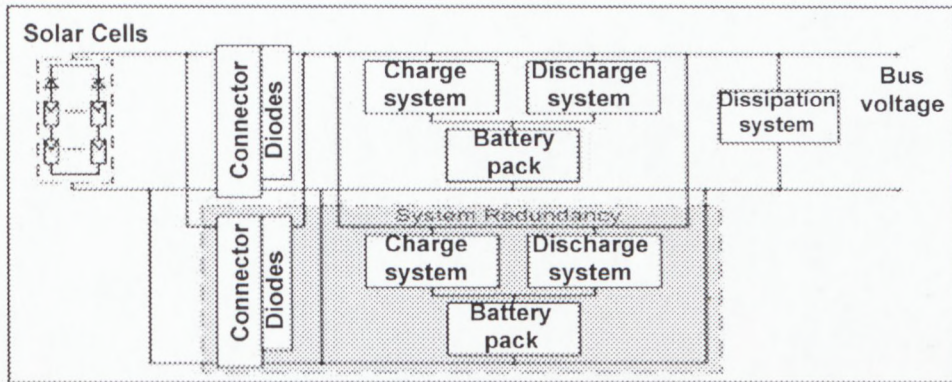
- Ali, I. 2002. *Doppler applications in LEO satellite communication systems*. Dordrecht: Kluwer Academic.
- Amils, R., Ellis-Evans, C. & Hinghofer-Szalkay, H. 2007. *Life in extreme environments*. Netherlands: Springer.
- Bagad, V. S. & Chitode, J. S. 2001. *Communication systems*. Technical Publications: Pune.
- Barrett, E.C. & Curtis, L.F. 1999. *Introduction to environment remote sensing*. Cheltenham Glos: Stanley Thornes.
- Boeker, E. & Grondelle, R.V. 2011. *Environmental Physics: Sustainable Energy and Climate Change*. 3^d Ed. New Jersey: John Wiley & Sons.
- Camarinha-Matos, L.M. Technological Innovation for Sustainability. Second IFIP WG 5.5/SOCOLNET. *Doctoral Conference on Computing, Electrical and Industrial Systems, DoCEIS 2011 Costa de Caparica, Portugal, February 2001*.
- Castaner, L. & Silvestre, S. 2002. *Modelling photovoltaic systems using PSpice*. Chichester: John Wiley & Sons.
- Chester, S. Power management applications: Linear and switching voltage regulator fundamentals. <http://www.national.com/assets/en/appnotes/f4.pdf>. [12 April 2011].
- Clyde Space Ltd. Small satellite solar panels. <http://www.clyde-space.com/documents/2410> [02 September 2010].
- Clyde Space Ltd: Evaluation of Lithium Polymer technology for small satellite applications. <http://www.clyde-space.com/documents/1500>. [04 October 2010].
- Collins, S. 1992. Geocentric Nadir and Range from Horizon Sensor Observations of the Oblate Earth. AIAA Paper No. 92-176 presented at the AAS/AISS Space-flight Mechanics Meeting. Colorado Springs, CO, Feb. 24-26.
- Donabedian, M. & Gilmore, D.G. 2003. *Spacecraft thermal control handbook: Cryogenics*. California: Aerospace Press.
- Edward, P.J. 1887. *The Earth in space: A manual of Astronomical geography*. Boston: D.C. Heath & CO.
- Eisenbud, M. & Gesell, T.F. (Eds). 1997. *Environmental radioactivity: from natural, industrial and military sources*. California: Academic Press.
- Fortescue, P.W., Stark, J. & Swinerd, G. 2003. *Spacecraft systems engineering*. Chichester: John Wiley & Sons.
- Goldin, D. 1992. National Aeronautics and Space Administration http://en.wikipedia.org/wiki/Daniel_Goldin [03 October 2011].
- Gottlieb, I.M. 1990. *Regulated power supplier, Switching regulators, Inverters, and Converters*. 2nd Ed. Howard W. North College: Mc Graw-Hill.
- Graham R.T. & Turk, J. (Eds.). 2006. *Earth science and the environment*. 4th Ed. Belmont: Thomson Learning.

- Green, R.M. 1985. *Spherical Astronomy*. Cambridge: Cambridge University Press.
- Helvajian, H. 1997. *Microengineering technology for space systems*. Los Angeles: Aerospace Press.
- Inglis, A.F. & Luther, A.C. 1997. *Satellite technology: an introduction*. 2nd Ed. Woburn: Butterworth-Heinemann.
- Jones, M. H., Lambourne, R. J. & Adams, D. J. 2004. *An introduction to galaxies and cosmology*. Cambridge University: Press Syndicate.
- Jordan, F. 2006. SwissCube: Electrical power system. HEIG-VD Yverdon: Switzerland
- Kaltschmitt, M., Streicher, W. & Wiese, A. 2007. *Renewable energy: technology, economics and environment*. Berlin Heidelberg: Springer.
- Kiehne, H. A. 2003. *Battery technology handbook*. 2nd Ed. Renningen-Malsheim: Expert Verlag.
- King-Hele, D. 1987. *Satellite Orbits in an Atmosphere: Theory and Applications*. Glasgow: Blackie and Son.
- Kramer, H.J. 2002. *Observation of the Earth and its environment: Survey of mission and sensors*. 4th Ed. Berlin Heidelberg: Springer.
- Kusky, T. 2010. *Encyclopedia of earth and space science*. New York: Facts on File Science Library.
- Lang, K.R. (eds). 2011. *The Cambridge guide to the solar system*. Cambridge-New York: Cambridge University Press.
- Ley, W., Wittmann, K. & Hallmann, W. 2009. *Handbook of space technology*. Chichester, West Sussex: John Wiley & Sons.
- Lida, T. 2000. *Satellite communications: system and its design technology*. Tokyo: Ohmsha.
- Linden, D. & Reddy, T. B. 2002. *Handbook of batteries*. 3^d Ed. Howard: McGraw-Hill.
- Luque, A. & Hegedus, S. (Eds). 2003. *Handbook of photovoltaic science and engineering*. 2nd Ed. Chichester, West Sussex: John Wiley & Sons.
- Mahalik, N.P. 2006. *Micromanufacturing and nanotechnology*. Berlin Heidelberg: Springer.
- Maini, A.K. & Agrawal, V. 2011. *Satellite Technology: Principles and Applications*. 2nd Ed. Chichester, West Sussex: John Wiley & Sons.
- Maloney, S., Travis, Mc.C., Stogsdill, J. & Waddle, H. 2007. Small satellite: Satellite Electrical Power System (EPS), conference paper, December 7, 2007.
- Maral, G., Bousquet, M. & Sun, Z. 2009. *Satellite communications systems: systems, techniques and technology*. Chichester: John Wiley & Sons.
- McEvoy, A., Markvart, T. & Castaner, L. 2011. *Practical handbook of photovoltaics: Fundamentals and applications*. Waltham: Elsevier.

- Melone, C.W. 2009. Preliminary design, simulation and test of the electrical power subsystem of the Tinyscope nanosatellite. NPSM California.
- Michael, J.R. & Norma C. 2002. *Smaller Satellites: Bigger Business? Concepts, Applications and Markets for Micro/ Nanosatellites in a New information world*. Netherlands: Kluwer Academic.
- Mohan, N., Undeland, T.M. & Robbins, W.P. 2003. *Power electronics: converters, applications and design*. 3^d Ed. Hoboken NJ: John Wiley & Sons.
- Montenbruck, O. & Eberhard, G. 2000. *Satellite orbits: models, methods and applications*. Berlin Heidelberg: Springer.
- Munshi, M.Z.A. 1995. Handbook of solid state batteries & capacitors. Farrer: Singapore.
- Pearsall, N.M. & Hill, R. 2001. Photovoltaic modules, systems and applications. Newcastle: University of Northumbria.
- Pistoia, G. 2008. *Battery operated devices and systems: from portable electronics to industrial products*. Amsterdam: Elsevier.
- Pressman, A.I. (Eds). 1991. *Switching power supply design*. New York: Mc Graw-Hill.
- Rashid, M.H. (Eds). 2010. *Power electronics handbook: Devices, circuits and applications*. 3^d Ed. Burlington: Elsevier.
- Redoute, J.M. & Steyaert, M. 2009. *EMC of Analog integrated circuits*. Heidelberg: Springer.
- Sandau, R., Roser, H.P. & Valenzuela, A. 2010. *Small Satellite Mission for Earth Observation: New Developments and Trends*. Heidelberg: Springer.
- Scott, D. 2004. Microchip Technology Inc datasheet: Power Management in Portable Applications: Charging Lithium-Ion/Lithium-Polymer Batteries. Microchip technology.
- Solanki, C.S. 2009. *Solar Photovoltaics: Fundamentals Technologies and Applications*. New Delhi: Asoke K. Ghosh.
- SREEY, Satellite Technology LTD. Small Satellites Home Page: Satellite Classification. http://centaur.sstl.co.uk/SSHP/sshp_classify.html [26/10/2011].
- Vallado, D.A. 1997. *Fundamentals of Astrodynamics and applications*. New York: McGraw-Hill.
- Wenhan, S.R., Green, M.A. & Watt, M.E. 2007. *Applied photovoltaics*. London: Earthscan.
- Wertz, J.R. & Larson, W.J. (eds) 1999. Space Technology Library: *Space Mission Analysis and Design*. Eds. Hawthorne: Microcosm Press & Springer.

APPENDICES
APPENDIX A: Electrical power source equation

The LPCS is based on a single orbit energy balance equation ($P_{bd} \times T_d \leq P_{bc} \times T_c$) and the equivalent circuit shown in Figure 3.9 is repeated here for convenience.



The efficiency of the system depends on the stages that compose the LPCS. A DC to DC regulator has a higher efficiency. The power required by the load is supplied first by the solar array with any remaining power which is taken from the batteries. Hence the power taken from the batteries is the difference between what the load requires and what the solar array supplies.

APPENDIX B: Adjustment of nominal cell efficiency and solar cells calculations

1. The adjustment of nominal cell efficiency (Spectrolab)

D42

	A	B	C	D
1	Adjustment of a nominal efficiencies of Spectrolab Solar Cell			
2		Summer	Winter	Note
3	Predicted Temperature [degree C]	55.7	60.5	From paper
4	Base Temperature [degree C]	28	28	Manufacturer Specification sheet
5	Temperature delta [degree C]	27.7	32.5	Line3 - Line4
6				
7	Voltage Coefficient [V/degree C]	-0.0067	-0.0067	From paper
8	Nominal Max Power Voltage [V]	2.35	2.35	Manufacturer Specification sheet
9	Average Max Power Voltage [V]	2.16441	2.13225	Line8 + (Line7*Line5)
10				
11	Current Coefficient [uA/cm^2/degree C]	9.00E-06	9.00E-06	From paper
12	Nominal Max Power Current [A]	0.0164	0.0164	Manufacturer Specification sheet
13	Average Max Power Current [A]	1.66E-02	-1.67E-02	Line12 + (Line11*Line5)
14				
15	Nominal Efficiency	0.283	0.283	Manufacturer Specification sheet
16	AMO [W/cm^2]	0.1353	0.141	Solar constant at Air Mass Zero (AMO)
17	Power [W]	3.60E-02	3.56E-02	Line9 * Line13
18	Average Efficiency	2.66E-01	2.52E-01	Line17 * Line16
19				
20				
21				
22	Final Average of a nominal Efficiencies of Spectrolab Solar Cell			
23		Summer	Winter	Note
24	Nominal Efficiency	0.283	0.283	Manufacturer Specification sheet
25	Average Radiation	1	1	Decided
26	Temperature Adjustment	0.954	0.881	From paper
27	Design and Assembly Adjustment	0.84	0.84	Manufacturer Specification sheet
28	Final Average Efficiency	0.22678488	0.20943132	Line24 * Line25 * Line26 * Line27
29				
30	Temperature Adjustment Voltage [V]	2.35	2.35	Manufacturer Specification sheet
31	Square Root of Design & Assy	0.92	0.92	From paper
32	Final Average Voltage [V]	2.162	2.162	Line30 * Line31
33				
34	Temperature Average Current [A]	0.0163	0.0163	Manufacturer Specification sheet
35	Square Root of Design & Assy	0.92	0.92	From paper
36	Final Average Current [A]	0.014996	0.014996	Line34 * Line35
37				
38	Final Average Voltage * Final Averaget Current	0.032421352	0.032421352	Line32 * Line36
39	Solar Constant at Air Mass Zero [W/cm^2]	0.1353	0.141	From paper
40	Final Average Efficiency	0.239625661	0.229938667	Line38 / Line39

2. Spectrolab predicted solar cell temperature at winter

#57

	A	B	C	D	E	F	G
28	Spectrolab Predicted Solar Cell Temperatures Winter Solstice						
29	If back side of SA sees all of Earth Enter "1" else "0"						
30	Item	Equation	Symbol	SMAD	Source		
31	Altitude		h	900	GIVEN		
32	Inclination		i	1.809951	GIVEN		
33	Solar/orbit angle		β	0	GIVEN		
34	Orbit angle from Solar Sub Point		ω	0	GIVEN		
35	Radiator normal WRT Nadir		λ	0.785398	GIVEN		
36	Earth angular radius	$\arcsin(R_e/R_0+H)$	ρ ₀	1.167	calculated		
37	Earth view factor	$\sin^2(\theta_0) \cos^2(\lambda)$	F _e	0.608	calculated		
38	Albedo view factor	$F_e \cos(\theta) \cos(\omega)$	F _a	0.608038	calculated		
39	Solar array temperature	$T = [(I_0 S \cos(\phi)) / (ab S_{eff} a + b F_e h^2 \rho_0 S \cos(\phi))]^{0.25}$	T _{sa}				
40	Albedo		al	0.3	GIVEN		
41	Emissivity solar cell side		ε _f	0.85	GIVEN		
42	Emissivity back side		ε _b	0.92	GIVEN		
43	Absorptivity front side		α _f	0.92	GIVEN		
44	Absorptivity back side		α _b	0.17	GIVEN		
45	Cell packing factor		fp	0.8	GIVEN		
46	Cell efficiency		η	0.28	GIVEN		
47	Max direct solar flux - W/m^2		S	1322	GIVEN		
48	Soak incidence angle - rad		Phi	0	GIVEN		
49	Max earth IP emission @ surface		E	326	GIVEN		
50	Solar array temperature - K	$[(I_0 S \cos(\phi)) / (ab S_{eff} a + b F_e h^2 \rho_0 S \cos(\phi))]^{0.25}$	T _{sa}	327.47	calculated	54.32	(Celsius)
51							

3. Solar cell series and parallel requirements for best case scenario

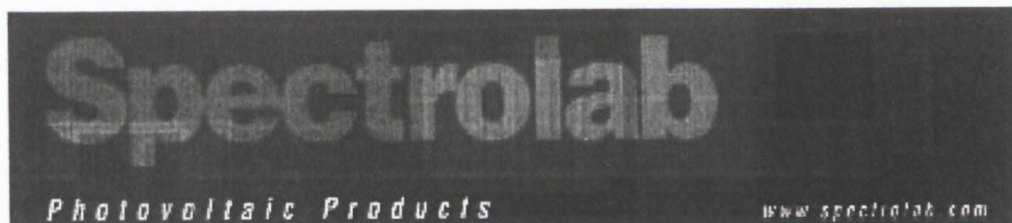
G23		A	B	C	D
1	Voltage value added to the Battery nominal voltage [V]		1.16666667		
2					
3	Solar Cell Series and parallel Requirements (Spectrolab) For Best case Scenario				
4					
5	Battery Nominal Voltage [V]		12.3	12.3	Battery Specification Sheet
6	Voltage Required to Charge Battery [V]		14.35	14.35	Battery Specification Sheet
7	Margin [%]		3.00%	3.00%	Decided
8	Net Voltage Required [V]		14.7805	14.7805	Line47 + (Line47 * Line48)
9	Average Power [W]		12	12	From Matlab/Simulink Model
10	Current Required [A]		0.811880518	0.811880518	Line50 / Line49
11	Net Current Required [A]		0.836236934	0.836236934	Line51 + (Line51 * Line48)
12	Dimension of a cell [6.89cm * 3.95cm]		#	#	From Specification Sheet
13	Area of Solar Cell [cm ²]		27.2155	27.2155	From Specification Sheet
14					
15	EOL Voltage [V]		2.162	2.162	The final Average voltage [Line32]
16	EOL Current Density [A/cm ²]		0.014996	0.014996	The final Average current [Line36]
17					
18	Number of cells connected in Series		6.836493989	6.836493989	Line49 / Line56
19	Number of cells connected in Parallel		2.048979416	2.048979416	Line52 / (Line54*Line57)
20	Number of cells Required		14.00783546	14.00783546	Line59 * Line60
21	Total Cells area required [cm²]		381.230246	381.230246	Line61 * Line54
22					
23	Solar Cells Body mounted Configuration				
24					
25	Total Area Available on the Unit [cm ²]		1981.156348	1981.156348	Dimension calculation
26	Packing factor		0.58	0.58	Decided
27	Effective Area Available [cm ²]		1149.070682	1149.070682	Line66 * Line67
28	Unsed Area Available [cm ²]		767.8404358	767.8404358	Line68 - Line62

4. Solar cell series and parallel requirements for worst case scenario

G8		A	B	C	D
1	Solar Cell Series and parallel Requirements (Spectrolab) For worst case Scenario 1				
2					
3	Battery Nominal Voltage [V]		13.8	13.8	Battery cell degradation up to 4.6 * 3
4	Voltage Required to Charge Battery [V]		16.1	16.1	Calculated value
5	Margin [%]		3.00%	3.00%	Decided
6	Net Voltage Required [V]		16.583	16.583	Line76 + (Line76 * Line77)
7	Average Power [W]		12	12	From Matlab simulation
8	Current Required [A]		0.723632636	0.723632636	Line79 / Line78
9	Net Current Required [A]		0.745341615	0.745341615	Line80 + (Line80 * Line77)
10	Dimension of a cell [6.89cm * 3.95cm]		#	#	From Specification Sheet
11	Area of Solar Cell [cm ²]		27.2155	27.2155	From Specification Sheet
12					
13	EOL Voltage [V]		2.162	2.162	The final Average voltage [Line32]
14	EOL Current Density [A/cm ²]		0.014996	0.014996	The final Average current [Line36]
15					
16	Number of cells connected in Series		7.670212768	7.670212768	Line78 / Line85
17	Number of cells connected in Parallel		1.826264262	1.826264262	Line81 / (Line83*Line86)
18	Number of cells Required		14.00783546	14.00783546	Line89 * Line88
19	Total Cells area required [cm²]		381.230246	381.230246	Line90 * Line83
20					
21	Solar Cells Body mounted Configuration				
22					
23	Total Area Available on the Unit [cm ²]		1981.156348	1981.156348	Dimension calculation
24	Packing factor		0.58	0.58	Decided
25	Effective Area Available [cm ²]		1149.070682	1149.070682	Line95 * Line96
26	Unsed Area Available [cm ²]		767.8404358	767.8404358	Line97 - Line91

5. Series and parallel final calculation

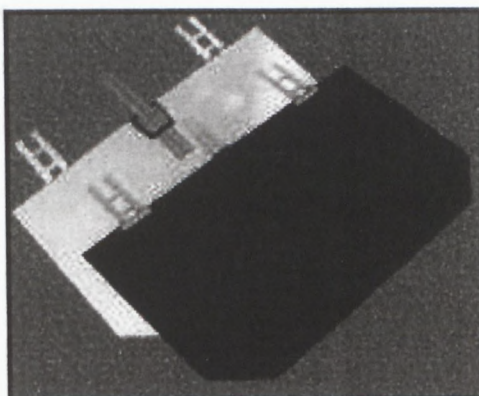
B41		A	B	C	D
1	Solar Cell Series and parallel Requirements (Spectrolab) For worst case Scenario 2				
2					
3	Battery Nominal Voltage [V]		9.6	9.6	Battery cell degradation down to 3.2 * 3
4	Voltage Required to Charge Battery [V]		11.2	11.2	Battery Specification Sheet
5	Margin [%]		3.00%	3.00%	Decided
6	Net Voltage Required [V]		11.536	11.536	Line105 + (Line105 * Line106)
7	Average Power [W]		12	12	From Matlab simulation
8	Current Required [A]		1.040221914	1.040221914	Line108 / Line107
9	Net Current Required [A]		1.071426571	1.071426571	Line109 + (Line109 * Line106)
10	Dimension of a cell [5.89cm * 3.95cm]		#	#	From Specification Sheet
11	Area of Solar Cell [cm ²]		27.2155	27.2155	From Specification Sheet
12					
13	EOL Voltage [V]		2.162	2.162	The final Average voltage [Line32]
14	EOL Current Density [A/cm ²]		0.014996	0.014996	The final Average current [Line36]
15					
16	Number of cells connected in Series		5.335800187	5.335800187	Line107 / Line114
17	Number of cells connected in Parallel		2.625254877	2.625254877	Line110 / (Line112*Line115)
18	Number of cells Required		14.00783546	14.00783546	Line118 * Line117
19	Total Cells area required [cm²]		381.230246	381.230246	Line119 * Line112
20					
21	Solar Cells Body mounted Configuration				
22					
23	Total Area Available on the Unit [cm ²]		1981.156348	1981.156348	Dimension calculation
24	Packing factor		0.58	0.58	Decided
25	Effective Area Available [cm ²]		1149.070682	1149.070682	Line124 * Line125
26	Unsed Area Available [cm ²]		767.8404358	767.8404358	Line126 - Line120
27					
28					
29					
30					
31	Solar Cells Wings Configuration				
32					
33	Total Area Available on Wings [cm ²]		1450	1450	Decided
34	Packing factor		0.8	0.8	Decided
35	Effective Area Available [cm ²]		1160	1160	Line73 * Line74



28.3% Ultra Triple Junction (UTJ) Solar Cells

Features

- High efficiency n/p design (28°C, AM0)
 - BOL: 28.3% min. average efficiency @ maximum power (28.0% @ load voltage)
 - EOL: 24.3% min. average efficiency @ maximum power, 1 MeV 1E15 e/cm²
- Heritage bypass diode protection
- 140 μm Ge wafer thickness



Product Description

Substrate	Germanium
Solar Cell Structure	GaInP ₂ /GaAs/Ge
Method of GaAs Growth	Metal Organic Vapor Phase Epitaxy
Device Design	Monoolithic, two terminal triple junction, n/p GaInP ₂ , GaAs, and Ge solar cells interconnected with two tunnel junctions
Sizes	Up To 32 cm ²
Assembly Method	Multiple techniques including soldering, welding, thermocompression, or ultrasonic wire bonding

Note: Other Variations Are Available Upon Request

Heritage

- More than 2000 kW of multi-junction cells delivered
- More than 675 kW of multi-junction arrays on orbit
- 1 MW annual capacity - cells, panels & arrays
- On orbit performance for multi-junction solar cells validated to ± 1.5% of ground test results

Intellectual Property

This product is protected by the following patents:

- 6,380,601
- 6,150,603
- 6,255,580

ISO 9001:2000
REGISTERED

AS 9100
REGISTERED



10EING 11/01/01

Spectrolab Inc. 12500 Glenhurst Avenue, Dayton, California 95424 USA • Phone: 916-265-4011 • Fax: 916-265-5712

Spectrolab

Photovoltaic Products

www.spectrolab.com

Typical Electrical Parameters

AM0 (135.3 mW/cm²) 28 °C, Bare Cell

$$J_{sc} = 17.65 \text{ mA/cm}^2$$

$$J_{mp} = 16.30 \text{ mA/cm}^2$$

$$J_{sc \text{ min max}} = 16.40 \text{ mA/cm}^2$$

$$V_{oc} = 2.665 \text{ V}$$

$$V_{mp} = 2.350 \text{ V}$$

$$V_{oc \text{ min}} = 2.310 \text{ V}$$

$$CR = 0.84$$

$$E_{\text{eff} \text{ max}} = 28.0\%$$

$$E_{\text{eff}} = 26.3\%$$

Radiation Degradation

(Fluence 1MeV Electrons/cm²)

Parameters	1x10 ¹⁴	5x10 ¹⁴	1x10 ¹⁵
J _{mp} /J _{mp0}	0.99	0.98	0.96
V _{mp} /V _{mp0}	0.94	0.91	0.89
P _{mp} /P _{mp0}	0.93	0.89	0.86

Thermal Properties

Solar Absorptance = 0.92 (Cerium Doped Microsheet)

Emissance (Normal) = 0.85 (Cerium Doped Microsheet)

Weight

84 mg/cm² (Bare) @ 140 μm (5.5 mil) Ge wafer thickness

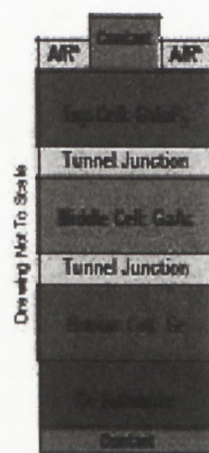
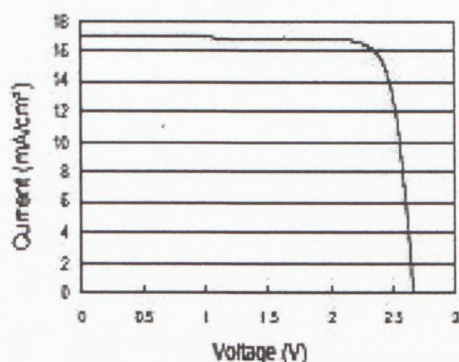
Temperature Coefficients (15 °C - 75 °C)

(Preliminary)

Parameters	BOL	5x10 ¹⁴ (1 MeV e/cm ²)
J _{mp} (μA/cm ² °C)	1	5
J _{sc} (μA/cm ² °C)	5	6
V _{mp} (mV/°C)	-6.5	-6.7
V _{oc} (mV/°C)	-5.9	-6.3

Typical IV Characteristic

AM0 (135.3 mW/cm²) 28 °C, Bare Cell



AR: Anti-Reflective Coating

ISO 9001:2000 REGISTERED AS9100 REGISTERED

SPECTROLAB

100100 111111

The information contained on this sheet is for reference only. Specifications subject to change without notice. 4/21/2008

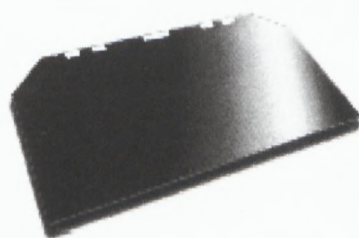
Spectrolab Inc. 11000 Galt Road, Aurora, Ontario, Canada L4R 1V4 • Phone: 416-765-4677 • Fax: 416-765-5117

ATJM Photovoltaic Cell

Advanced Triple-Junction with Monolithic Diode Solar Cell for Space Applications



SPACE PHOTOVOLTAICS

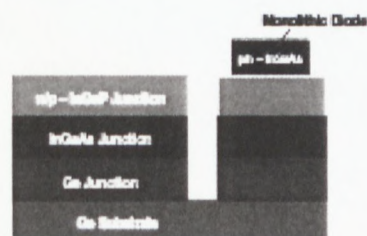


Typical Performance Data

Solar Cell Electrical Output Parameters	
Electrical Parameters @ AMO (135.2 mW/cm ²)	27%
V _{oc}	2.575V
J _c	16.3 mA/cm ²
V _{mp}	2.285V
J _{mp}	16.0 mA/cm ²

Monolithic Diode Electrical Performance	
V _{bi} < 0.5V @ I _b	500 nA, 20T
I _b < 50 μA @ V _{bi}	2.5V (Dark), 20T
I _b < 200 μA @ V _{bi}	2.5V (Sunsim3), 20T
I _b < 10 μA @ V _{bi}	2.5V (Dark), -150C
I _b < 1 μA @ V _{bi}	2.5V (Dark), +130C

ATJM Cell Structure



Schematic Cross-Sectional View

27.0% Minimum Average Efficiency

Features & Characteristics

- Advanced Triple-Junction (ATJ) InGaP/InGaAs/Ge Solar Cells with n-on-p Polarity on 140-μm Uniform Thickness Substrate
- Fully space-qualified with proven flight heritage in LEO and GEO environments
- Fully Space-Qualified Monolithic Bypass Diode Protection
- Lowest solar cell mass of 84 mg/cm²
- Excellent radiation resistance with P/Po = 0.89 @ 1-MeV, SE14 e/cm² fluence
- Excellent Mechanical Strength for Reduced Attrition during Assembly and Laydown
- Weldable or Solderable contacts
- Available at EPI, cell, CIC or panel configuration
- Standard and Custom Sizes Available

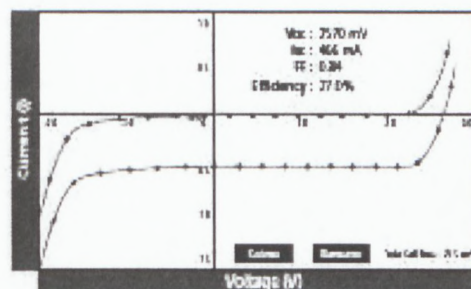
ATJM Photovoltaic Cell

Advanced Triple Junction with Monolithic Diode Solar Cell for Space Applications



SPACE PHOTOVOLTAICS

Typical Current (I) / Voltage(V) Plot



Key Space Qualification Results

Test Parameters	Industry Quality Standard	Typical Test Results
Metal Contact Thickness	4-70 µm	6 µm
Dark Current Degradation after reverse bias	A spec <2%	<0.4%
Electrical performance after 1,000 thermal cycles -80°C to +125°C	<2%	<0.7%
High-Temperature Arrest at 200°C for >5,000 hrs.	<2%	No measurable difference
Contact pull strength	>300 grams	>600 grams
Electrical performance degradation after 40 day humidity exposure at 80°C and 95% relative humidity	<1.5%	No measurable difference

For complete qualification results, please request EMCORE's ATJ Qual Report EWRP036

About EMCORE Corporation



EMCORE Photovoltaics
Albuquerque, NM

- Incorporated in 1984
- Appx. 800 Employees
- Nasdaq: EMCR

Radiation Performance at 1 MeV Electron Irradiation, EOL/BOL Ratios

Device (size)	Voc	Isc	Vmp	Imp	ηmp	Efficiency
SE 13	0.97	1.00	0.97	1.00	0.97	0.97
TE 14	0.96	1.00	0.96	1.00	0.96	0.96
SE 14	0.97	0.98	0.97	0.94	0.89	0.89
TE 15	0.98	0.96	0.98	0.94	0.85	0.85
SE 15	0.86	0.90	0.85	0.87	0.74	0.74

Temperature Coefficients

Device (size)	dVoc/dT (mV/°C)	dIsc/dT (µA/°C)	dVmp/dT (mV/°C)	dImp/dT (µA/°C)
SE	-5.48	+17	-5.93	+11
SE TE	-5.48	+30	-5.88	+7
TE TE	-5.46	+11	-5.68	+7
SE TE	-6.61	+12	-5.92	+12
TE TE	-5.77	+17	-6.14	+12

• ^m Isc is the symbol for normalized Isc

• ^m Imp is the symbol for normalized Imp

Regulatory



EMCORE CORPORATION
ISO 9001 CERTIFIED



EMCORE PHOTOVOLTAIC
& SPACE ELECTRONICS
AS9100 CERTIFIED

APPENDIX D: Matlab codes

```
%%%%%%%%%%%%%%%%%%%%%%%%%%%%%%%%%%%%%%%%%%%%%%%%%%%%%%%%%%%%%%%%%%%%%%%%%%
Solar Panel Power Simulation with different angles (0, 30 and 60 degrees)
%%%%%%%%%%%%%%%%%%%%%%%%%%%%%%%%%%%%%%%%%%%%%%%%%%%%%%%%%%%%%%%%%%%%%%%%%%

% Constants

SCD = 6.89*3.95; % Surface area of standard size of spectrolab solar
cell (cm^2)
CEff = 0.28; % Spectrolab solar cell
efficiency (28%)
AMO = 1368; % Solar constant
(W/m^2)
NCS = 7; % Number of cells per
surface

% Variable

MCP = (SCD/10000)*CEff*AMO; % Maximum power per solar
cell (W)
power = NCS*MCP % Power from 1
solar panel

% Initialition

yangle = 0;
count = 1;
while (count <4)
yangle = (pi/6)*(count-1);
x = 0;
y=1;
angle = 0;
totalpower = 0;
while (x<(90*(pi/180)))
anglecorrect = cos(yangle);
anglecorrect;
panell = abs(cos((pi/2)+x));
```

```

panel2 = cos(x);
power1(y)= panel1 .* (power * anglecorrect);
power2(y)= panel2 .* (power * anglecorrect);
totalpower(y) = power1(y)+power2(y)
angleshort(y) = (180/pi)*x;
angle(y) = angleshort(y);
y = y+1;
x = x+(pi/180);
end
subplot (3,1,count)
plot (angle, totalpower)
xlabel('Degrees')
ylabel('Power (W)')
title('Power vs. Angle @ 0 degrees inclination')
grid on
count = count+1;
end
subplot (3,1,2)
title('Power vs. Angle @ 30 degrees inclination')
subplot (3,1,3)
title('Power vs. Angle @ 60 degrees inclination')

```


=====
I(V) characteristic curve of series connection of cells
=====

function Ia =solar (Va, G, TaC)

% Constants

k = 1.38e-23; % Boltzmann's
constant
q = 1.60e-19; % charge on an
electron
G = 1368; % G = Irradiance (1G = 1368 W/m²),
scalar
n = 1.64; % Diode quality factor
for GaAs
Vg = 1.42; % Band voltage of
the GaAs
TaC = 28; % Solar cell nominal temperature in degree
Celsius
Ns = 7; % Number of cells in
series
Voc_T1 = 2.3; % Open circuit voltage per cell at temperature T1
(in V)
Isc_T1 = 0.5; %Short circuit current of the cell at temperature T1
(in mA)
Voc_T2 = 2.25; % Open circuit voltage per cell at temperature T2
(in V)
Isc_T2 = 0.495; % Short circuit current of the cell temperature T2
(in A)

% Variable

T1 = 273 + 28; % Solar cell nominal temperature in degree
Kelvin
T2 = 273 + 75; % Solar cell temperature changed in degree
Kelvin
TaK = 273 + TaC; % Temperature of the array

```

K0 = (Isc_T2 - Isc_T1) / (T2 - T1); %
Equation (4)

% Initialition

for G = .2:.2:1;
IL_T1 = Isc_T1 * G %
Equation (3)
end
IL = IL_T1 + K0 * (TaK - T1); %
Equation (2)
I0_T1 = Isc_T1 / (exp (q * Voc_T1 / (n * k * T1)) -1);
I0 = I0_T1 * (TaK/T1).^ (3 / n) .* exp (-q * Vg / (n * k )).*((
1./TaK) - (1/T1));
Xv = I0_T1 * q / (n * k * T1) * exp (q * Voc_T1 / (n * k * T1)); %
Equation (8)
dVdI_Voc = - 1.15/Ns / 2; % dV / dI at Voc by cell from the
manufacturer data
Rs = - dVdI_Voc - 1/Xv; % Rs series resistance
per Cell
Vt_Ta = n * k * TaK / q;
Va = linspace (0, 15-TaC/22, 200);
Vc = Va / Ns;
Ia = zeros (size (Vc));

```



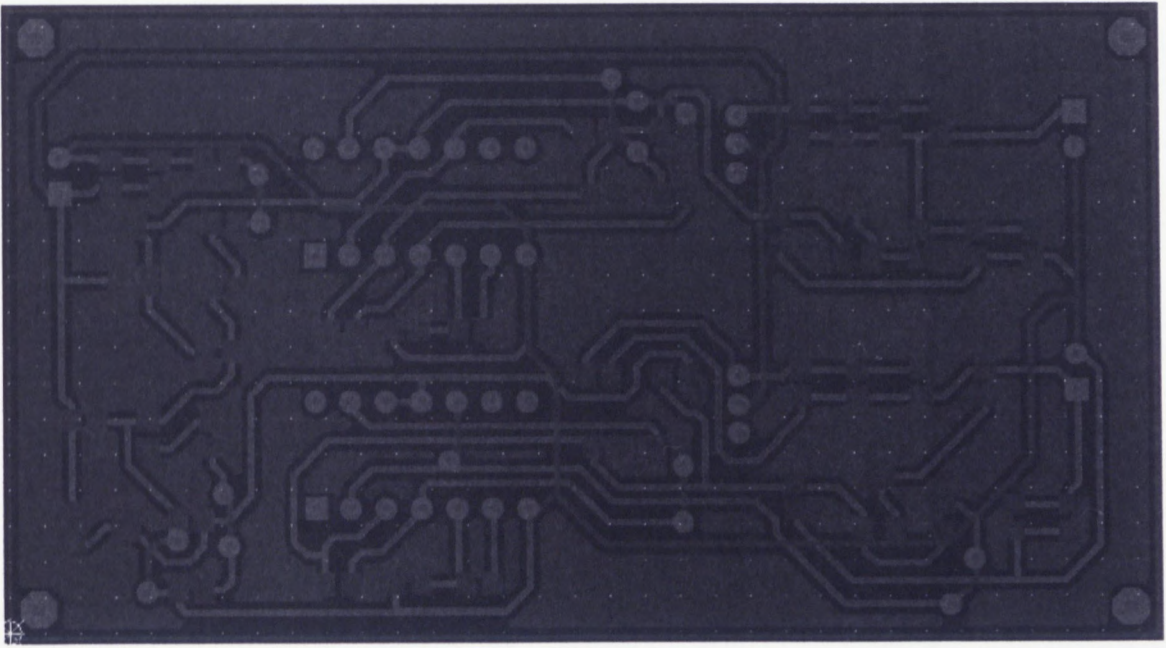
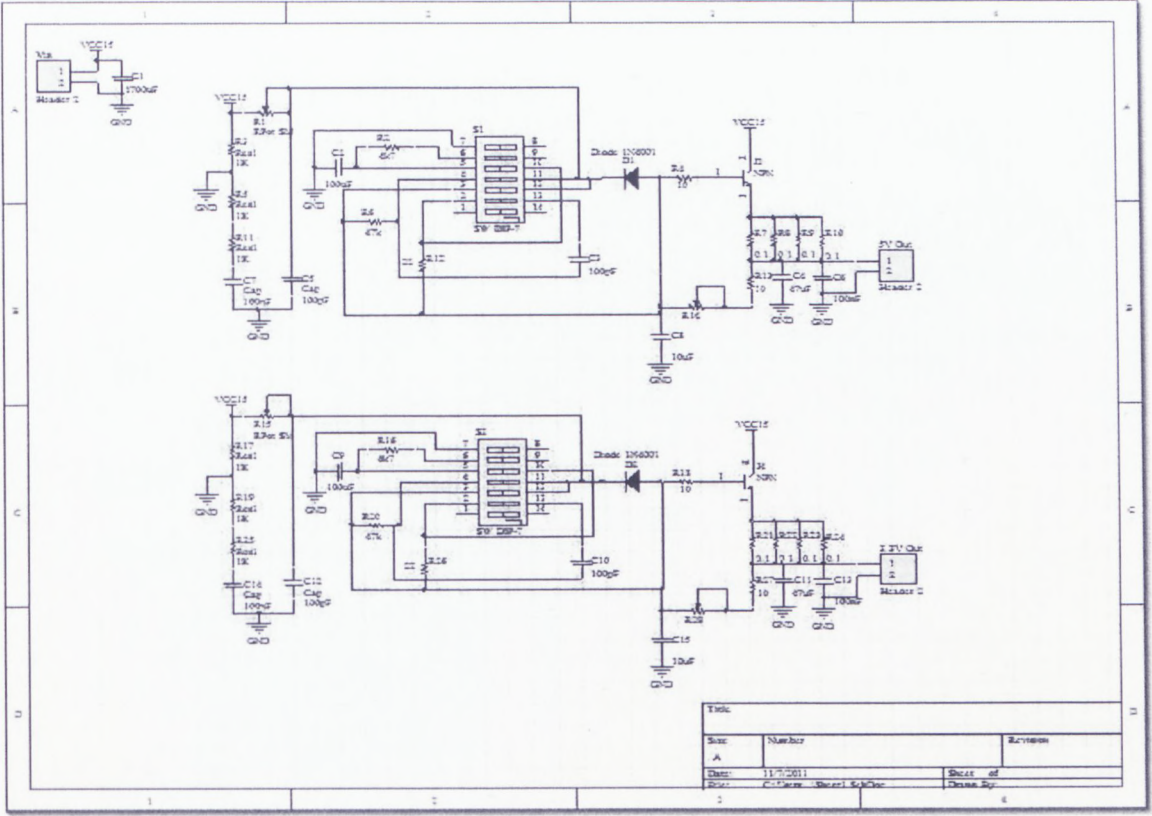
```
=====
Newton's method
=====
```

```
% Initialising

for j = 1:1;
Ia = Ia - (IL - Ia - I0 .* (exp((Vc + Ia .* Rs) / Vt_Ta) - 1)) ...
    ./ (-1 - (I0 .* (exp((Vc + Ia .* Rs) / Vt_Ta) - 1)) .* Rs ./ Vt_Ta);
End

% Functions to plot

figure
hold on
for G=0.1:0.1:1,
%for TaC=0:25:75;
plot(Va, Ia)
end
grid on
title('Solar Cells I-V Characteristic vs Temperature')
xlabel(' Solar Cells Voltage (V)')
ylabel(' Solar Cells Output Current (I)')
gtext('0C')
gtext('25C')
gtext('50C')
gtext('75C')
% gtext('100C')
% gtext('0.2G')
% gtext('0.4G')
% gtext('0.6G')
% gtext('1G')
hold
```

CAPE PENINSULA
UNIVERSITY OF TECHNOLOGY

